



**NAVFAC**  
Naval Facilities Engineering Command

**ENGINEERING SERVICE CENTER**  
Port Hueneme, California 93043-4370

**TECHNICAL MEMORANDUM**  
**TM-2411-AMP**

**HYDRODYNAMIC RESPONSES OF MODULAR  
HYBRID PIERS (MHP) TO PASSING SHIPS**

By:  
Erick T. Huang, PhD, PE  
Hamn-Ching Chen, PhD, PE

September 2008

---

Approved for public release; distribution is unlimited.

<b>REPORT DOCUMENTATION PAGE</b>				Form Approved No. 0704-0811		OMB	
<p>The public reporting burden for this collection of information is estimated to average 1 hour per response, including the time for reviewing instructions, searching existing data sources, gathering and maintaining the data needed, and completing and reviewing the collection of information. Send comments regarding this burden estimate or any other aspect of this collection of information, including suggestions for reducing the burden to Department of Defense, Washington Headquarters Services, Directorate for Information Operations and Reports (0704-0188), 1215 Jefferson Davis Highway, Suite 1204, Arlington, VA 22202-4302. Respondents should be aware that notwithstanding any other provision of law, no person shall be subject to any penalty for failing to comply with a collection of information, if it does not display a currently valid OMB control number.</p> <p><b>PLEASE DO NOT RETURN YOUR FORM TO THE ABOVE ADDRESS.</b></p>							
1. REPORT DATE (DD-MM-YYYY) 31-07-2008			2. REPORT TYPE Final		3. DATES COVERED (From – To)		
4. TITLE AND SUBTITLE <b>HYDRODYNAMIC RESPONSES OF HYBRID MODULAR PIERS (MHP) TO PASSING SHIPS</b>					5a. CONTRACT NUMBER		
					5b. GRANT NUMBER		
					5c. PROGRAM ELEMENT NUMBER		
6. AUTHOR(S) Erick T. Huang, NAVFAC ESC Hamn-Ching Chen, Texas A&M University					5d. PROJECT NUMBER		
					5e. TASK NUMBER		
					5f. WORK UNIT NUMBER		
7. PERFORMING ORGANIZATION NAME(S) AND ADDRESSES NAVFAC ESC 1100 23 <sup>rd</sup> Ave, Port Hueneme CA 93043-4370					8. PERFORMING ORGANIZATION REPORT NUMBER TM-2411-AMP		
9. SPONSORING/MONITORING AGENCY NAME(S) AND ADDRESS(ES) NAVFAC ESC 1100 23 <sup>rd</sup> Ave, Port Hueneme CA 93043-4370					10. SPONSOR/MONITORS ACRONYM(S)		
					11. SPONSOR/MONITOR'S REPORT NUMBER(S)		
12. DISTRIBUTION/AVAILABILITY STATEMENT Approved for public release; distribution is unlimited.							
13. SUPPLEMENTARY NOTES							
14. ABSTRACT <p>This study explores the passing ship effects on a floating pier in typical navy waterfront environments. The goal is to observe the pier performance in the passing ship episode, identify disturbances due to the buoyancy hull of the pier to the ambient water and client ships, and assure the design capacity of the founding system for the pier. The study addresses relevant hydrodynamics with a proven simulation model replicating the hydraulic model test procedure. The results indicate that the buoyancy hull of the pier does not substantially disturb the ambient water activities. Passing ships hardly move the floating pier nor contest the design capacity of its founding system. For example, the maximum load on an individual founding shaft in the worst case passing ship scenario varies from about 8 to 40 percent of the design capacity of the fenders around the founding shaft. The variations depend primarily on the number of client ships and their layout at the pier.</p>							
15. SUBJECT TERMS <p>Passing ship effects; irregular seabed; ship-to-ship couplings; floating pier; time domain simulation; viscous flows; real site conditions.</p>							
16. SECURITY CLASSIFICATION OF:			17. LIMITATION OF ABSTRACT	18. NUMBER OF PAGES 63	19a. NAME OF RESPONSIBLE PERSON Erick Huang		
a. REPORT U	b. ABSTRACT U	c. THIS PAGE U			19b. TELEPHONE NUMBER (include area code) (805) 982-1256		

Standard Form 298 (Rev. 8/98)  
Prescribed by ANSI Std. Z39.18

# **EXECUTIVE SUMMARY**

## **Objective**

This study explores the hydrodynamic influence on the Modular Hybrid Pier (MHP) induced by ship traffic in a nearby navigation channel. The goal is to observe the MHP performance in the passing ship scenario, identify disturbances peculiar to the MHP hull, and assure the design capacity of the anchoring system for the pier.

## **Background**

The United States Navy is developing a floating pier concept, known as the Modular Hybrid Pier (MHP), as an alternative to the standard pile-supported berthing piers. The MHP concept integrates functional versatility, construction flexibility, and operational simplicity in a robust structure that remains largely maintenance-free over a service life of 100 years. This new generation pier can rapidly adapt to the changing needs of a naval base, allowing quick replacement of piers at capital cost comparable to functionally equivalent fixed piers.

Despite its technical and economical merits, the MHP, like any other floating facilities, is subject to the actions of ambient water and client ships through hydrodynamic and structural couplings. A variety of environmental and operational loadings concerning the pier performance and system survivability has been identified by an Integrated Project Team (IPT) at the early stage of conceptual development. These include hydrodynamic forces imposed by docking ships, drifting ships, seismic actions, meteorological and oceanographic (metocean) events, and transit ships. This study assesses the impact induced by ship traffic in the nearby navigation channel.

## **Scope**

The core effort encompasses a series of numerical simulations to quantify the passing ship effects on the MHP in the exact site conditions of a typical navy waterfront. The simulations were conducted for a variety of pier and ship configurations to attain a general vision of the passing ship effects on the MHP. Selected cases were repeated in exactly the same scenario but replacing the MHP with a pile supported pier. This provides a baseline to assess the influence of the MHP hull to the ambient water and client ships. All simulations were conducted with the largest containership admissible to Suez Canal, known as the Suezmax class ship, in the fully authorized channel configuration of Norfolk Harbor Reach (NHR) of 1,500 feet (457 meters) wide and 55 feet (16.8 meters) deep. This model passing ship assumes the existing outbound lane of NHR for most cases. Four other lanes were also investigated to inspect the sensitivity of passing ship locations to the results of passing ship effects. The effects are presented in terms of passing ship induced fluid excitations and dynamic responses of the MHP, client ships, as well as the coupling members.

## **Methodology**

The immense water area and the size of ships involved in the passing ship scenario overwhelm present hydraulic modeling technology and suitable analytical solutions are not

available. This study addresses the relevant hydrodynamic events with a proven simulation model in a manner closely resembling hydraulic model testing in a towing tank. The process includes model fabrications, model calibrations, test executions, and data reduction.

## **Documentation**

This report describes the methodology, model setup, and simulation tool in use, as well as simulation results and findings. A brief description of the site condition and analysis procedure was also provided for reference. The results comprise a large database of flow fields over the entire fluid domain and the motion histories of the MHP and client ships. Raw data in terms of discrete velocity and pressure fields were electronically archived. For brevity, the passing ship effects are presented in integral forms of fluid forces, vessel motion, and dynamic performance of coupling members. The first half of this report describes the nature of passing ship induced flow in the typical waterfront environment with a brief justification. The second half articulates the impact of the MHP hull as opposed conventional pile supported to the pier on ship operations, and summarizes the intensity of passing ship effects and their significance to the MHP design.

## **Conclusions**

Passing ships engage the MHP and its client ships through pressure pulses in coastal water. Their effects on a specific hull are dictated by the speed and separation distance of the passing ship and the water depth at the pier site relative to the drafts of client ships. Most potential the MHP sites at typical navy waterfronts are relatively deep, considering client ships of no larger than the LHD class. Under this circumstance, the flow pattern around the pier site for a specific ship layout remains nearly invariant. This nature allows the passing ship induced excitations be addressed by parametric models. However, these models are site, hull shape, and ship layout dependent and hence require extensive calibrations by empirical data. Besides, a full account of passing ship effects at the pier shall address the dynamic responses of pier, client ships, coupling members, and ambient fluid. These induced entities are highly transient and fully coupled. A seamless, self-sustain model capable of assessing the instant structure and fluid activities concurrently is required to preserve the phase relations among the component entities for a faithful description of the pier and client ship performances in the event of passing ship scenario. Otherwise, numerical uncertainties in one entity may propagate to the others and accumulate in time.

This study indicates that the MHP hull does not substantially disturb the ambient flow and client ship performance. The disturbance introduced by the presence of the MHP hull is much less significant than the influence due to water depth variations at the pier site. In fact, a client ship on the weather side provides far more sheltering than does the MHP hull. This observation is substantiated by evidences extracted from flow patterns around the pier site and fluid excitations on the MHP and client ships.

Passing ship induced fluid excitations are roughly proportional to the displacement of the MHP and client ships. Large client ships of the LHD class draw comparable fluid forces as does the MHP. A smaller hull of DDG class bears about 20 percent of the forces on the MHP. These forces are eventually transferred to the founding system of the pier. For instance, the founding shafts of the MHP may endure three to five times the fluid forces on the pier alone in a scenario

with four the LHD hulls in double mooring. Nevertheless, an equivalent pile supported pier with the same client ships would experience similar fluid excitations. The MHP differs from the pile supported berthing pier in the load transfer path to the founding system. The MHP is apparently more sensitive to the layout of client ships.

The present simulation addresses an adverse passing ship scenario in the typical naval waterfront environment close to the worst case event in which a future MHP may face in reality. Lessons learned from this effort provide a tangible measure to gauge the design load for the founding system. The scenario features a large cargo ship of Suezmax class cruising by the model pier site at 14 knots in a ship lane at 190 meters from the offshore end of the pier. The MHP is secured to the seabed with four founding shafts and stands nearly perpendicular to the navigation channel. Each founding shaft interfaces the MHP hull through a set of internal fenders around the shaft. One the LHD hull is moored to the offshore end of the pier on its downstream side. Figures 51 and 52 summarize the passing ship effects in terms of fluid excitations and system responses, respectively. Under the prescribed conditions, the passing ship imposes a sway force of 520 Kilonewtons (KN) and a surge force of 220 KN on the LHD hull and a sway force of 400 KN and a surge force of 150 KN on the MHP, respectively. These forces hardly move the MHP. The MHP surges 1 centimeter (cm), sways 2 cm, and yaws 0.005 degrees at the maximum. The maximum load on a founding shaft is 520 KN, which is about 8 percent of the design buckling load of these fenders. Taking the passing ship scenario and client ship layout to the worst conditions possible for a 396-meter MHP at the waterfront under consideration, the maximum load on the internal fenders could reach 40 percent of their design buckling load by linear extrapolation.



## TABLE OF CONTENTS

	Page
<b>INTRODUCTION .....</b>	<b>1</b>
Objective .....	1
Background.....	1
Scope .....	3
<b>METHODOLOGY .....</b>	<b>4</b>
<b>SITE DESCRIPTION .....</b>	<b>5</b>
<b>SIMULATION MODEL .....</b>	<b>8</b>
Status of Technology .....	8
Theoretical Considerations .....	9
Model Layouts .....	10
Numerical Grids .....	13
Validations .....	19
<b>FEATURES OF PASSING SHIP EFFECTS IN REAL SITE</b>	
<b>ENVIRONMENT .....</b>	<b>22</b>
Basic .....	22
Prevailing Parameters .....	24
<b>RESULTS .....</b>	<b>28</b>
Structure Layouts .....	28
Model Calibrations .....	29
Outputs .....	37
<b>PASSING SHIP EFFECTS ON THE MHP SYSTEM .....</b>	<b>47</b>
Hydrodynamic Interference Introduced by the MHP Hull .....	47
Fluid Excitations on the MHP and Client Ships .....	53
Dynamic Responses of the MHP and Client Ships .....	54
<b>CONCLUSIONS .....</b>	<b>59</b>
<b>REFERENCES.....</b>	<b>61</b>

## LIST OF FIGURES

	Page
Figure 1. The Modular Hybrid Pier, structural layouts, and founding (mooring) system .....	2
Figure 2. The Modular Hybrid Pier, a floating pier concept .....	3
Figure 3. Site map (a) Hampton Roads area, (b) navy waterfront.....	6
Figure 4. NAVSTA Norfolk waterfront .....	7
Figure 5. Simulation domain, model layouts, and seabed bathymetry .....	7
Figure 6. Geometries of the navigation channel .....	8
Figure 7. Structure layouts and nomenclatures .....	11
Figure 8. Definition of ship lanes .....	12
Figure 9. Coordinates and nomenclatures .....	13
Figure 10. Numerical grids on seabed and free surface .....	14
Figure 11. Surface pressure contours around modular hybrid pier and moored ship	16
Figure 12. (a) Test setup and (b) velocity and vorticity fields .....	20
Figure 13. (a) Test setup and (b) fender loads .....	20
Figure 14. Ship-ship couplings .....	21
Figure 15. Towing tank measurements.....	21
Figure 16. Flow patterns induced by the passing ship .....	22
Figure 17. Pressure profiles .....	24
Figure 18. Influence of separation distance on the passing ship effect .....	27
Figure 19. Structure layouts and nomenclatures .....	28
Figure 20. Load deflection curve of the internal fenders.....	29
Figure 21. The MHP undergoes forced vibration in surge .....	30
Figure 22. The MHP undergoes forced vibration in sway.....	31
Figure 23. The MHP undergoes forced vibration in yaw .....	31
Figure 24. The MHP undergoes forced vibration in sway with LHD fixed .....	32
Figure 25. The LHD undergoes forced vibration in sway with MHP fixed .....	32
Figure 26. Free decays of the MHP in (a) surge, (b) sway, and (c) yaw .....	34
Figure 27. Forced vibrations of the MHP near resonance periods .....	34
Figure 28. Motion responses to an initial offset in surge of the MHP.....	36
Figure 29. Motion responses to an initial offset in sway of the MHP .....	36
Figure 30. Motion responses to an initial offset in yaw of the MHP.....	37
Figure 31. The LHD-MHP couplings due to sinusoidal yaw excitations on the MHP .....	37
Figure 32. An example of passing ship induced flow fields.....	39
Figure 33. Currents under the ship hulls induced by outbound Suezmax .....	40
Figure 34. Example of passing ship induced forces .....	42
Figure 35. Shape of force histories .....	42
Figure 36. Example of ship motions .....	45
Figure 37. Example of fender and mooring line reactions .....	45
Figure 38. Influences of mooring lines .....	46
Figure 39. Fluid reaction forces versus ship motion.....	46
Figure 40. Comparison of flow fields at the free surface .....	49
Figure 41. Comparison of flow fields near seabed .....	50

## LIST OF FIGURES (cont)

	Page
Figure 42. Hydrodynamic coupling between moored ships and piers .....	51
Figure 43. Sheltering between moored ships: currents .....	51
Figure 44. Sheltering between moored ships: excitation forces .....	52
Figure 45. Influences of hip locations and water depths .....	52
Figure 46. Impacts introduced by the presence of floating pier the MHP .....	53
Figure 47. Example of passing ship induced forces .....	54
Figure 48. Impacts introduced by MHP hull: motion excursions .....	57
Figure 49. Impacts introduced by MHP hull: kinematics and excitation .....	57
Figure 50. Impacts introduced by MHP hull: coupling member reactions .....	58
Figure 51. Summary of passing ship induced excitations on the MHP and client ship .....	59
Figure 52. The MHP responses and fender reactions .....	59

## TABLE OF TABLES

Table 1. Prevailing parameters of passing ship effects considered in this study .....	5
Table 2. Summaries of ship particulars.....	12
Table 3. Locations of ship lanes .....	12
Table 4. Locations of moored ships.....	12
Table 5. Summary of passing ship induced forces on moored ships (normalized) ....	27

# INTRODUCTION

## Objective

This study explores the hydrodynamic impacts on the Modular Hybrid Pier (MHP) induced by ship traffic in a nearby navigation channel. The goal is to verify the design capacity of the founding shafts, observe the MHP performance, and identify disturbances due to the intrusion of the MHP hull to the ambient water and the client ships.

## Background

Most of the United States Navy piers and wharves are at the late stage of their design life and require substantial maintenance and repairs. Shutdown during repair or replacement often results in high collateral cost to Navy operations. As such, the Navy is seeking an alternative relocatable pier with reduced life-cycle cost. The Naval Facilities Engineering Command Atlantic (NAVFAC LANT) is leading a consortium in the development, testing and evaluation of concepts and materials technology for a new generation of berthing piers. The Naval Facilities Engineering Service Center (NAVFAC ESC) is developing an innovative concept known as the MHP. In contrast to the conventional pile supported piers, the MHP is comprised of standardized pontoon floats on buoyancy support (Berger/Abam Engineers Inc. (2001)). The MHP concept integrates functional versatility and construction flexibility in a robust structure that remains largely maintenance-free over a service life of 100 years. This new generation pier can rapidly adapt to the changing needs of a Navy base, allowing quick replacement of piers at capital cost comparable to functionally equivalent fixed piers.

A typical MHP assembled from four modules is illustrated in Figure 1(a). Each module measures 27-m width by 99-m length by 9-m height with a 4.3-m draft when fully loaded. Pier modules can be added/subtracted and disassembled/reassembled as needed. This floating pier is founded by two to four steel shafts extending from underwater pile dolphins (Figure 1(b)). The number of shafts and their design depends on local geology and environmental loads. This is the only portion of the MHP that is “site adapted.” Buckling rubber fenders located in the founding well absorb energy and limit motion (Figure 1(c)). The founding design isolates the modules from seafloor ground motion; therefore, it can be sited in areas of high seismicity without excessive costs for strengthening.

The MHP is accessed from land via a ramp of nominally 30-m long depending on tidal variations (Figure 2(a)). This pier along with its client ships ride on tides concurrently and thus maintain a constant elevation differential from ship decks to the pier deck (Figure 2(b)). This reduces labor spent in tending brows, mooring lines, and utility cables. Ships can be berthed at less standoff since there is no risk that flared hulls or ship appendages will contact the pier as the tide drops. MHP modules are double-decked for efficient ship support. Ship berthing, re-supply and intermediate maintenance are conducted on the top, “operations”, deck. Utilities for ship “hotel” services are on the lower, “service”, deck. This leaves the operations deck uncluttered for operation of mobile cranes. Utilities are readily accessible for maintenance and eventual change-out to meet new ship requirements.

Despite the operational and constructional merits, MHP, like any other floating facility, is subject to the actions of client ships and ambient water through hydrodynamic and structural

couplings. A variety of environmental and operational loadings concerning the pier performance and system survivability has been identified. For instance, sea level rise, land settlement, storm surge, tsunami, harbor seiche, ship collision, and severe metocean loading are risks for survivability whereas passing ships, docking ships, operational loads, and normal metocean loading are risk factors for pier performance. Several high priority hydrodynamic issues relevant to the pier performance at site were identified by an Integrated Project Team (IPT) at the early stage of conceptual development as follows.

- (a) Response of the MHP and client ships to docking ships
- (b) Response of the MHP to impact from a large drifting ship
- (c) Response of the MHP and client ships to harbor oscillation
- (d) Response of the MHP to hurricane level current, wave, and wind forces
- (e) Response of the MHP and client ships to nearby ship traffic

Item (a) quantifies the berthing loads imposed by a docking ship on MHP and the subsequent motion responses of MHP and its client ships alongside. Item (b) explores the consequence of accidental collision by a large drifting ship. These two items were rigorously addressed in 2003. Findings were documented in Chen and Huang (2003). The results indicate the MHP will be suitable for operation of mobile cranes and the founding shafts and fenders are sufficient to absorb the impacts by docking ships and drifting ships in the prescribed ambient currents. Items (c) and (d) are currently addressed under separate tasks. The present task addresses item (e). This study quantifies the hydrodynamic impact induced by ship traffic in the navigation channel on vessels moored at the piers along the waterfront. The influence of ship traffic on the MHP system is demonstrated in a real waterfront environment at the NAVSTA Norfolk Virginia.

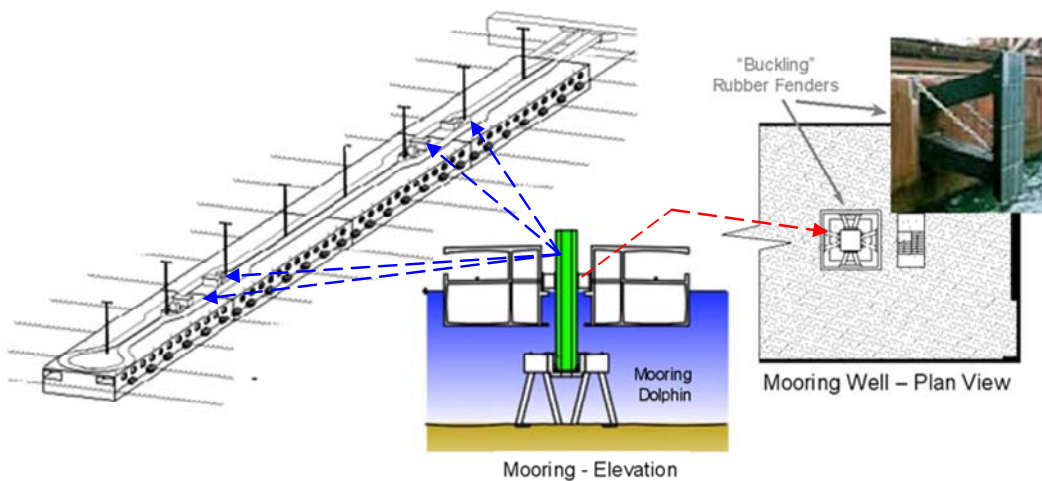


**Figure 1. Modular Hybrid Pier, structural layouts, and founding (mooring) system**

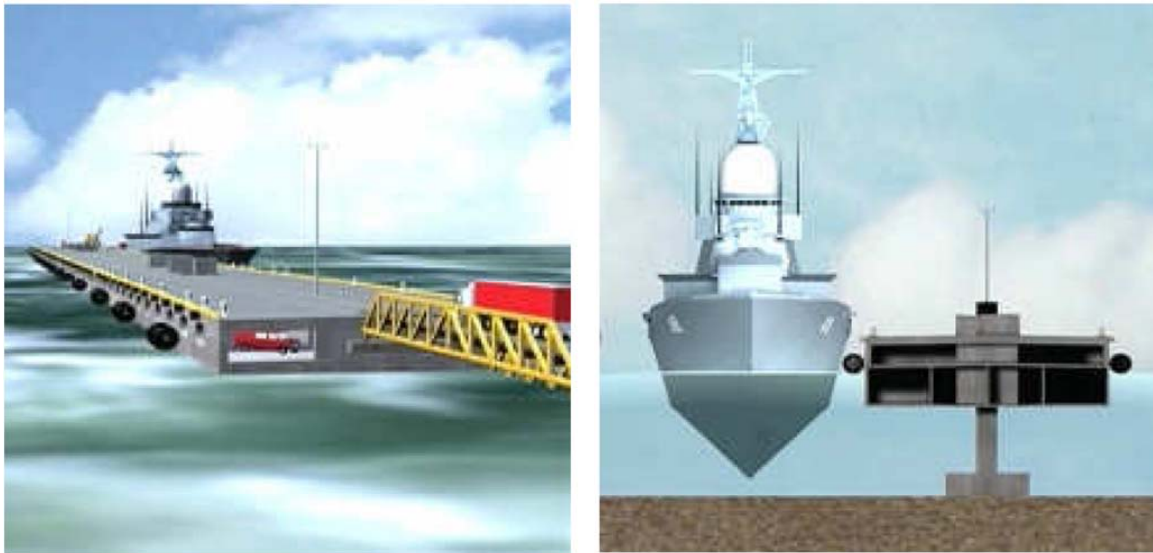


**Figure 2. Modular Hybrid Pier, a floating pier concept**

## Scope

**Simulation.** This study assesses the hydrodynamic issues concerning the design and operation of the MHP induced by transit vessels in a nearby navigation channel. The core effort encompasses a series of numerical simulations to quantify the passing ship effects on the MHP in the exact site conditions at the NAVSTA Norfolk waterfront. The ultimate goal is to verify the design capacity of the mooring shafts and fenders and quantify the dynamic performance of the MHP in the prescribed scenario. To provide a contrast between a floating pier and a traditional pile supported pier, simulations were also repeated for selected cases in exactly the same conditions with the substitution of the MHP by a traditional pile supported pier. The results provide a contrast to assess the influence to the ambient water and client ships introduced by the presence of the MHP hull. The influence was presented in terms of flow patterns and force excitation observed by the client ships. The simulation was conducted with the largest containership admissible to Suez Canal, or the Suezmax class ship in the fully authorized channel configuration of NHR of 1,500 feet wide and 55 feet deep. The assessment is conducted with the model passing ship at the existing outbound lane of NHR. Four other lanes were also conducted to inspect the sensitivity of passing ship locations to the results of passing ship effects.

**Documentation.** This report describes the methodology, model site, and simulation tools in use, as well as simulation results and findings. This effort generated a large database of the flow fields induced by passing ships. Raw data and reduced data directly relevant to the passing ship effects on the MHP and client ships were electronically archived to an external hard drive. For the sake of brevity, this report addresses primarily the flow fields in the specific site conditions of the NAVSTA Norfolk waterfront, their effects on a moored ship, and the consequence of ship lane relocations concerning the passing ship effects. A brief description of the site condition and analysis procedures was also provided for reference.

## METHODOLOGY

Passing ships engage vessels at nearby berths via two primary paths: the pressure pulse and the wave trains. However, a ship cruising at the low speed permissible in the inland water is unlikely to generate noticeable wave disturbances. As such the passing ship effect in the inland water is dictated by pressure pulses. Ship induced flow, although well defined in open water, becomes more involved in restricted waterway. The flow field constantly changes subject to the restraints of seabed and shoreline and varies the most drastically as the ship passes by other ships or structures. Its assessment requires proper treatment of the nonlinear nature of water viscosity and precise description of the irregular seabed and shoreline. This transient flow is traditionally assessed by hydraulic modeling in tow tanks. However, the immense water areas affected by a large passing ship and the ship size per se overwhelm present hydraulic modeling techniques and analytical solution taking into account the irregular waterways in reality is not yet available. This effort therefore resorts to an advanced CFD based simulation model. The model in use is capable of tracing the ship induced flows and their couplings with nearby ships in a manner closely resembling the hydraulic model testing. This is accomplished through a self-sustained viscous flow solver, which is further integrated to a three-dimensional ship motion tracer. The flow solver constantly tracks the flow activities over the entire fluid domain and concurrently feeds fluid forces to the motion tracer for ship location updates. The flow field is resolved in a refined grid mesh on curvilinear coordinates to catch the exact site conditions. The results provide a complete database of the velocity and pressure fields over the entire fluid domain throughout the passing ship episode. All other engineering parameters may be derived from this database.

This study assesses the performance of the MHP subject to passing ship effects in the exact site environment at Pier 7 of NAVSTA Norfolk waterfront. A brief description of the site configurations and ship layouts at this location are provided in the next section. To avoid possible bias the assessment is further conducted in a comprehensive matrix of revised scenarios to explore the influence of site specific parameters, including water depth, pier type, hull shape, and ship layouts. Table 1 summarizes the parameters in consideration. The passing ship effects are quantified in terms of the excitation forces imposed on the MHP and client ships. The trends of force variation with respect to governing parameters provide a sanity check of the performance of the simulation model. The ultimate goal is to validate the design capacity of founding shafts and observe the dynamic performance of the MHP subject to the influence of passing ships. This parametric analysis also identifies the disturbance to the ambient water and client ships introduced by the presence of this floating pier.

**Table 1. Prevailing parameters of passing ship effects considered in this study.**

<b>Parameters</b>	<b>Comments</b>
Hull characteristics of passing ships	Suezmax and Panamax
Hull characteristics of moored ship	LHD, DDG, and MHP
Layout of passing ships	Outbound, inbound, and both
Layout of moored ships	Single LHD, double LHD, double DDG, MHP alone, and MHP with LHD
Orientations of moored ship	Perpendicular or parallel to the ship path
Features of seabed geometry	Full details. Water depths at ship slip may vary
Quay wall	With or without quay wall constraints
Separation distance of passing ship	Varies from 270 to 950 feet as measured from the bottom of the east bank of the navigational channel.
Passing ship speeds	14 knots
Pier sites	Pier 7

## **SITE DESCRIPTION**

NAVSTA Norfolk lies on the eastern shore of Hampton Roads, immediately east of the north-south oriented Norfolk Harbor Reach (NHR) as shown in Figures 3(a) and 3(b). NAVSTA Norfolk maintains 14 piers along this two-mile long waterfront (Figure 4(a)). NHR is the main thoroughfare to the commercial facility of Norfolk Harbor located at about five miles south of the navy waterfront. Heavy traffic of large cargo ships is common. As containerships continue to grow in size, this waterway is under incremental expansion to the authorized ultimate configuration of 55 feet deep and 1,500 feet wide as shown in Figure 5(a). This ultimate cross section is sufficient to accommodate post Suez and post Panama class ships in the future. The solid lines in Figure 3(a) mark current locations of the inbound lane (green) at the western side of the channel and the outbound lane (blue) at the eastern side adjacent to the navy waterfront. The outbound lane at the closest location is within several hundred feet of the offshore end of navy piers, or roughly two beam-widths of modern containerships. When large containerships had been brought into Norfolk Harbor, on rare occasions, ships at the navy piers reported harmful disturbances. The eventual goal of the channel expansion project includes an option to shift the outbound lane by 250 feet toward the navy waterfront as indicated by the dashed blue line in Figure 3(a) to provide a wider safety margin to ship traffic in heavy weathers. The result would notably escalate passing ship disturbances at the navy waterfront. This perhaps represents the worst case scenario that future MHP could be exposed to the influence of ship traffic. The site of Pier 7 is the closest to the navigation channel along the waterfront. An MHP comprised of four standard modules will be placed at this site to observe the passing ship effects.

To minimize the possibility of distorting the passing ship induced flow, this simulation considers a large water domain enclosed in the red box in Figure 4(a). This area includes most of the navy waterfront with the Pier 7 near the center, a section of NHR, and the open water across from the channel. Figure 3(b) illustrates the seabed geometry of the study area under consideration. The seabed bathymetry in the open water area (in green) was duplicated from Hydrographic Chart number 18773 published by National Oceanic and Atmospheric Administration (NOAA). The seabed at the waterfront is more complicated. The two strips at the

right hand side of Figure 4(b) illustrate the seabed geometry. The one in the middle presents the seabed as is, while the one at the far right presents the approved ultimate seabed. It is noted that a series of ship slips along the waterfront were cut out from the natural seabed and separated by unimproved shoals in-between. Water depths in the ship slip varies from 20 to 50 feet. The majority of the seabed of the waterfront is higher than the bottom of the fully authorized navigation channel. The open water and the navigation channel are in fact fairly shallow in comparison to the fully-loaded drafts of large containerships. The deepest area is only a few feet more than these ship drafts. Much of the open water near Craney Island at the south is less than 10 feet deep. The influences of these geometric complexities to the passing ship effects at this location have been addressed in a previous study (Huang and Chen, 2008). In general, seabed bathymetry influences passing ship effects through the large scale geometry. Influences by minor depth irregularities are negligible. Figure 5(a) illustrates the numerical representation of the simulation domain and overall layouts. This domain is roughly centered at Pier 7 and covers an area of 10,000 feet long in the north-south direction and 8,000 feet wide in the east-west direction. An MHP is implemented at the location of Pier 7 with an LHD hull as the model client ship on its north side as shown in the close-up view of Figure 5(b). Figure 5(c) provides an orthogonal view of the simulation area in bird's eye. The red lines specify 12 cross sections, whose profiles are illustrated in Figure 5(d). It can be seen that the open water across the channel from the waterfront, except the north end, is extremely shallow. For instance, the cross section number 7 near Pier 7 (as perceived from north to south) is enlarged in Figure 6(a). Note that the vertical scale is highly exaggerated relative to the horizontal scale. The seabed of the west bank is about 12 meters above the bottom of the channel and the seabed in the waterfront is also substantially higher than the bottom of the channel. This water domain is relatively shallow in comparison to the model passing ship of Suezmax class. It can be seen from Figure 5(b) that the keel of Suezmax is lower than most of the seabed (red lines) in the waterfront and is only 8 feet above the bottom of the fully expanded channel. The MHP and the LHD on the other hand present much more comfortable under keel clearances. As a result, the simulation domain near Pier 7 is essentially confined shallow water. Passing ship effects normally increase in confined shallow water.

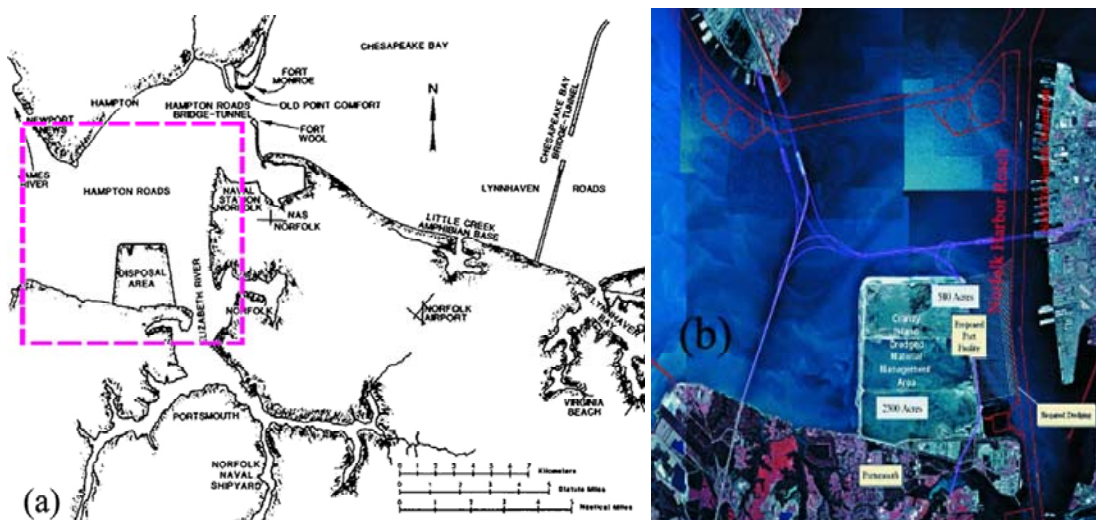


**Figure 3. Site map (a) Hampton Roads area, (b) navy waterfront.**

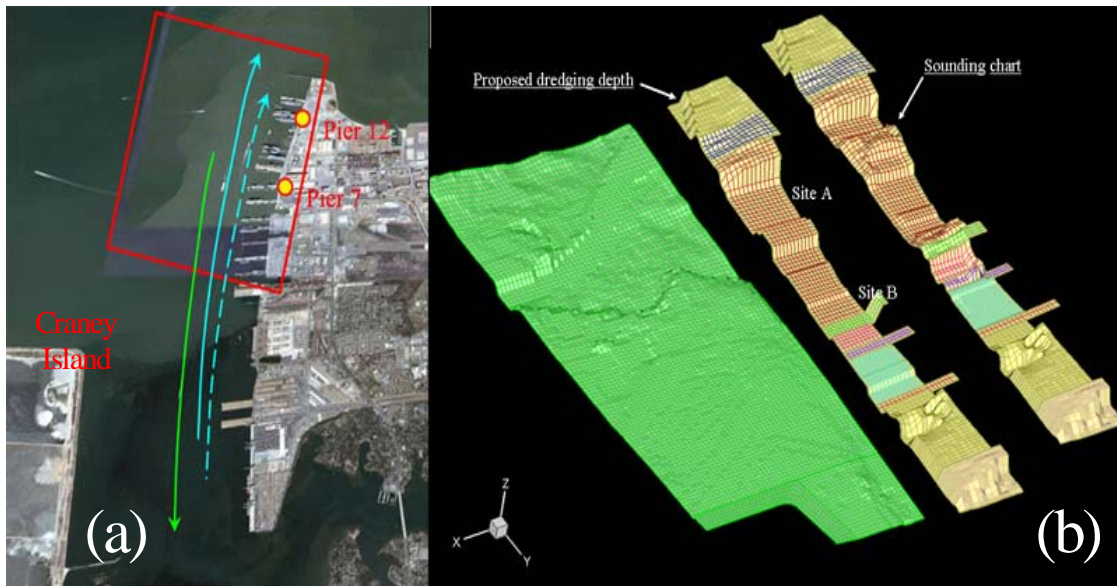


Figure 4. NAVSTA Norfolk waterfront

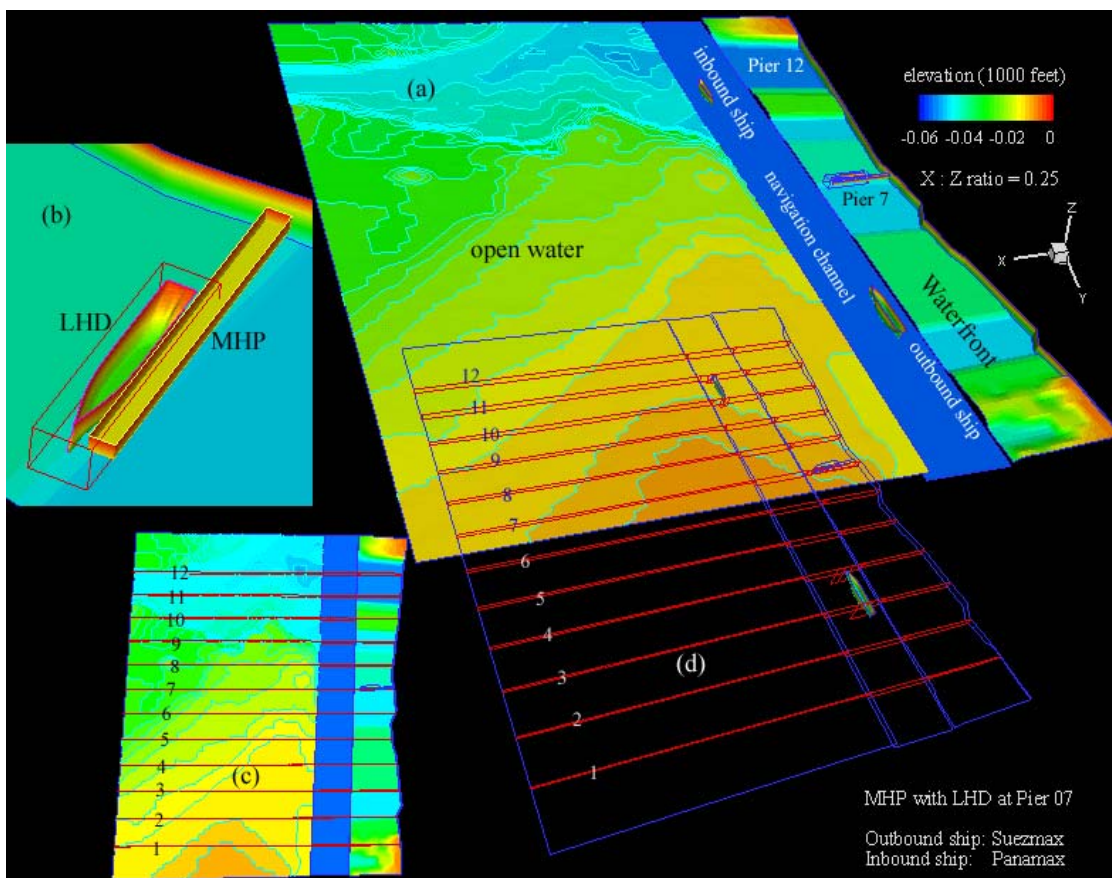
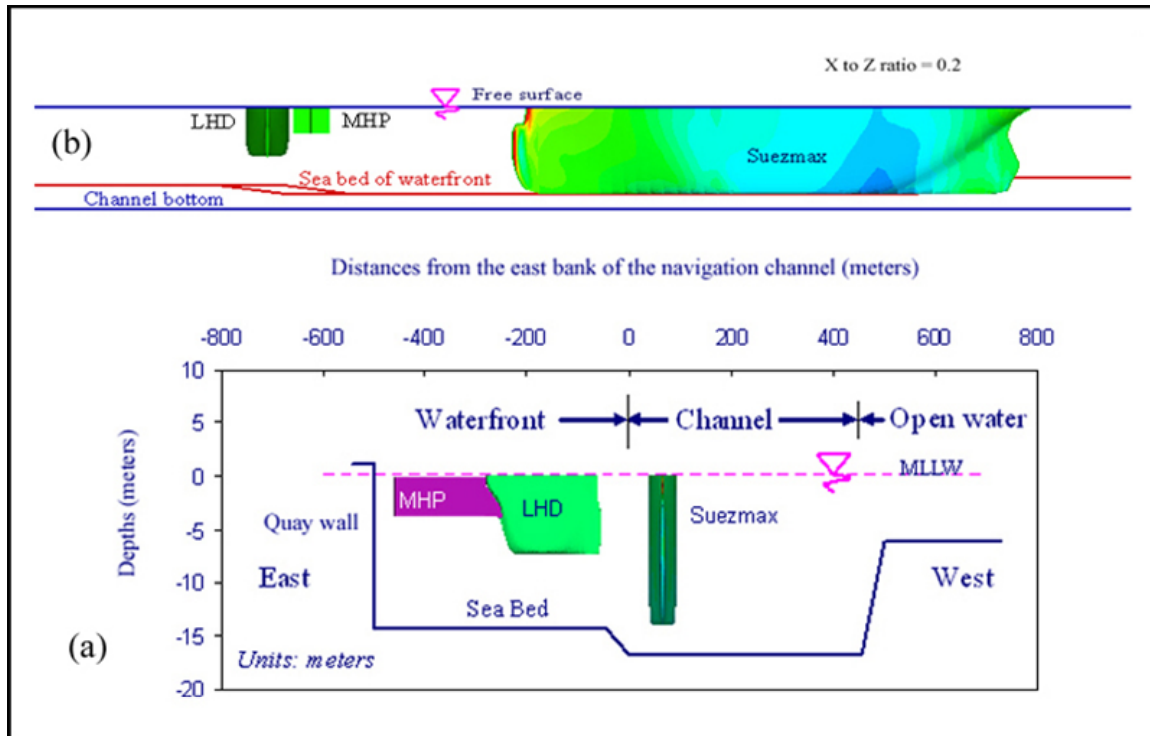


Figure 5. Simulation domain, model layouts, and seabed bathymetry



**Figure 6. Geometries of the navigation channel**

## SIMULATION MODEL

### Status of Technology

Current perception of passing ship effects is built on previous works of Tuck et al. (1974), Remery, (1974), Wang (1975), Muga et al. (1975), and Varyani et al. (2006). Their findings were mostly drawn from an open water environment of flat seabed with passing ships on a straight path parallel to the moored ship. Results to date reached a consensus that the contributions of various parameters are highly coupled. With all other parameters remaining constant, the excitation forces on the moored ship increase with the ship size; increase in proportion to the square of the ship speed; decrease with the increase of separation distance; and decrease with the increase of under keel clearance. It is also noted that this process is heavily influenced by the presence of seabed and basin borders. Wang (1975) assessed the influence of finite water depth using an image reflection technique. He suggested that a shallow seabed would enhance the excitations by 10 percent if the water depth is no less than the separation distance and that this correction increases rapidly as the water depth decreases. Varyani et al. (2006) proposed an empirical correction factor for the influences of finite water depth based on an observation that the shape of excitation force histories remains nearly invariant for passing ships at various lateral separation distances in various water depths. Their test data lead to a correction inversely proportional to the relative water depth with respect to ship draft. Nevertheless, these corrections are limited to the influence of a flat seabed in highly simplified scenarios. The influences of other site specific features on passing ship effects in confined shallow water remain

unresolved. A short list of the missing factors includes at least the irregular seabed and basin borders, pier layouts, size and heading of the moored ship, and elastic properties of the mooring system.

Chen et al. (2002a) successfully applied an advanced viscous flow solver built on the Reynolds-Averaged Navier-Stokes (RANS) equation to the transient flow induced by ship-to-ship coupling in confined water of finite depth. This flow solver, in conjunction with chimera domain decomposition technique, demonstrated a remarkable potential to capture all details of ship hull, seabed, and basin boundaries in confined shallow water. Its performance was fully verified with the towing tank observations presented by Dand (1981). Chen et al. (2002b) extended this model to address the excitation forces imposed on a moored ship induced by passing ships in a straight channel parallel to the moored ship. Its function to track irregular seabed and dynamic boundaries of a moving body was fully confirmed. The present study further integrates this flow code to a ship motion tracer to explore the dynamic performance of a ship moored at a finger pier perpendicular to the navigation channel. A parametric study was conducted to explore the influences of seabed and basin boundaries on passing ship effects in an actual waterfront surrounding.

## Theoretical Considerations

In the present study, calculations have been performed using the free-surface chimera RANS method of Chen and Chen (1998) and Chen et al. (2000, 2001, and 2002) to determine the multiple-ship interactions in a shallow-water bay including a major navigation channel. This method solves the non-dimensional RANS equations for incompressible flow in general curvilinear coordinates  $(\xi^i, t)$ :

$$U_{,i}^i = 0 \quad (1)$$

$$\frac{\partial U^i}{\partial t} + U^j U_{,j}^i + \overline{u^i u^j}_{,j} + g^{ij} p_{,j} - \frac{1}{\text{Re}} g^{jk} U_{,jk}^i = 0 \quad (2)$$

where  $U^i$  and  $u^i$  represent the mean and fluctuating velocity components,  $g^{ij}$  is the conjugate metric tensor,  $t$  is time,  $p$  is pressure, and  $\text{Re} = UL/\nu$  is the Reynolds number based on a characteristic length  $L$ , a reference velocity  $U$ , and the kinematic viscosity  $\nu$ . Equations (1) and (2) represent the continuity and mean momentum equations, respectively. The equations are written in tensor notation with the subscripts  $,j$  and  $,jk$  represent the covariant derivatives. In the present study, the two-layer turbulence model of Chen and Patel (1988) is employed to provide closure for the Reynolds stress tensor  $\overline{u^i u^j}$ . The RANS equations have been employed in conjunction with a chimera domain decomposition technique for accurate and efficient resolution of turbulent boundary layer and wake flows around the moving and moored ships. The method solves the mean flow and turbulence quantities on embedded, overlapped, or matched multiblock grids including relative motions. Within each computational block, the finite-analytic method of Chen, Patel and Ju (1990) is employed to solve the RANS equations in a general, curvilinear, body-fitted coordinate system. The overall numerical solution is completed by the hybrid PISO/SIMPLER pressure solver of Chen and Korpup (1993) that satisfies the equation of continuity at each time step. The present method was used in conjunction with the PEGSUS program of Suhs and Tramel (1991) that provides interpolation information between different

grid blocks. The free surface boundary conditions for viscous flow consist of one kinematic condition and three dynamic conditions. The kinematic condition ensures that the free surface fluid particles always stay on the free surface:

$$\eta_t + U\eta_x + V\eta_y - W = 0 \quad \text{on} \quad z = \eta \quad (3)$$

where  $\eta$  is the wave elevation and  $(U, V, W)$  are the mean velocity components on the free surface. The dynamic conditions represent the continuity of stresses on the free surface. When the surface tension and free surface turbulence are neglected, the dynamic boundary conditions reduce to zero velocity gradient and constant total pressure on the free surface. A more detailed description of the chimera RANS/free-surface method was given in Chen and Chen (1998) and Chen et al. (2000, 2001, 2002).

In order to predict the responses of moored ships and their feedback to the ambient flows, the RANS code was coupled with a six-degree-of-freedom motion analyzer, Compound Ocean Structure Motion Analyzer (COSMA), developed by Huang (1990). Coupling forces on fenders and mooring lines may be assessed based on the relative motion between moored ships and piers. The equation of motion implemented in the COSMA can be written in the following general form:

$$[M + a]\{\ddot{X}(t)\} + [b]\{\dot{X}(t)\} + [K + C]\{X(t)\} = \{f(t)\} \quad (4)$$

in which  $[M]$  represents the generalized inertia matrix,  $[a]$  is the hydrodynamic mass matrix,  $[b]$  is the hydrodynamic damping matrix,  $[K]$  is the hydrodynamic restoring force matrix,  $[C]$  is the restoring forces due to coupling members,  $\{X(t)\}$  is the generalized displacement vector, and  $\{f(t)\}$  is the generalized external excitation force vector.

The present method solves the unsteady RANS equations at each grid node for the transient velocity and pressure fields induced by the passing and moored ships. Therefore, the hydrodynamic force vector  $\{F_h(t)\}$  can be readily obtained by a direct integration of the surface pressure and shear stresses over the wetted hulls of the floating structures. This term includes the external excitations,  $f(t)$ , as well as the added mass and damping forces. Consequently, Equation (4) can be rearranged in a convenient form as follows:

$$[M]\{\ddot{X}(t)\} + [K + C]\{X(t)\} = \{F_h(t)\} \quad (5)$$

For ship induced flows, the chimera RANS method was employed first to calculate the transient flow field and the associated hydrodynamic forces  $\{F_h(t)\}$ . The COSMA program was then used to solve the displacement vector  $\{X(t)\}$  from Equation (5). Once the new ship position and the corresponding fender deflection are determined, the numerical grids can be updated by following the ship motion. A more detailed description of the COSMA program and the coupled RANS / COSMA method is given in Huang and Chen (2003) and Chen et al. (2000).

## Model Layouts

For the purpose of testing the design capacity of mooring shafts and fenders, a model MHP was implemented at Site B around Pier 7 as illustrated in Figure 4. This site was chosen for

its close proximity to the navigation channel and full exposure to the passing ship actions. Figure 5 gives a synoptic view of the water domain and ship layouts of the numerical model under consideration. The baseline model includes two transit ships and on the MHP with a client ship at the location of Pier 7. This represents the largest model permissible to the available PC workstation. Two large cargo ships of Panamax and Suezmax classes were selected to represent the worst case inbound and outbound ships, respectively. Particulars of the model ships are listed in Table 2. Most simulation cases were, however, conducted with one outbound ship alone, except the scenario to test the coupling effects between two passing ships. The inbound ship, if presents, will stay in the existing inbound lane at 1,000 feet away from the east bank of the channel. The outbound ship cruises in one of the five ship lanes, designated as Lane 1 to Lane 5, as depicted in Figure 8. Note that the locations of ship lanes used for the cases of the MHP (with or without the LHD) and DDG cases are slightly different, except Lane 2, which represents the existing outbound lane. The locations of these ship lanes as measured from the bottom of the east bank of the channel are listed in Table 3. While the locations of the MHP and moored ships are given in Table 4. The outbound ship maintains a draft of 47 feet throughout this study. That leaves a clearance of 8 feet under keel. The MHP and client ship may be reconfigured or replaced with a pile supported pier or other ship hulls for the purpose of identifying influences introduced by the presence of the MHP hull. For instance, the layouts illustrated in Figure 9 are designed to show the significance of sheltering or interference to the client ship performance due to the MHP hull. The passing ship effects in terms of fluid forces on the moored ship were computed in all seabed configurations with the outbound ship. Coordinates and key nomenclatures are specified in Figure 9.

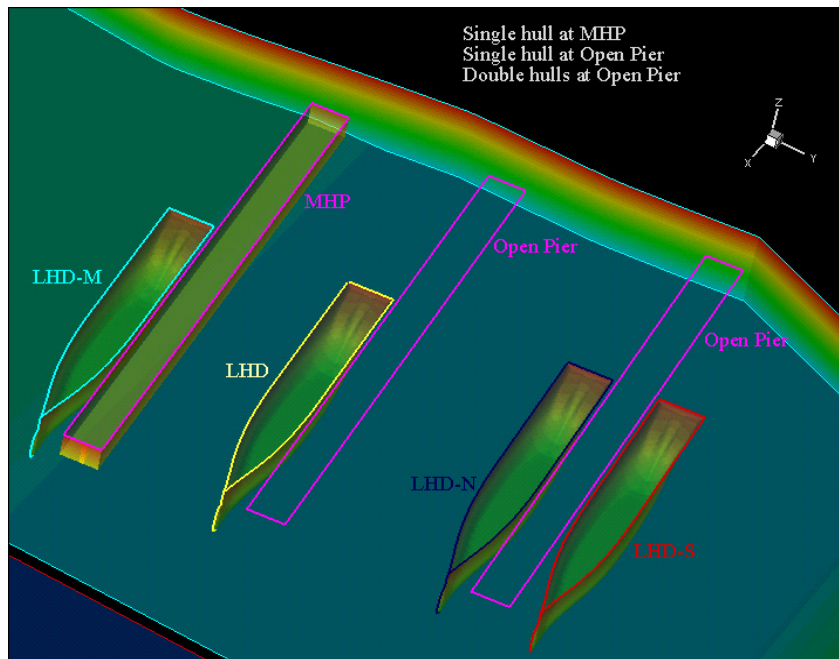


**Figure 7. Structure layouts and nomenclatures**

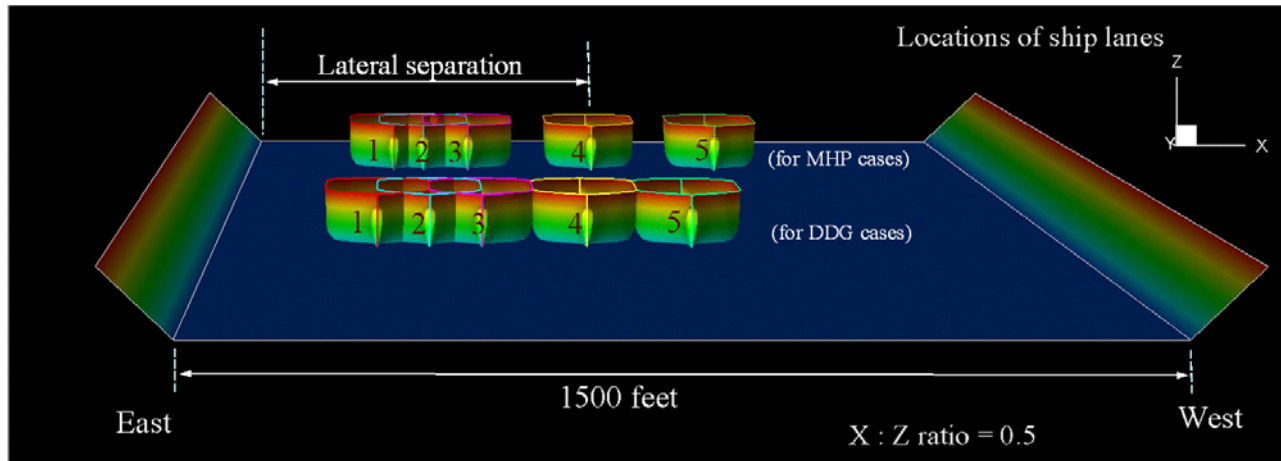


**Figure 8. Definition of ship lanes**

**Table 2. Summaries of ship particulars**

	Suezmax	Panamax	CVN	LHD	DDG	MHP
Displacement (tons)	-	-	87300	41150	8300	43116
Lwl (meters)	379	283	318	237.13	142.04	396.24
Beam (meters)	55	32	41	32.31	20.12	26.82
Draft (meters)	14.3	13.1	11.6	8.23	9.45	4.36
Mass (tons)	-	-	8900	4190	846	4400
Izz (ton-m <sup>2</sup> )	-	-	7.5E7	2.0E7	1.4E6	5.7E7

**Table 3. Locations of ship lanes**

Case	units	Lane 1	Lane 2	Lane 3	Lane 4	Lane 5	Lane 6
LHD	feet	300	360	450	700	950	-
	meters	91.44	109.73	137.16	213.36	289.56	-
	normalized	0.2419	0.2903	0.3629	0.5645	0.7661	-
DDG	feet	270	360	450	630	810	-
	meters	82.30	109.73	137.16	192.02	246.89	-
	normalized	0.2177	0.2903	0.3629	0.5081	0.6532	-
CVN	feet	110	360	610	860	235	485
	meters	33.53	109.73	185.93	262.13	71.63	147.83
	normalized	0.0887	0.2903	0.4919	0.6935	0.1895	0.3911

**Table 4. Locations of the MHP and moored ships**

Distances from the east border of the channel at bottom		
Moored ship	feet	meters
CVN	965.31	294.23
MHP	833.47	254.04
LHD-S	578.79	176.41
DDG_N	465.15	141.78
DDG_S	489.20	149.11

Note: The offshore end of the MHP is at 55 meters east of the east border of the navigation channel at the bottom.

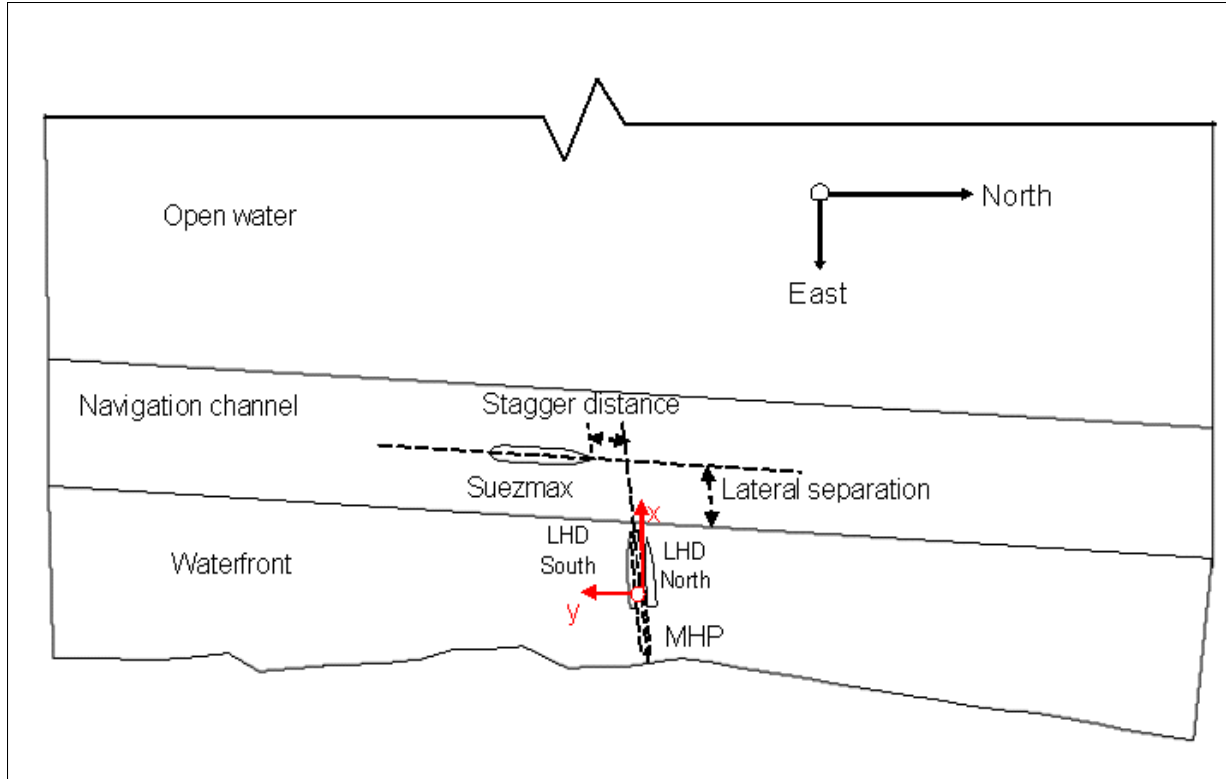
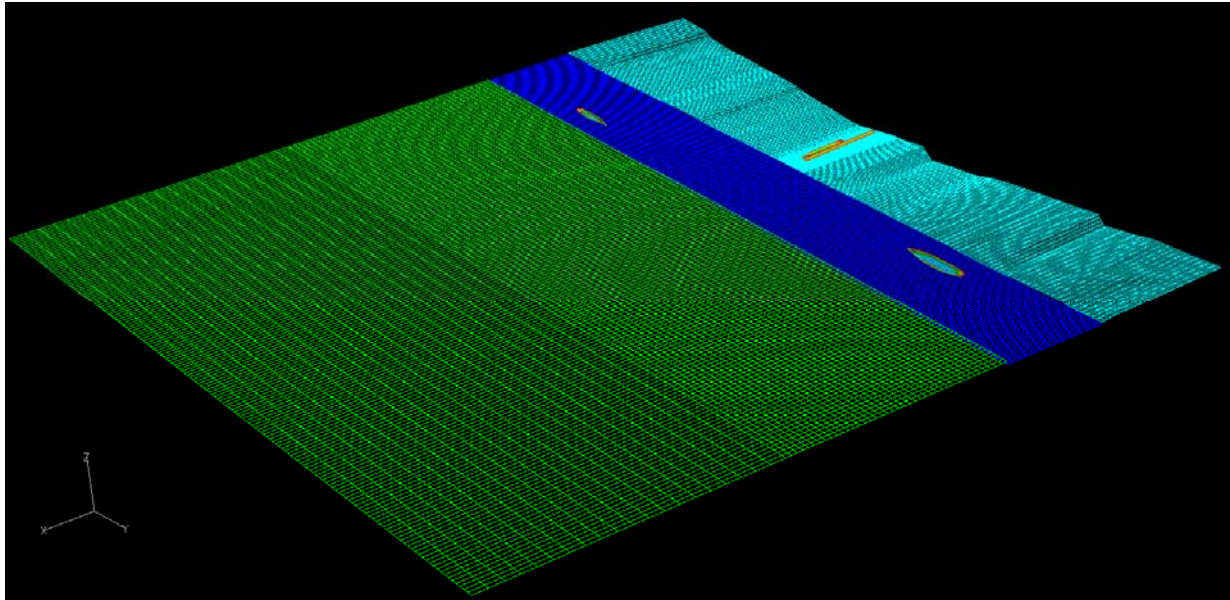


**Figure 9. Coordinates and nomenclatures**

## Numerical Grid

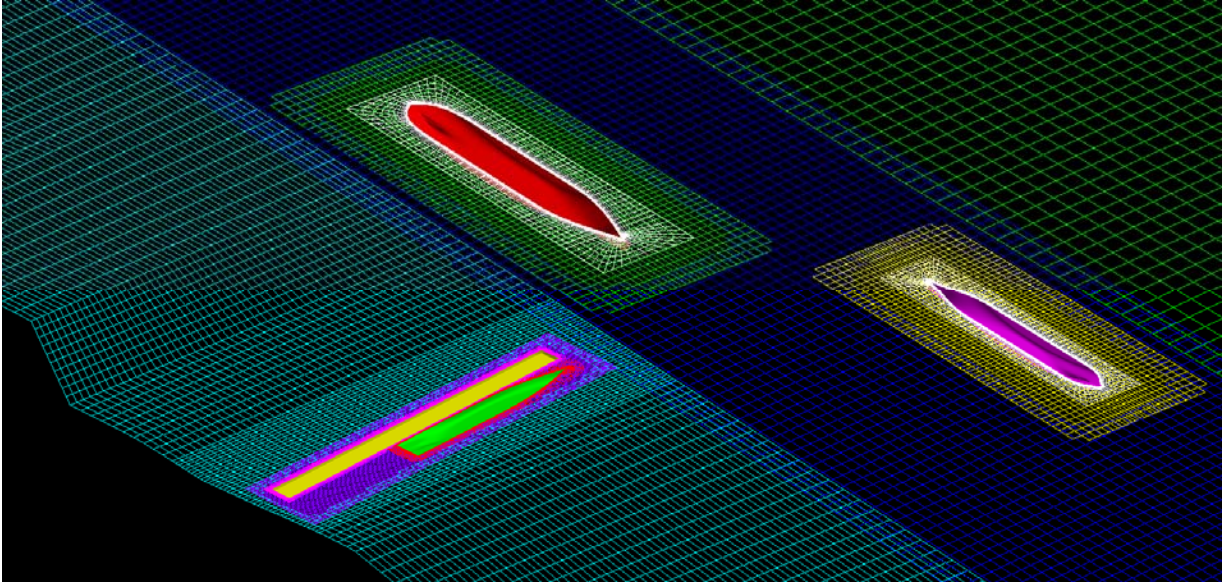
The irregular water domain was digitized into a numerical grid system using a chimera domain decomposition approach. The grid system prepared for Site B is a typical example. Figure 10(a) shows a scenario involving both the inbound and outbound ships, and a moored ship docking next to a floating pier. Figure 10(b) shows the overset numerical grids on sea floor and free surface at select time instants. The chimera domain decomposition approach substantially simplifies the grid generation process for passing ships traveling at prescribed speeds. For convenience, the flow domain is divided into three computational blocks with  $251 \times 41 \times 15$  points for the water front,  $197 \times 61 \times 15$  for the navigation channel, and  $165 \times 61 \times 11$  for the open water area. Both the inbound and outbound ship grid blocks consist of  $51 \times 31 \times 61$  grid points, while the moored ship block is surrounded by a  $61 \times 29 \times 61$  boundary-fitted grid and the modular pier is covered by a  $122 \times 21 \times 31$  grid block. Both the moored ship and the pier are embedded in a  $151 \times 61 \times 11$  rectangular background grid block to provide accurate resolution of the near-field flow around the modular hybrid pier and the moored ship. The inbound and outbound ship blocks are also embedded in  $61 \times 31 \times 15$  rectangular grid blocks which move together with the passing ships as shown in Figures 10(b) thru 10(d). This enables us to accurately resolve the wake flow behind each passing ship without significant increase of the total grid points for the entire water basin. In addition, three phantom grid blocks with  $2 \times 2 \times 2$  grids were used to blank out any ship grids which fall below the channel bottom or sea floor. The total number of grid points including the 10 computational blocks and 3 phantom blocks are slightly below 1 million.

Time-domain simulation was performed for this test case with both the inbound and outbound ships moving at the same speed of 14 knots. **Figure 10** shows the predicted surface pressure contours on the modular hybrid pier and the moored ship at selected time instants. It is seen that the passing ships have negligible influence on the moored ship up to the normalized elapse time  $t/T = 2.5$  since the flow induced by the motion of passing ships has not yet reached the moored ship. The symbol  $T$  is the time scale factor. Between  $t/T = 3.5$  and  $4.5$ , the bows of the passing ship and pier are subjected to positive pressures which push the moored ship away from the navigation channel. After the inbound and outbound ships have passed each other around  $t/T = 4.5$ , a suction pressure is developed on the bows of the modular hybrid pier and moored ship. The suction force is expected to pull the pier and moored ship toward the navigation channel. In addition, the side forces and yaw moments induced by the passing ships will also produce lateral motions of the moored ship. The simulation results clearly illustrated the capability of the present RANS method to provide detailed prediction of passing ship effects.

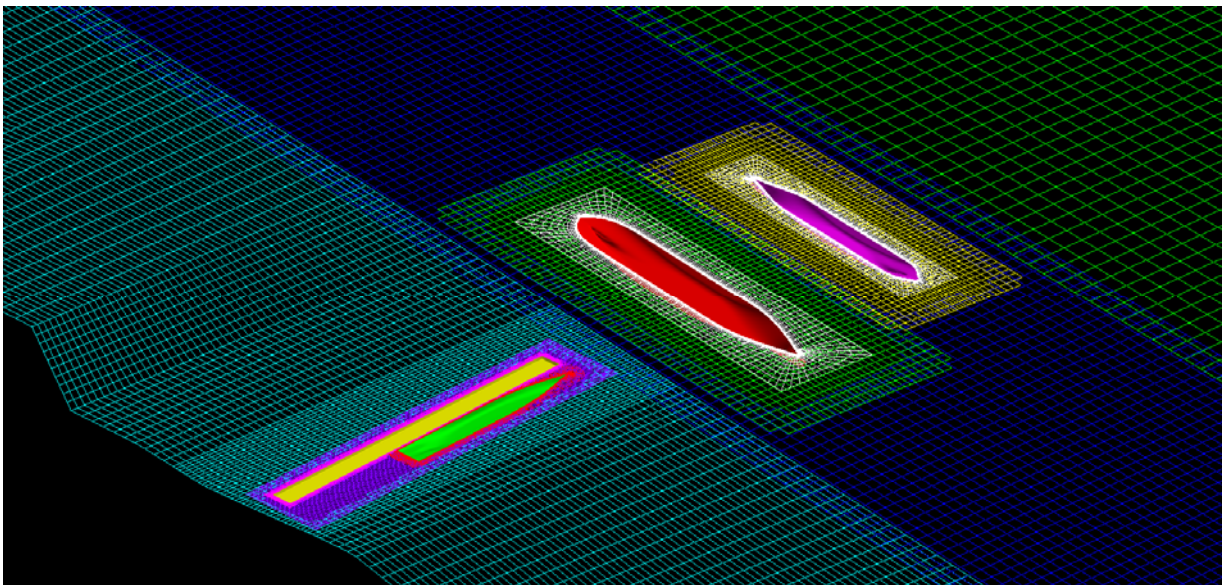


(a) Seabed grid

**Figure 10. Numerical grids on seabed and free surface**

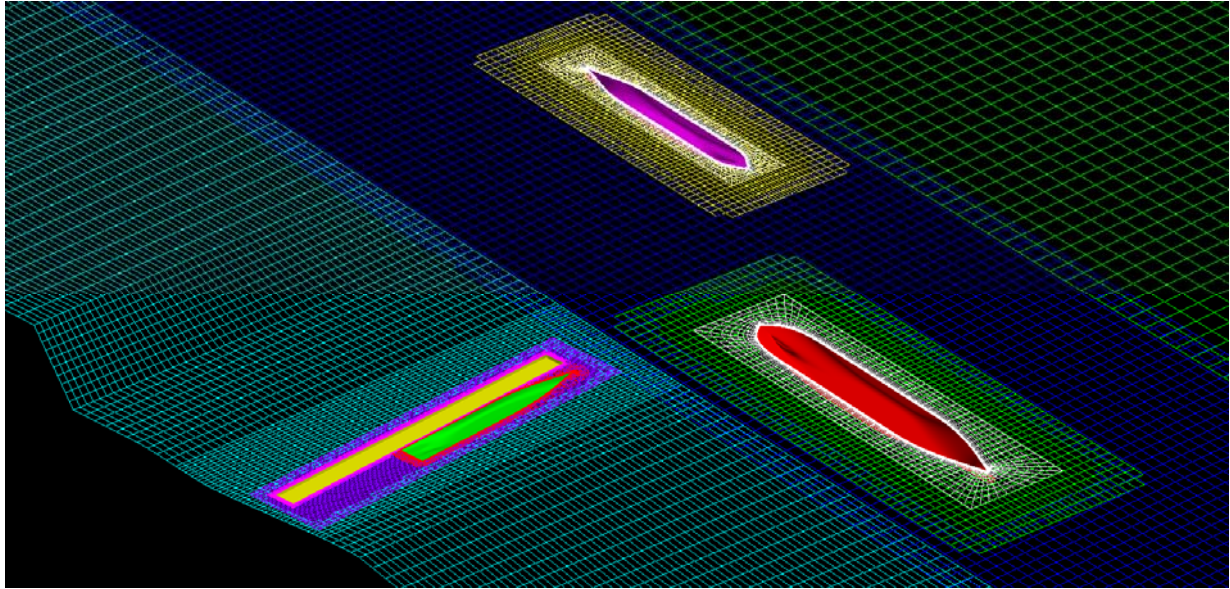


**(b) Free surface grid;  $t/T = 3.6$**



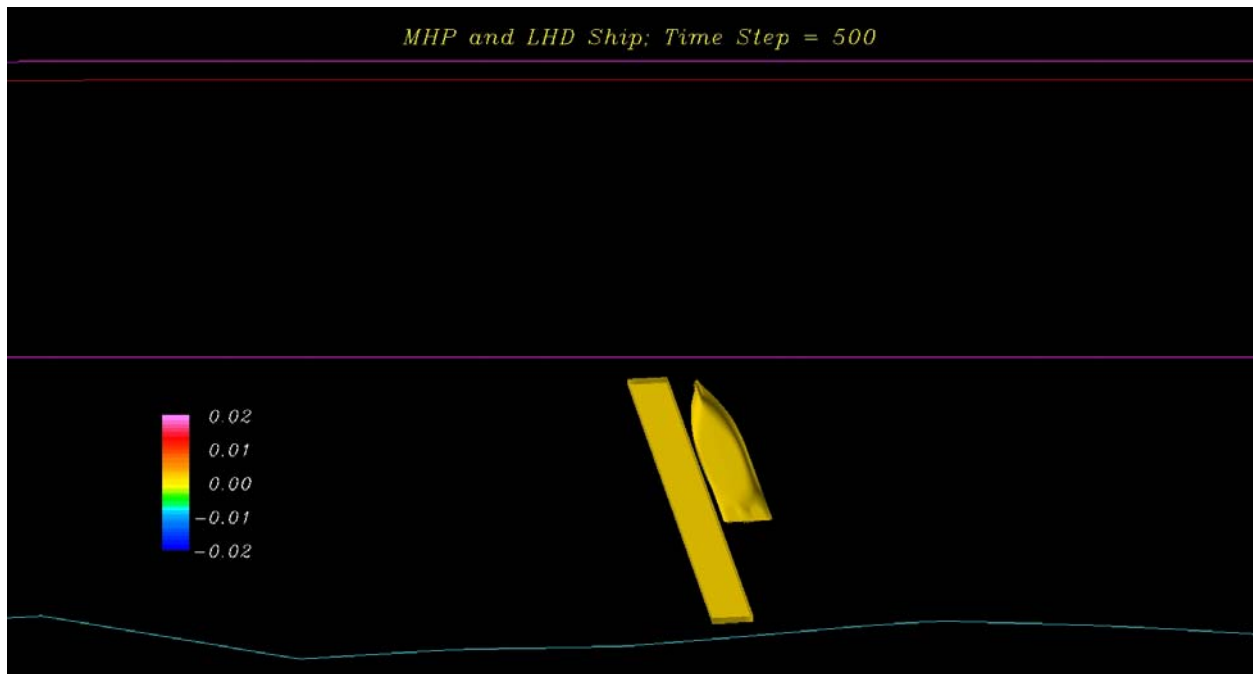
**(c) Free surface grid;  $t/T = 4.6$**

**Figure 10. Continued**



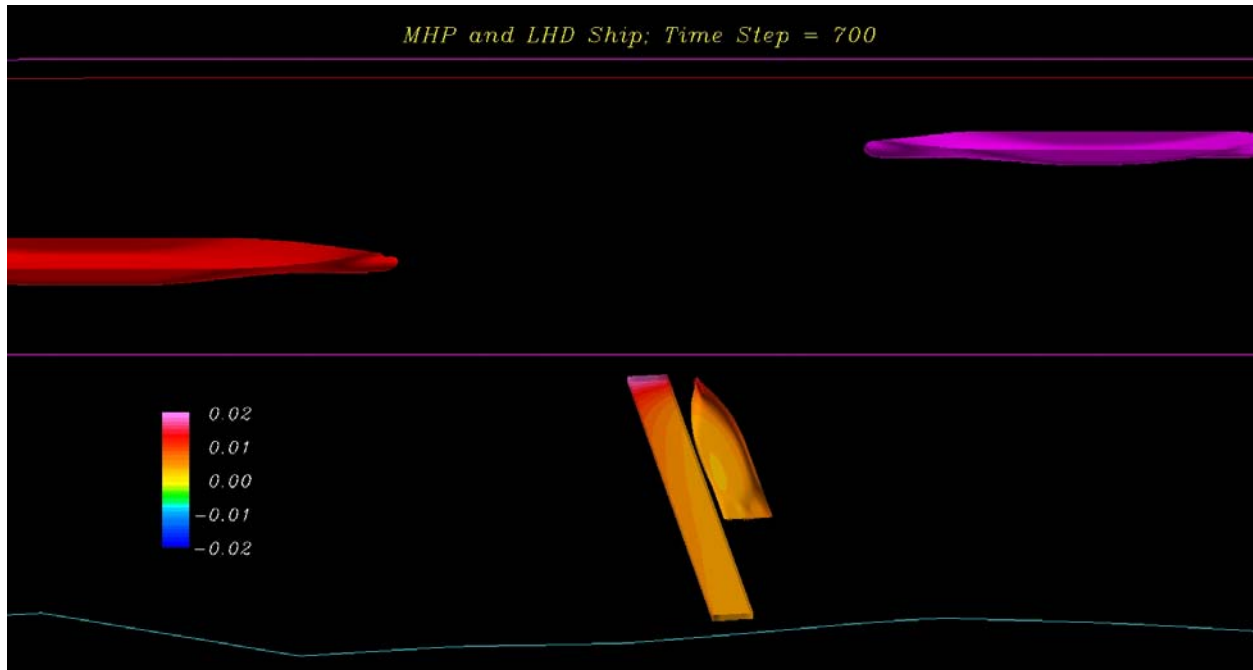
(d) Free surface grid;  $t/T = 5.6$

Figure 10. Continued

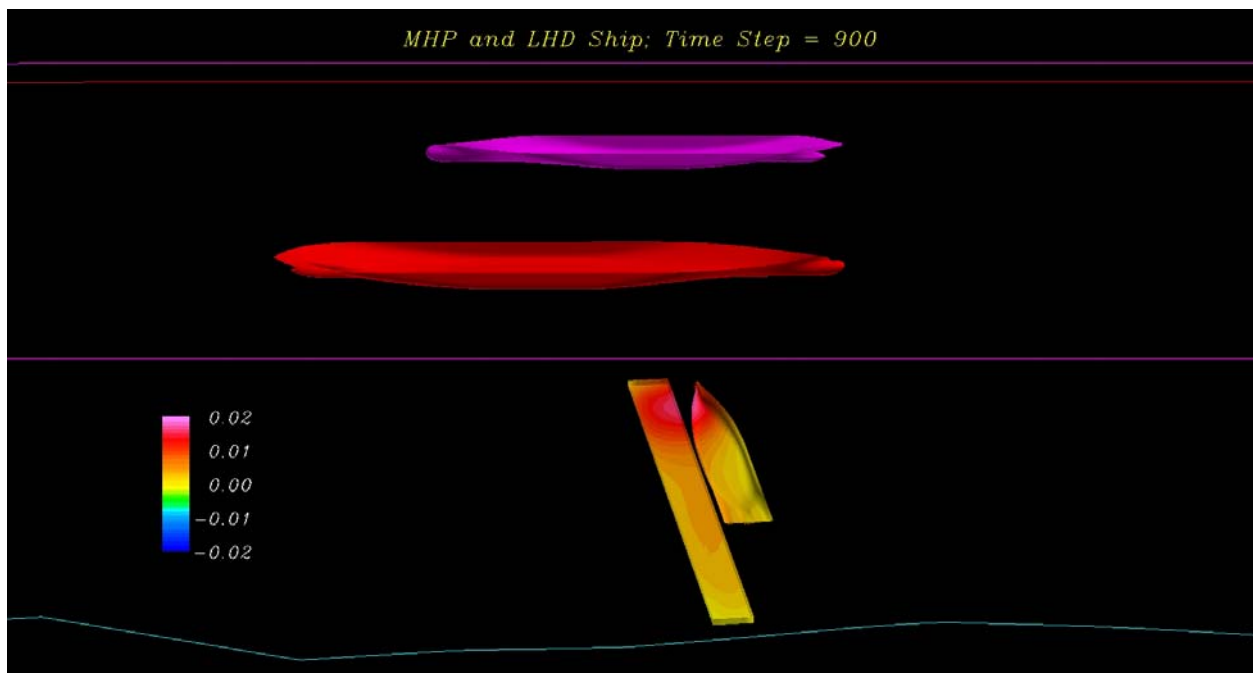


(a)  $t/T = 2.5$

Figure 11. Surface pressure contours around modular hybrid pier and moored ship.

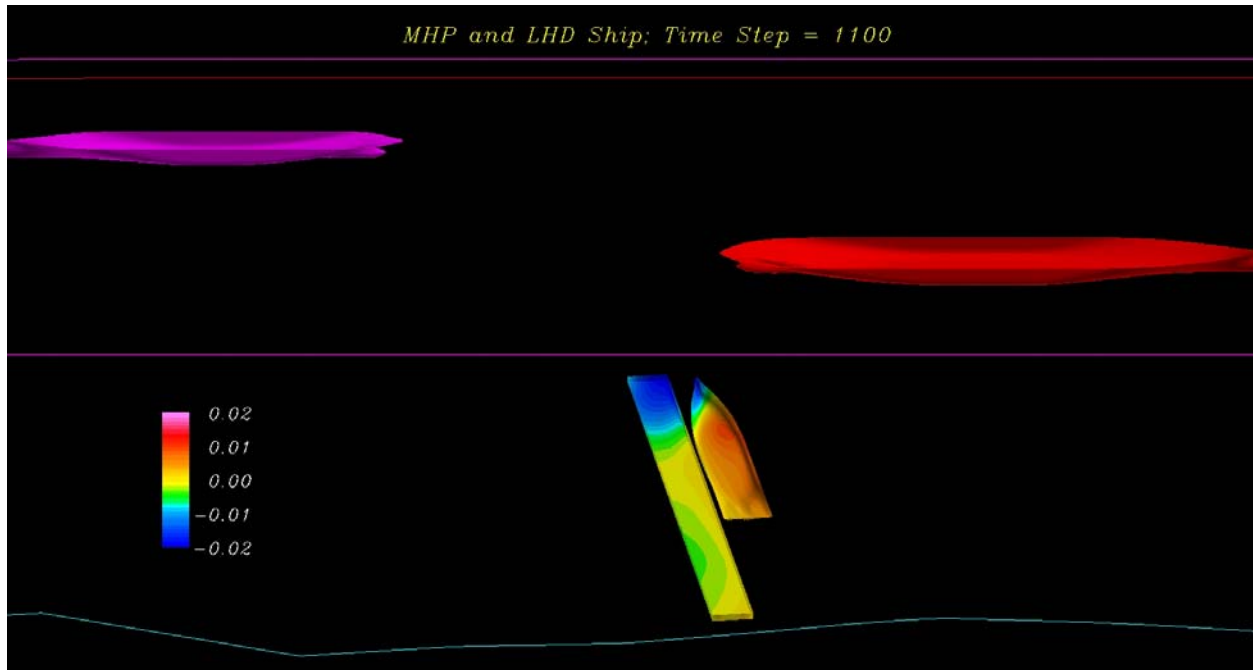


(b)  $t/T = 3.5$



(c)  $t/T = 4.5$

**Figure 11. Continued**



(d)  $t/T = 5.5$   
Figure 11. Continued

## Validations

The performance of the present simulation model had been validated with a series of field and towing tank tests. This simulation model consistently reproduced field and laboratory measurements at great accuracy. Two important evidences acquired by NAVFAC ESC are recaptured here for references. One is a laboratory observation of wave-induced water particle velocity and vorticity fields around the corner of a partially submerged rectangular cylinder in regular wave trains as illustrated by Figure 12(a). Figure 12(b) compares the measured and simulated free surface elevations, velocity vectors, and phase-averaged vorticities at a selected instant. More details of this test were described in Appendix D and Chen et al. (2002). It is clearly seen that the computed free surface elevations are in close agreement with the corresponding measurements. Furthermore, the locations and sizes of the computed vortices were also accurately predicted. This feature is critical in the case that broadside currents prevail and significant flow separations present at sharp edges of the ship hull.

The other is a field measurement of berthing forces and flow patterns induced by a docking ship as shown in Figure 13(a). During the test a ship was docking against two instrumented fenders where the berthing forces were monitored. An array of eight current meters (see the top right insert of Figure 13(a)) was placed under the path of docking ship to record the ship induced currents throughout the process. More details of this test were described in Appendix D and Chen et al. (2000). The test results indicated that the present simulation model is very effective in capturing the flow field induced by broadside ship motions. It is also very reliable in the prediction of global force parameters as illustrated in Figure 13(b). This figure compares the predicted fender reactions to the corresponding measurements from the test. The results are exceptionally convincing.

Chen et al. (2003) further demonstrated the credibility of the present simulation model for the event of passing ships with a hydraulic model test conducted by Dand (1981). The latter conducted a series of tests to measure the coupling forces between two ships encountered in a straight channel in either overtaking or head-on scenarios. Figures 14 (a) to (c) compare the forces felt by the ship in green outline as shown in Figure 13(d) in the head-on encounter scenario. In general, the predicted force and moment coefficients are in good agreement with the model test data, although the numerical results present more oscillatory components. More discussions may be found in Chen et al. (2003).

Kriebel (2007) conducted a towing tank test to measure the loads on a moored ship resulting from a passing ship moving in perpendicular to the moored ship. The test configuration (Figure 15(d)) is similar to the site conditions at the NAVSTA Norfolk waterfront. The size and hull shape of model ships used in the test are also reasonably close to the vessel considered in the present simulations. However, the test was performed in constant water depths somewhat deeper than the present site conditions. These test observations provide a direct validation to the simulation results. Figures 15 (a) to (c) compare the time histories of surge and sway forces as well as the yaw moment experienced by the moored ship. In these figures, discrete symbols represent the test data and solid lines are simulation results. It can be seen that the present simulation model precisely captured the shapes and intensities of passing ship excitations. However, apparent phase differences are also noticed. The predicted forces occur roughly 1/2 ship length behind the test measurements. This disparity may be attributed to the hull shape differences between the passing ships and discrepancies in the model configurations. Nevertheless the results from both sources are in reasonable agreement.

Overall, this experimental evidence unanimously confirms the performance of the present simulation model over a wide range of applications. Its credibility for use with the present passing ship effect assessment at NAVSTA Norfolk waterfront is robustly validated.

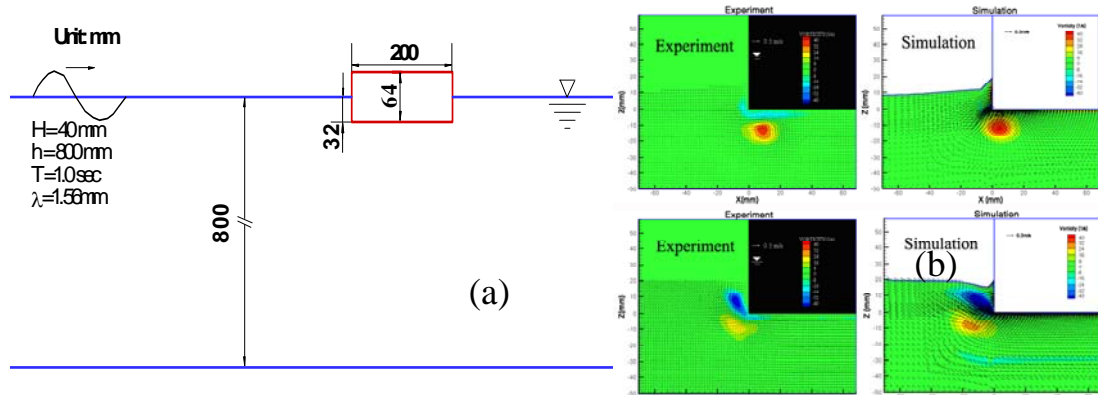


Figure 12. (a) Test setup and (b) velocity and vorticity fields.

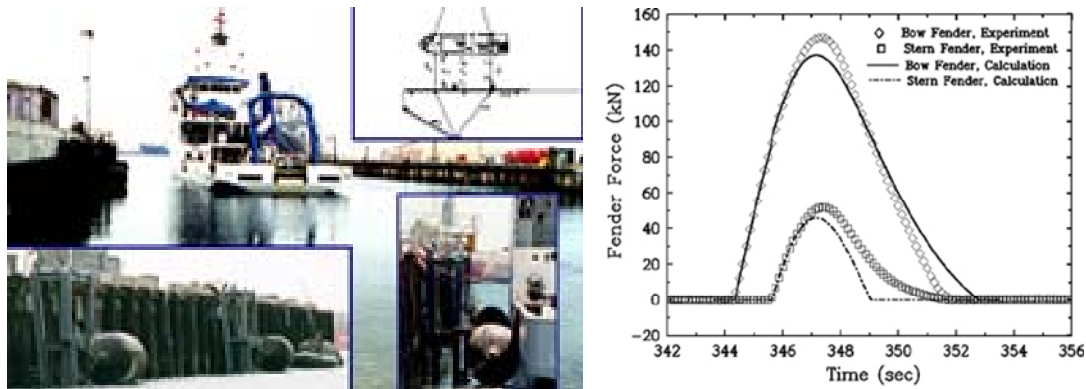


Figure 13. (a) Test setup and (b) fender loads.

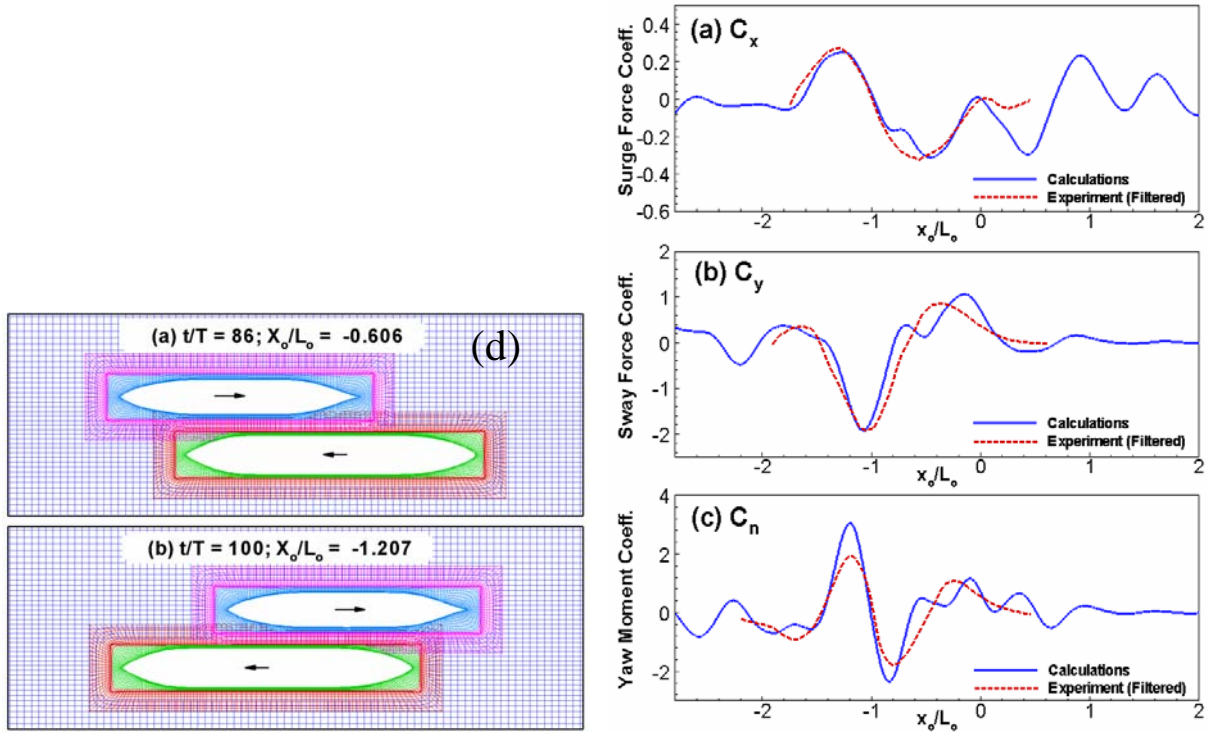


Figure 14. Ship-ship couplings

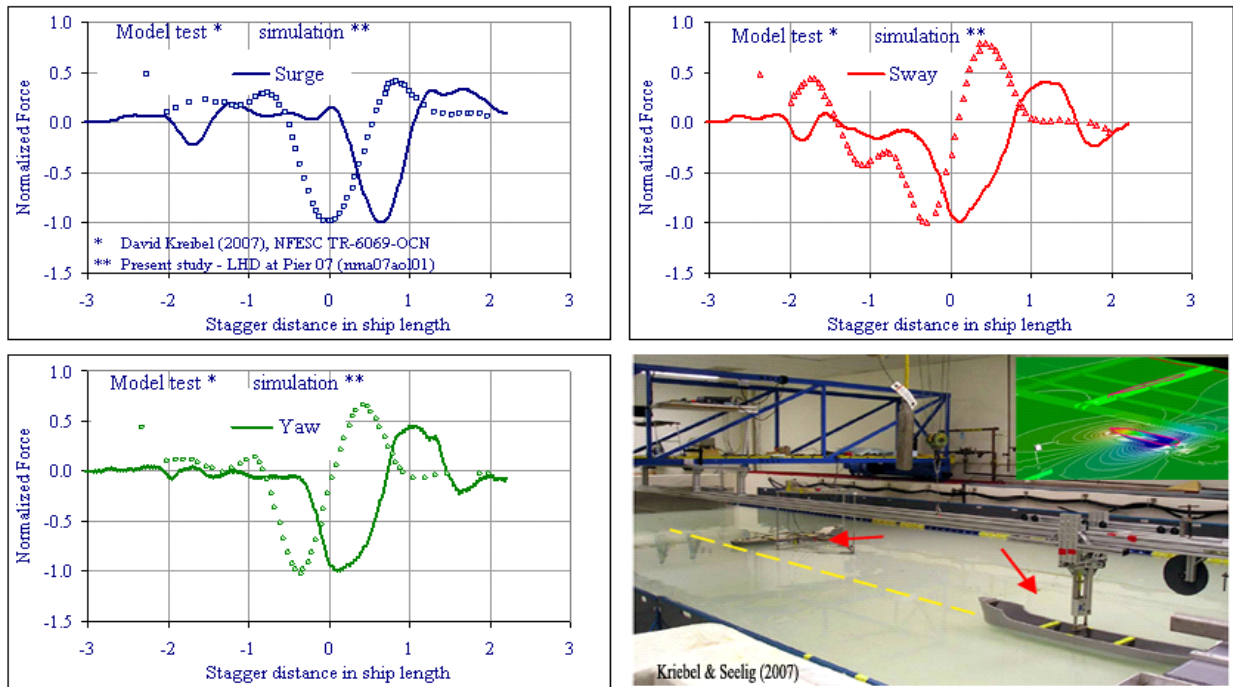
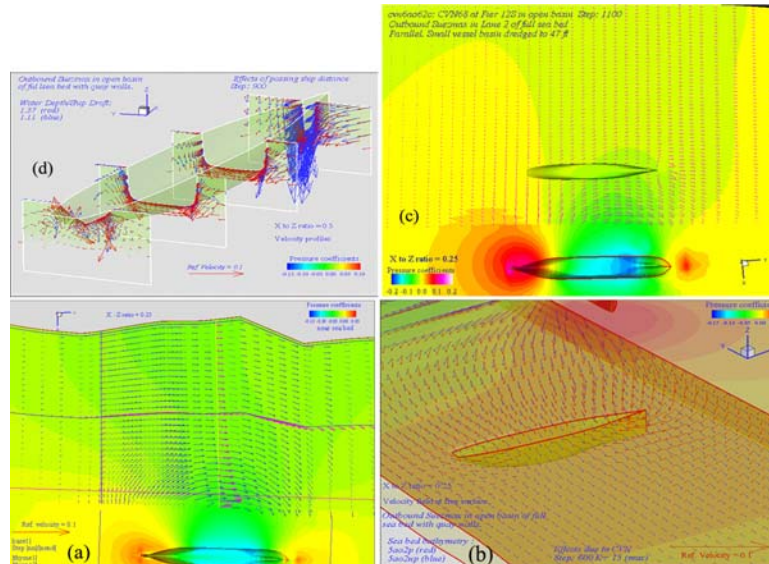


Figure 15. Towing tank measurements

## FEATURES OF PASSING SHIP EFFECTS IN REAL SITE ENVIRONMENT

### Basic

A passing ship generates an oval circulation around itself in laterally unbound water (Figure 16 (a)). This flow pattern essentially travels with the moving ship in a pseudo-steady state if the ship advances at constant speed along a straight course. Nevertheless, seabed, coastal features, and artificial facilities tend to mildly regulate the flow pattern. Moored ships at nearby pier facilities are perhaps the most obvious causes altering the flow pattern. A perpendicular hull cutting in the circulation path forces the ambient water to go around and severely changes both intensity and heading of the water velocities. The altered flow field is illustrated by the red arrows in Figure 16(b), while the blue arrows in harmony represent the flow field in the absence of the ship hull. The extent of interruption depends much on the amount of under keel clearance. In the case of an extremely small under keel clearance, the surrounding water may have to circulate around the far end of the ship hull (Figure 16 (d)). This mechanism will be revisited later. A moored ship in parallel to the passing ship obviously disturbs the circulation pattern much less (Figure 7 (c)) than would a perpendicular moored ship. Yet, its influence of flattening the pattern on both sides of its own hull is still noticeable.



**Figure 16. Flow patterns induced by the passing ship.**

Passing ship induced pressure pulses can be intense near the ship hull, but decays rapidly as they move away from the ship hull. In open waters, these pressure pulses are anticipated to decay at a rate proportional to the distance squared. Nevertheless, the simulation domain under consideration is essentially a thin layer of water, which allows much less room for the pressure pulses to decay in the vertical direction. As a result, the passing ship effects are expected to be more pronounced at confined shallow water like the present waterfront. Figure 17 presents the lateral profiles of the pressure pulses at a specific instant extracted along four key cross sections shown in the inserts of this figure. The top chart shows the pressure profiles at the water surface, while the bottom chart shows the same at the seabed. The curves in cold colors represent the positive pressures (above hydrostatic pressures) ahead of the bow and behind the stern, where as

the curves in warm colors represent the negative pressures in the transverse directions. These curves refer to different scales of matching colors. Note that the values of pressure pulses are normalized by the maximum pressure of each respective profile. The results indicate their decaying rate with respect to spatial distances on a consistent basis. Several obvious features can be observed from these charts.

1. The positive pressures decay much faster than the negative pressures.
2. Both positive pressures decay to nearly the ambient pressure in one ship length, however, reinforced noticeably near the open boundary of the simulation domain. This is perhaps due to reflections by the open boundary due to numerical approximation of the boundary. The effect is more pronounced at the stern than at the bow because the passing ship is closer to the south boundary at this moment.
3. Positive pressures at the seabed directly under the stern is negligible but increase rapidly aft to the maximum and then decay at roughly the same rate as do the positive pressures at the free surface. Due to the constraint of this shallow seabed, the pressures never reach ambient pressure.
4. The negative pressures in the transverse directions decay linearly initially up to a distance of roughly 0.3 ship lengths and then decay at a substantially slower rate since. This clearly reflects the effect of boundary constraints by quay walls and the sheer west bank of the channel. The pressures on the waterfront side decay to a constant level of 20 percent and maintain nearly constant for the most part of the waterfront. However, the pressures on the open water side continue to decay to negligible because of the shallow opening above the seabed. The profiles at the free surface and seabed look almost identical.

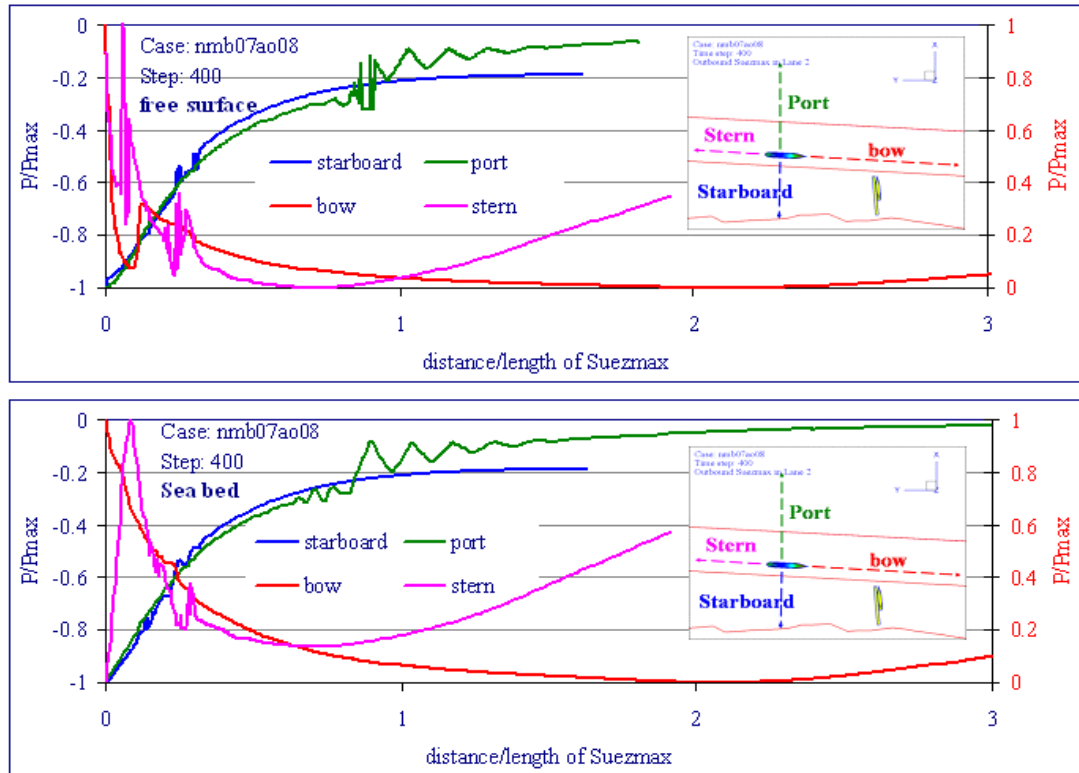


**Figure 17. Pressure profiles.**

### Prevailing Parameters

Huang and Chen (2008) conducted a series of numerical simulations to observe the nature of passing ship effects in the specific environment of the NAVSTA Norfolk waterfront. Prevailing parameters are identified and their influences are quantified. Full details of the simulation results were documented in Appendix C of their report. This section highlights the significant findings. In general the passing ship effects in the confined shallow water environment retain much of the nature observed in open water. The effects are primarily governed by the speed and location of the passing ship as well as the relative water depth with respect to ship drafts. However, the influence of site specifics is noticeable. Under certain conditions, the passing ship effects on a perpendicular moored ship are remarkably different than the observations with a parallel moored ship in open waters of constant depth.

**Ship speed.** Ship speed is perhaps the most efficient factor to escalate the passing ship effects. This effort confirms that exciting forces increase consistently in proportion to the square of speed over the range of 7 to 20 knots. The force histories induced by passing ships at various speeds are essentially identical after normalized by the square of the respective ship speeds.

**Seabed bathymetry.** Seabed bathymetry influences passing ship effects through the large scale geometry, such as the size, shape, and mean depth of ship slips and the seabed elevation of open water across the channel. Influences by minor depth irregularities are negligible. In general, passing ship effects increase in confined shallow water. Most influences can be correlated to seabed features within short distances of roughly two ship lengths from the moored ships.

Seabed features beyond this distance hardly impact the passing ship effects. For instance, the influence imposed by the elevated seabed in the open water near Craney Island is much more noticeable at Pier 7 than at Pier 12.

**Quay walls.** Quay walls of the NAVSTA Norfolk waterfront are at least two ship lengths<sup>1</sup> away from the ship channel and are more or less parallel to the oval shaped circulation flow induced by the passing ship (see Figure 16). They are unlikely to significantly interfere with the circulation, unless the moored ship or floating pier facility extends very close to the quay walls and guides the passing ship induced currents perpendicular to the walls. As a result, the presence of quay walls only slightly increases the passing ship induced excitations on moored ships very close to the wall.

**Water depth.** Water depth influences the passing ship effects in waterfront ambience in at least three ways. In general, the shallow depth of waterfront ambience confines angular spreading of the pressure pulses and thus carries the passing ship effect to a greater distance. As a result, the passing ship effects are expected to be more pronounced. Water depth further impacts the passing ship induced excitations on moored ships through the size of under keel clearance. Present consensus expects the excitations to diminish as the under keel clearance increases. This recognition is derived from the premise that a larger under keel clearance provides an easier path for broadside current to go under. However, previous simulation results of Huang and Chen (2008) observed a different trend in extremely shallow water. In this condition, water driven by a passing ship chooses to go around the far end of the moored ship or circulate vertically along the ship sides instead of squeezing transversely through the tiny clearance underneath. These unique flow patterns lead to a drastic reduction of excitation forces on the moored ship. A slight increase in the under keel clearance from this status tends to draw more current across the hull and thus push the hull harder. This trend continues until the under keel clearance is sufficiently large that the majority of the cross-hull current would not have to feel its way along the ship hull before cutting across the keel. Furthermore, the unique seabed configuration at the NAVSTA Norfolk waterfront introduces an additional consequence to the passing ship effects. Recall that the majority of the seabed of the waterfront is higher than the bottom of the navigation channel. A part of the passing ship is below the seabed of this waterfront (see Figure 6(b)). Consequently, only part of the passing ship induced pressure pulse is transmitted into the waterfront and thus a deeper ship slip, due to dredging or high tides, is more exposed to the influence of passing ship and thus allows a greater portion of the pressure pulse to engage the moored ships. Besides, it was observed in the extremely shallow water that ambient currents induced by a passing ship or circulate around the ship ends or circulate in vertical planes parallel to the ship length instead of squeezing across the keel under the ship hull. Much less water cuts across the ship hull to push the ship transversely. Therefore, the excitations on the moored ships in waterfront ambience are governed by the collective influences of the under keel clearance and the seabed elevation relative to the navigation channel.

**Separation distance.** The passing ship induced forces, in general, decrease rapidly as the ship lane shifts away from the pier. The results of Huang and Chen (2008) confirm this observation as shown by Figure 18. Dashed lines show the general trend of force variations with respect to the separation distance of the passing ship. Each line fits to the data set of the same color using a

---

<sup>1</sup> Distances are measured in the length of Suezmax in this study unless otherwise mentioned.

power equation,  $y=ax^b$ . Data presented are listed in Table 5. This figure summarizes the maxima of excitation forces observed by a CVN hull at Pier 12 (Site A in Figure 4) as well as the LHD and DDG at Pier 7 (Site B). This covers a range of ship length from 142 to 318 meters and ship draft from 8.2 to 11.6 meters (see Table 2). All simulations were conducted with an outbound Suezmax in identical site conditions. To facilitate comparison on the same basis, simulations for each moored ship include at least one case with the passing ship in the present outbound lane. This was designated as the baseline case for each moored ship. Forces observed in other cases are normalized by the corresponding component of the baseline case and presented in terms of percentage. A value above 100 indicates force increase and a value below 100 indicates force decrease. Tables 3 and 4 provide the locations of ship lanes and moored ships considered in the simulations. The overall trend clearly confirms the anticipated correlation between excitation forces and the separation distance. However, it is also noted that the excitations on CVN at Pier 12 uncharacteristically increase as the lateral distance increases from 0.3 to 0.4. The exact cause of this complexity is not clear. This is likely due to site specific effects associated with the hull shape and water depth, because the same trend is not seen in the cases with DDG and the LHD at Pier 7, where the under keel clearances are much larger than the case of CVN. It can be seen that passing ship effects vary only slightly as long as the passing ships remain within the range of the present outbound lane. The excitation forces will increase by 50 percent with the passing ship at the eastern boundary of the present outbound lane. However, the excitations increase drastically when the passing ships move closer to the waterfront. For instance, with the passing ship in the middle of the fairway ledge, the excitation forces will be quadrupled.

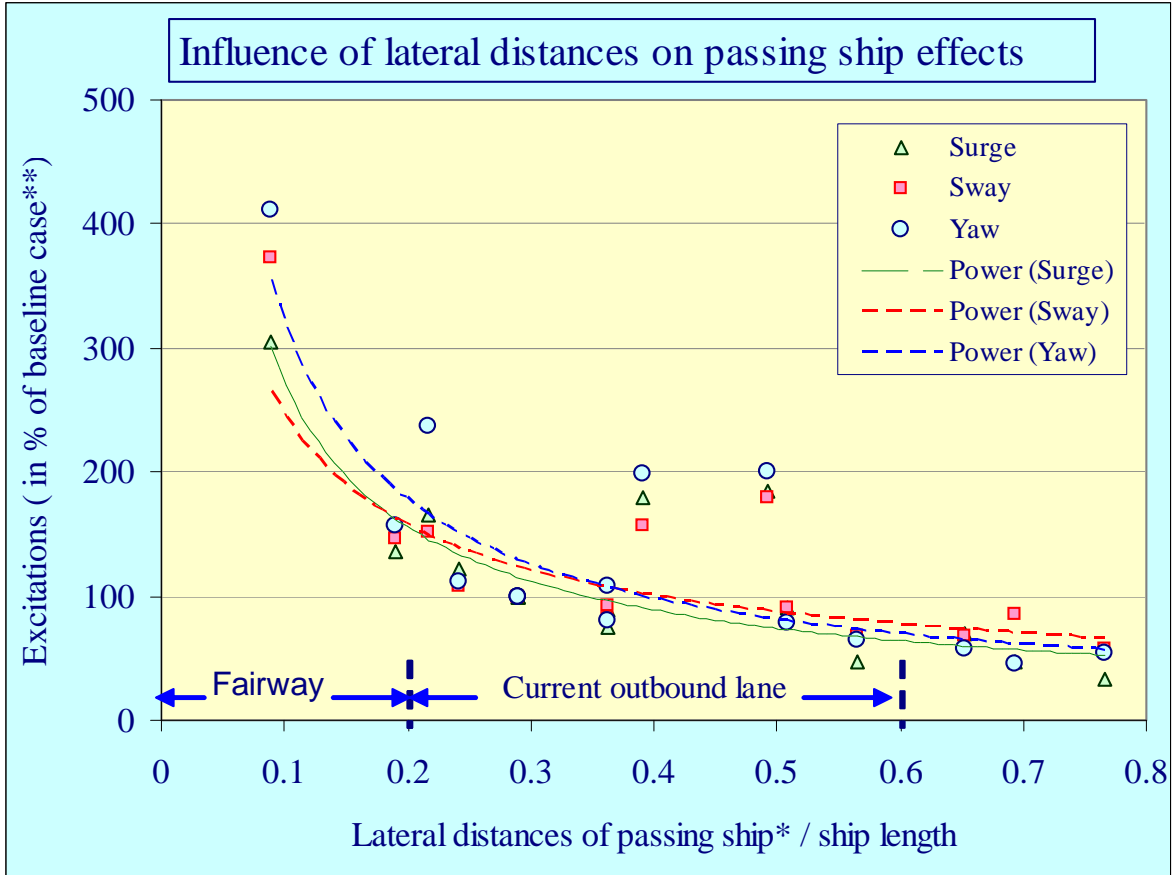


**Figure 18. Influence of separation distance on the passing ship effect.**

**Table 5. Summary of passing ship induced forces on moored ships (normalized).**

Case	Ship lane	Separation distance	Surge	Sway	Yaw
CVN at Pier 12	1	0.088710	304.13	373.19	411.56
CVN at Pier 12	5	0.189516	135.14	146.42	156.00
CVN at Pier 12	2	0.290323	100.00	100.00	100.00
CVN at Pier 12	6	0.391129	179.89	157.45	199.30
CVN at Pier 12	3	0.491935	183.94	179.81	200.47
CVN at Pier 12	4	0.693548	46.56	86.15	46.11
LHD at Pier 7	1	0.241935	122.19	108.46	110.74
LHD at Pier 7	2	0.290323	100.00	100.00	100.00
LHD at Pier 7	3	0.362903	75.26	81.89	80.60
LHD at Pier 7	4	0.564516	46.79	68.69	65.31
LHD at Pier 7	5	0.766129	32.49	56.94	53.52
DDG at Pier 7	1	0.217742	164.71	151.12	236.45
DDG at Pier 7	2	0.290323	100.00	100.00	100.00
DDG at Pier 7	3	0.362903	88.88	92.00	107.16
DDG at Pier 7	4	0.508065	89.81	91.24	79.02
DDG at Pier 7	5	0.653226	69.08	67.74	57.83

## RESULTS

### Structure Layouts

Figure 19 is a numerical representation of the structural layouts of the MHP with one client ship along side. MHP is modeled with a rectangular pontoon of 1,300 feet long and 80 feet wide with a mean draft of 14 feet. This floating pier is moored by four steel shafts (magenta) founded in underwater pile dolphins. These mooring shafts are treated as rigid members and do not deform subject of external forces in consideration. They interface with the MHP hull through a set of four buckling rubber fenders as illustrated in Figure 1. All relative movements between the MHP hull and mooring shafts are absorbed by these rubber fenders. These rubber fenders are represented by one-dimensional members with elastic property shown in Figure 20. One client ship (the LHD in this case) was secured to the MHP by four theoretical mooring lines (green) with two foam fenders (white) in-between. These mooring lines and fenders are treated as linear elastic members in the present study; even the simulation model in use is capable of addressing many aspects of relevant nonlinearities. The MHP hull is placed at the location of Pier 7 of NAVSTA Norfolk waterfront. This hull may be removed to inspect the client ship performance in the environment of traditional pile supported pier. The client ship may be relocated to any position along the pier. The MHP hull may also be replaced with another ship hull to explore the couplings between multiple client ships. In some cases, the LHD was replaced by a DDG to observe the impact of hull characteristics to the passing ship effects.

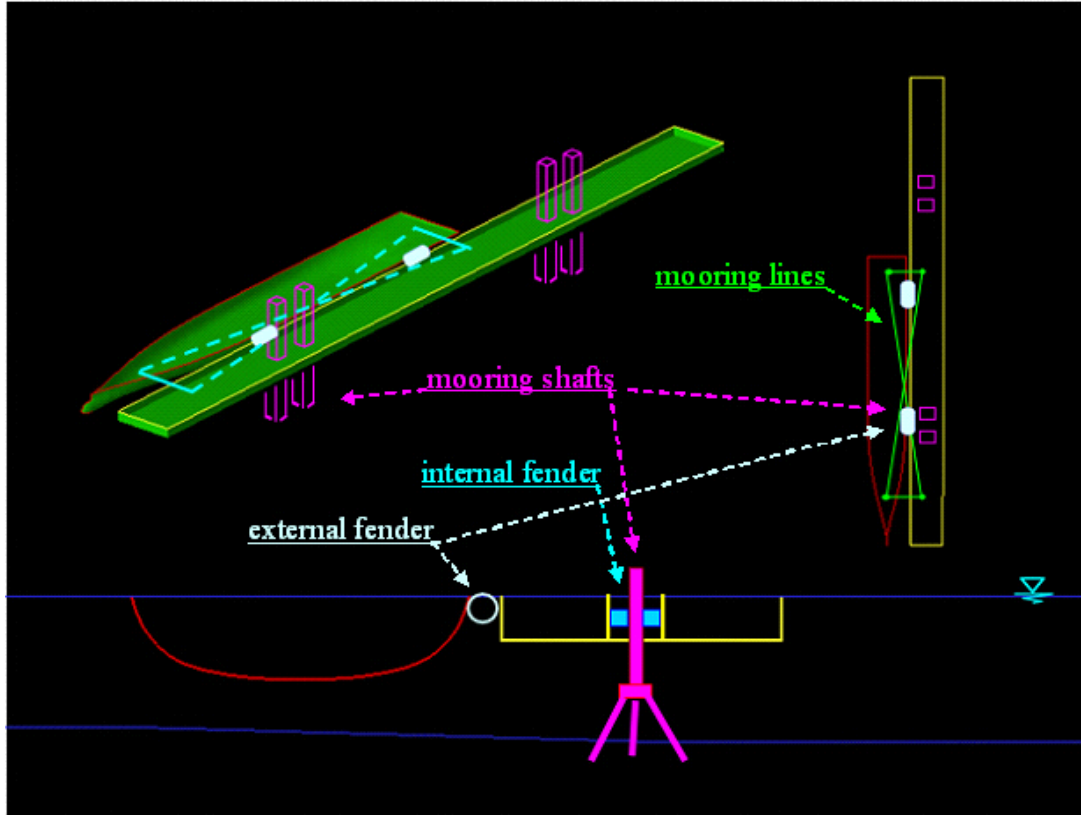
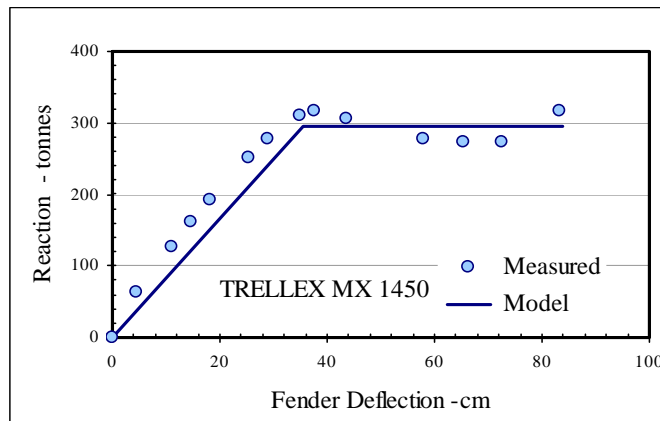


Figure 19. Structure layouts and nomenclatures.



**Figure 20. Load deflection curve of the internal fender.**

## Model Calibrations

A sequence of pilot studies was conducted to verify the effectiveness of the numerical grid system and calibrate the performance of floating hulls as well as coupling members. The former is achieved through an inspection of flow pattern generated by forced vibration and free decay test of the MHP and client ships. The latter is achieved by inspecting the dynamic responses in the air of the coupled structural system comprising of the MHP, client ship, mooring members, and fenders.

**Flow fields generated by forced vibrations.** Numerical grids describe the geometry of the simulation domain. The present simulation model utilizes a chimera domain decomposition technique to simplify the grid generation process, in which, the irregular simulation domain is divided into multiple blocks for the benefit of topography flexibility and resolution control. All coupled blocks must be properly connected to ensure the continuity of flow activities across the block boundaries. Surface waves and pressure pulses generated by a ship undergoing simple harmonic motions in open water are well documented. The influences of irregular seabed and coastline of the present waterfront environment to these flow patterns are traceable, at least qualitatively, by theories. These features may be used to test the quality of the numerical grid system. An effective grid system should capture sufficient details and maintain continuity of the induced flow, showing no sign of numerical decay or reflections. A sequence of test runs was performed with the MHP or the LHD undergoing simple harmonic oscillation in a selected translation mode, Figure 21 presents a snap shot of the pressure and velocity fields at a specific moment generated by the MHP in surge oscillation. There are four views in this figure with view (a) in the background and the rest overlaying on top. View (a) illustrates the pressure distribution at the seabed; view (b) correlates the pressure field with velocity field at the free surface; view (c) gives an overview of the pressure field, and view (d) shows a vertical profile of velocity field across the MHP hull. The primary goal is to inspect the continuity and overall quality of the flow fields and, in the mean time sway, observe the correlation between pressure velocity fields. Figures 22 and 23 are the corresponding results generated by the MHP motion in sway and yaw, respectively. In all cases, the pressure contours are smooth and continuous across the entire

simulation domain without noticeable kinks. The patterns of pressure and velocity fields are closely conforming to the theoretical anticipations.

Figure 24 illustrates the hydrodynamic coupling between the MHP and the LHD. In this case, the flow is generated by the MHP in sway motion while the LHD is held fixed. It can be seen, by comparing with Figure 22, that the LHD hull substantially shelters the pressure waves induced by the MHP from propagating to the port side of the LHD. Figure 25 is a reversed version with the LHD in sway motion and the MHP held fixed. Note that the MHP, of a shallower draft than the LHD, obviously provides less sheltering than does the LHD. The pressure waves of elongated ring shape induced by the LHD are clearly seen beyond the MHP. This case adds another source of disturbance introduced by an outbound Suezmax. In this scenario, the Suezmax accelerates from zero speed at its initial location to 14 knots and suddenly stops. This action produces a clear ring wave of pressure pulses (Figure 25(c)) as anticipated. The associated movie clip gives a complete view of the pressure wave evolvement.

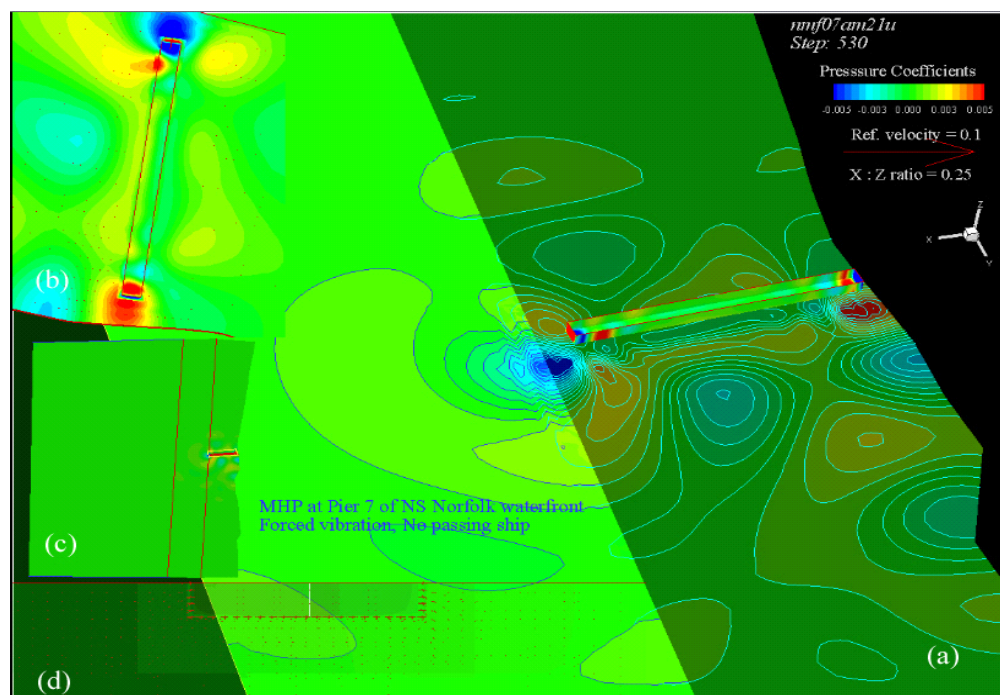


**Figure 21. The MHP undergoes forced vibration in surge.**

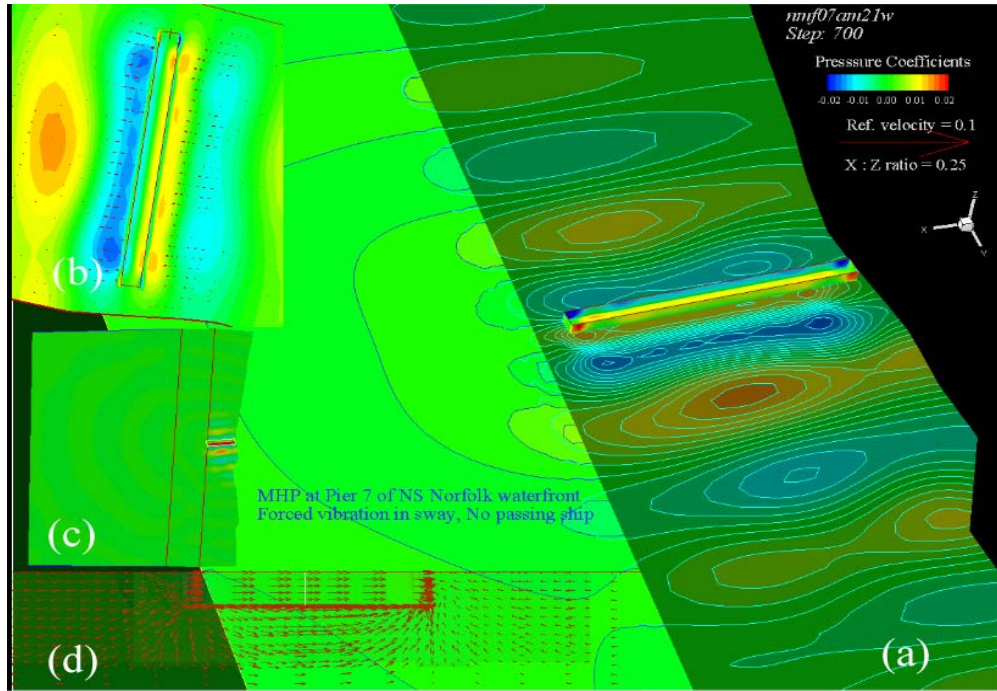


Figure 22. The MHP undergoes forced vibration in sway.

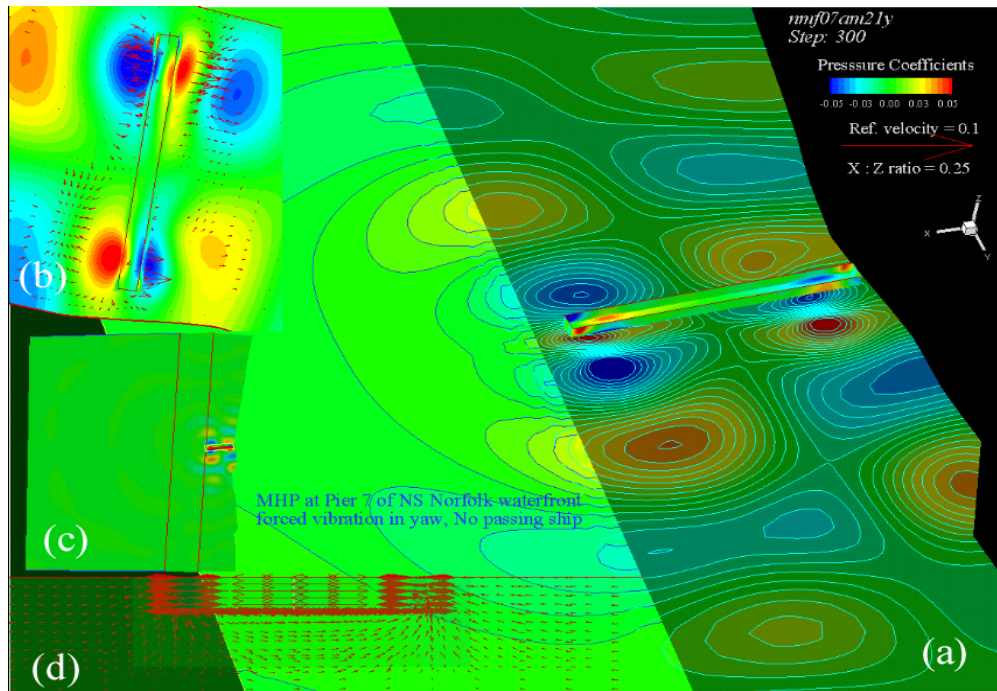


Figure 23. The MHP undergoes forced vibration in yaw.

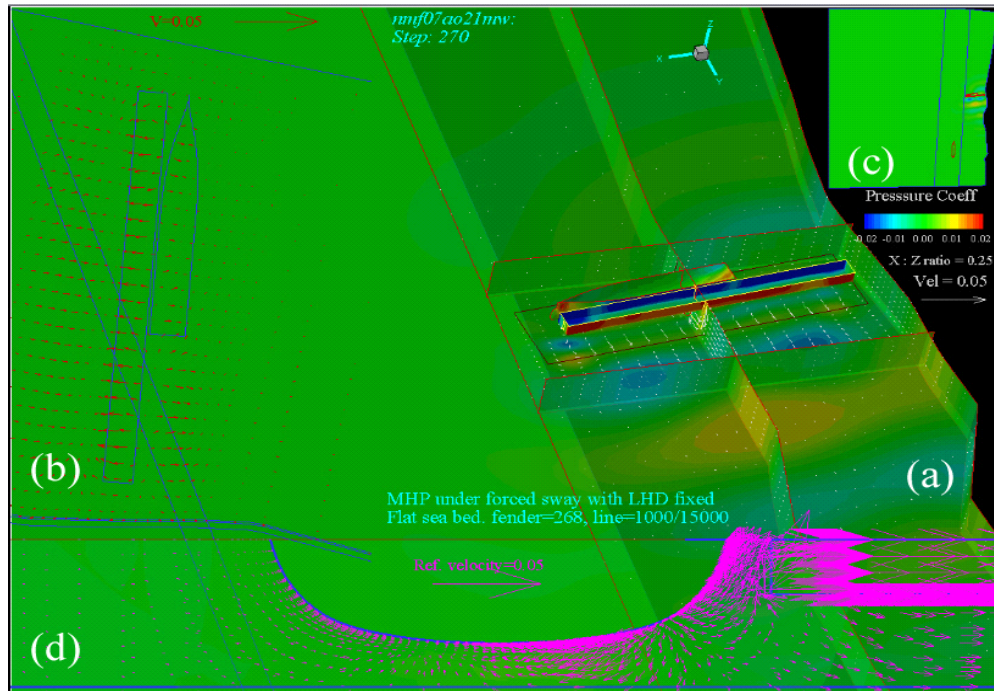


Figure 24. The MHP undergoes forced vibration in sway with LHD fixed.

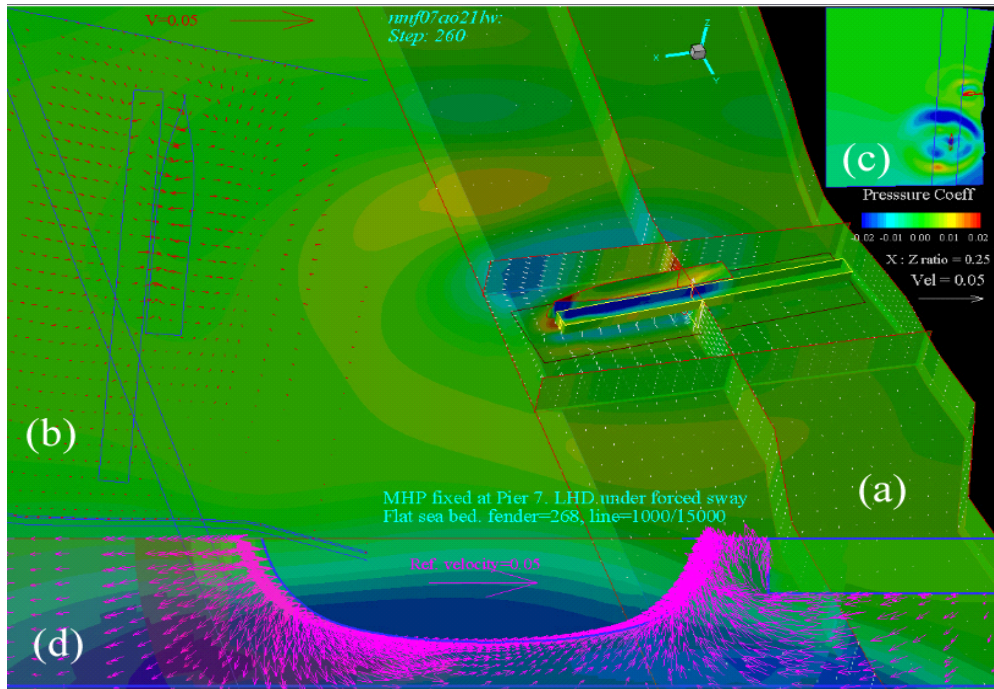
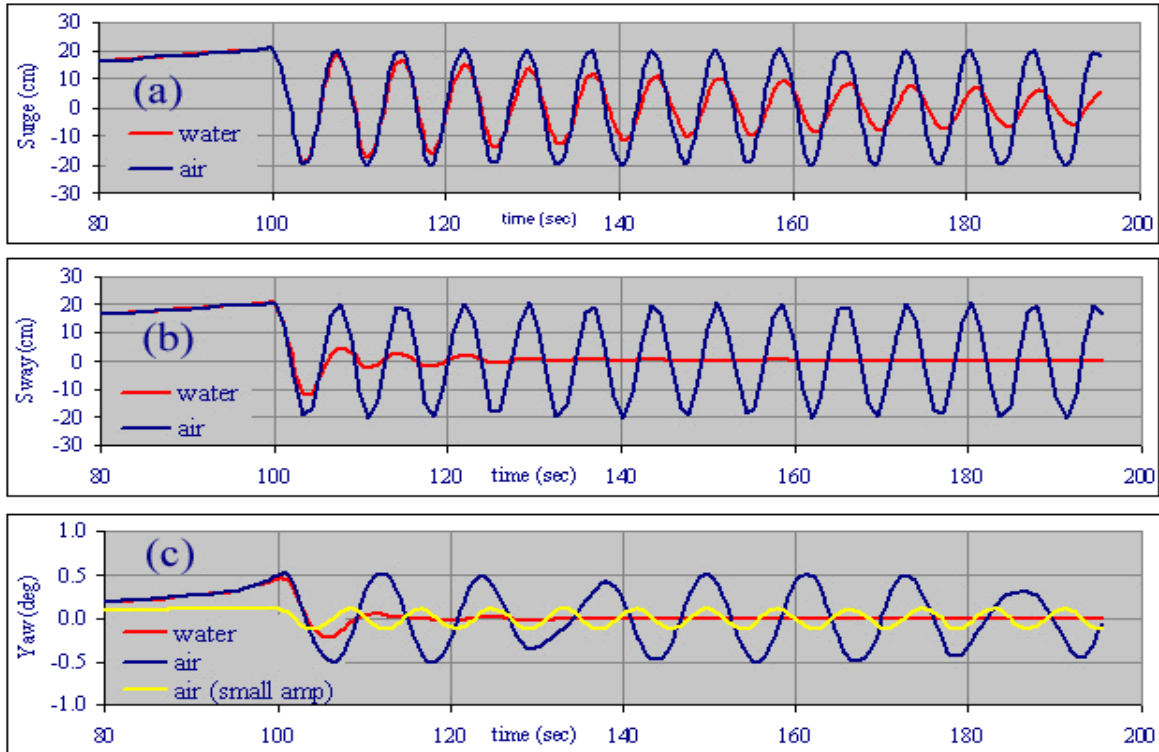


Figure 25. The LHD undergoes forced vibration in sway with MHP fixed.

**Free Decay.** Fluid damping is one of the dictating factors to the performance of surface piercing structures in the water. It is considered a fundamental hydrodynamic character of a floating structure. Its influence is particularly pronounced for floating structures of blunt hull shape in shallow water. The mechanism inducing fluid damping involves the process of flow separation behind sharp edges and fluid viscosity. Traditionally, these essential damping factors can only be experimentally determined through a free decay test, most often in the towing tank. This test observes the motion of the structure after being released from an initial offset in a specific principal direction without further disturbance. The resulting motion histories constitute a basis to determine the fluid damping and the nature frequency of the structure. This procedure can be reproduced with the present simulation code. The dynamic nature of the MHP alone at the NAVSTA Norfolk waterfront secured by four mooring shafts through single Trellex fender on each side was explored. Figure 26 summarizes the motion histories of the MHP (red curves) in response to an initial offset in surge, sway, and yaw, respectively. The blue curves represent the MHP performance in the air without the influence of fluid damping. Note that the surge motion decays much slower than do the sway and yaw motions. The surge and sway periods in the air are identical at the theoretical anticipation of 7.3 seconds because of the identical fender layouts in the longitudinal and transverse directions. The yaw period is however substantially longer than the theoretical value at 12.4 seconds. The nature periods in the water are only slightly longer in all modes. However, the profile of yaw excursion even without fluid damping (blue curve) are noticeably distorted. A closer inspection of the internal fender reactions reveals that these fenders buckle and become softer during more than half of the oscillation cycle in this test. An additional test run was executed with one tenth of the previous initial yaw offset. The resulting yaw oscillation (yellow curve) resumes the simple harmonic nature with the anticipated resonance period of 8.4 seconds. This example clearly demonstrates the significance of coupling members to the dynamic performance of a floating structure.

Figure 27 further confirms the accuracy of these resonance periods. The MHP responses to a simple sinusoidal excitation near the resonance period (red) are substantially stronger than the same excitation at slightly different period (blue). Again, the large excitation excursion of the MHP near resonant period buckles the internal fenders and subsequently induces motion components of longer periods. The induced components combined with the active excitations to create a clear harmony effect as shown by the red curves. Note that this effect is highly exaggerated with the MHP in the air. In reality, the fluid damping will greatly mitigate the MHP responses. However, the idea is the same. Similar effects are anticipated with the mooring lines through coupling with client ships.



**Figure 26. Free decays of the MHP in (a) surge, (b) sway, and (c) yaw.**

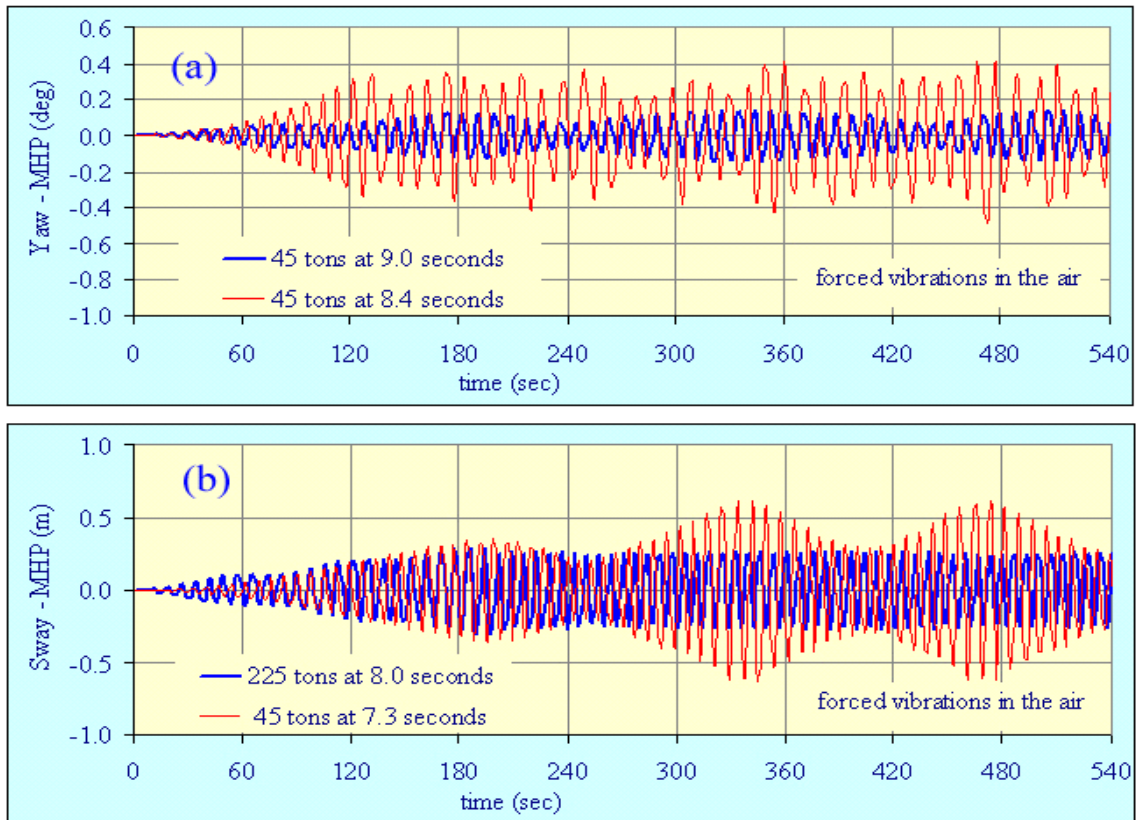


**Figure 27. Forced vibrations of the MHP near resonance periods**

**Structural Couplings.** The MHP couples with client ships through ambient water and coupling members such as mooring line and external fenders. The former is addressed by the flow solver and the latter are determined by relative motions between floating structures, which are handled by the motion tracer. The *consequence* of structure coupling depends on inertia properties of floating structures, dynamic character of coupling members, as well as the system layouts. A series of tests was conducted with the MHP/LHD assembly described by Figure 19 to inspect the model setup, including inertia properties of floating structures, connectivity and dynamic properties of coupling members, and vessel layout. The effectiveness of the model setup is measured by the system responses to a prescribed forced vibrations or initial offsets in a specific mode of a selected structure. All tests were conducted with the structure assembly in the air free from the influence of ambient water. (Explore the basic pattern of coupled motion for interpretation of the results in the full model.)

Figures 28 to 30 summarize the system responses induced by an initial displacement offset of the MHP in surge, sway, and yaw, respectively. Several obvious features were observed from these results.

- (a) The MHP and the LHD oscillate at respective frequencies that properly reflect the drastic differences in the elasticity properties of their respective coupling members. The internal (Trellex) fenders are much stiffer than the assembly of mooring lines and external foam fenders.
- (b) Asymmetric layouts of the foam fenders and of the mooring lines with respect to the center of gravity of the LHD induce cross coupling effects and geometry nonlinearity.
- (c) The motion responses of the LHD properly reflect the elastic property of mooring lines.

Figure 31 summarizes the vessel responses to a sinusoidal yaw moment at period of 8.4 seconds applied to the MHP. All displacements are assessed at the midship of respective vessel. This example illustrates the general feature of structural couplings between the MHP and its client ships. Note that the client ship, the LHD, is located at the offshore end of the MHP. Again, the yaw motion of the MHP presents the beat effect due to buckling of the internal fenders. The yaw excursion (cyan) oscillates within 0.2 degrees on each side, which produces a sway oscillation of about 12 inches at the midship of the LHD. This displacement in turn excites the LHD in substantial sway motion (yellow). The LHD undergoes a slow drift initially and then kicks in an irregular oscillation. This significant change in the LHD performance is a result of structural coupling between two vessels. Note that the orderly yaw vibration of the MHP about its midship subject to a pure yaw moment at the beginning, as reflected by its negligible sway displacement (green), is gradually modified by the influence of the LHD motion. The heavy mass of the LHD forces the MHP to sway more significantly at the offshore end. As a result, the sway displacement of the MHP increases significantly at its midship. At this moment the LHD kicks in the oscillatory mode. Furthermore, the surge motion of the LHD is also noticeable even the excitation imposed by the MHP is essentially in the transverse direction. This is caused by the asymmetric mooring line layout with respect to the center of gravity of the LHD.

This exercise confirms the model setup and structural connectivity. Results further indicate that the system responses are very sensitive to the features of coupling structures, including elastic properties, configurations, ship position, and histories of external excitations.

Linear coupling members do not imply linear responses. Asymmetry in any link of the structure layouts may trigger substantial nonlinear behaviors. The stiffness of mooring lines used in this exercise are arbitrarily selected to reflect their sensitivity to the motion excursions.

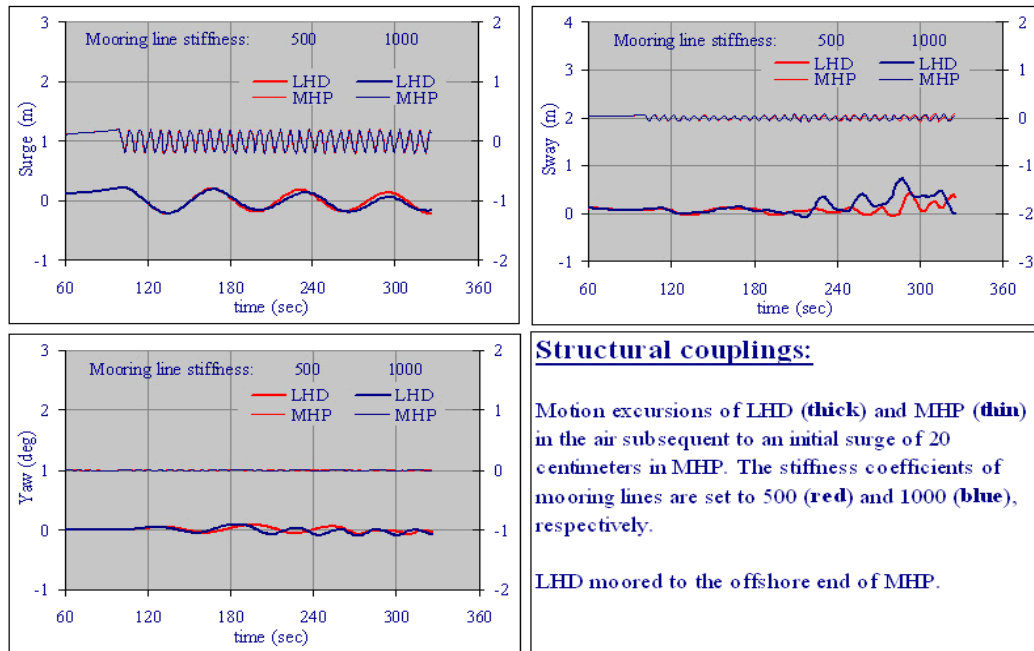


**Figure 28. Motion responses to an initial offset in surge of the MHP.**

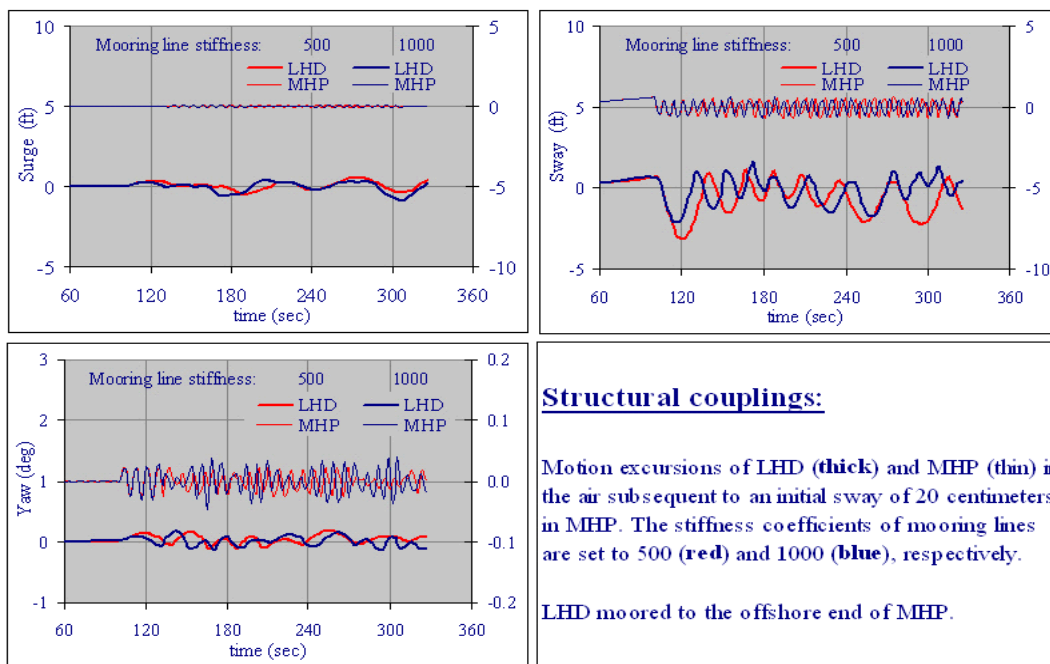


**Figure 29. Motion responses to an initial offset in sway of the MHP.**

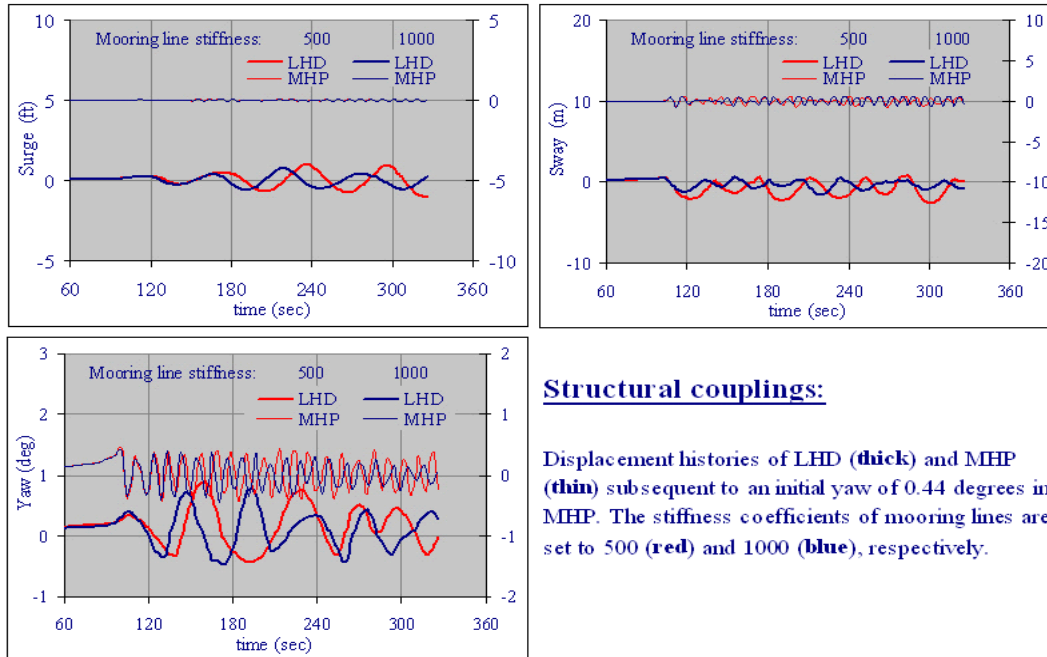


**Figure 30. Motion responses to an initial offset in yaw of the MHP.**

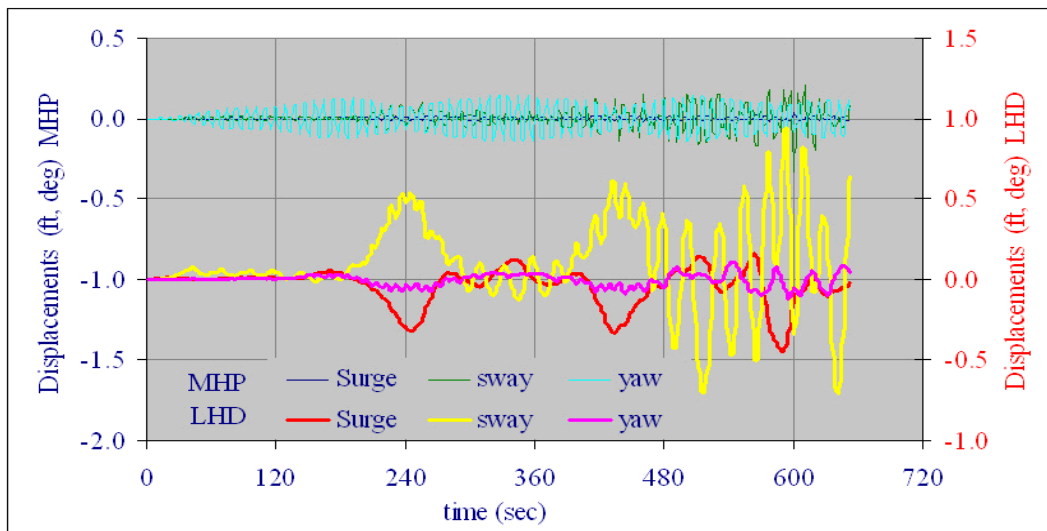


**Figure 31. The LHD-MHP couplings due to sinusoidal yaw excitations on the MHP**

## Outputs

The simulation encompassed a complete parametric study and generated a large database of passing ship induced flow fields of the entire water domain over the entire simulation duration. The complete database of more than 500 GB was permanently archived to an external hard drive. Data reduction was performed primarily to extract crucial results relevant to ultimate objective of testify the design capacity of the mooring shafts, observe the MHP performance, and identify disturbances due to the intrusion of the MHP hull to the ambient water and the client

ships. Due to the large number of cases involved and the transient nature of the flow activities, it is impractical to address the results of individual cases in this report. For the sake of brevity, only a selected case is presented to illustrate the format of reduced data and the nature of the flow fields and key parameters deduced thereof, such as fluid excitations, structural responses, and reaction forces on coupling members. Results from other cases are similar.

**Flow field.** The viscous flow solver generates a complete flow field description in terms of pressure (P), particle velocity (U, V, W), and other microscopic flow parameters such as vorticity. For the purpose of the present study, only the pressure and velocity fields were saved and archived in full details. Other features like surface wave patterns and excitation forces may be derived from this fundamental database. The resulting flow fields may be summarized in a concise format like Figure 32. This figure presents a snap shot of the flow field at a specific instant. In order to provide easy cross references among pressure and velocity fields and correlations of activities at different locations, multiple scenes at the same instant were stacked in layers. The scene in the background layer (a) focuses on the area near the moored ship. Colors illustrate the pressure field, while the white arrows represent the velocity field. It can be seen that the passing ship generates positive pressure at the bow and stern and a negative pressure along the shoulder. Even the pressure field decays rapidly in distance, the velocity intensity remain substantial across the entire width of the waterfront. The small insert (b) at the top right corner tracks the passing ship location and an overview of the pressure field over the entire simulation domain. A velocity profile may be shown at any location as required. It is also possible to place numerical transducers at any location to extract the time history of a certain parameter if required. The overlay (c) at the top left corner gives a bird's eye view of the flow field around the moored ship. Another overlay (d) at the bottom zooms in on the vertical profile across the moored ship and pier. The last two overlays are transparent and only velocity vectors are shown. Colors in these areas are pressure activities of the background layer. These two velocity profiles are chosen because they are often critical to the interpretation of the simulation results. Figure 33 is a close up of the passing ship induced currents across the ship and pier along the vertical profile near the middle of the waterfront extending roughly parallel to the quay wall as shown in Figure 32. These three pictures when spliced in sequence give a complete view of the lateral currents under the ship hulls. It is interesting to see the circulations in the wake of a sharp corner. The attached movie clips illustrate the evolution of this current while a passing ship goes by in either direction. In fact, the dynamic nature of this transient flow can only be captured in a movie clip. Examples are provided through the links in blue fonts in the figure title. Click the links to play.

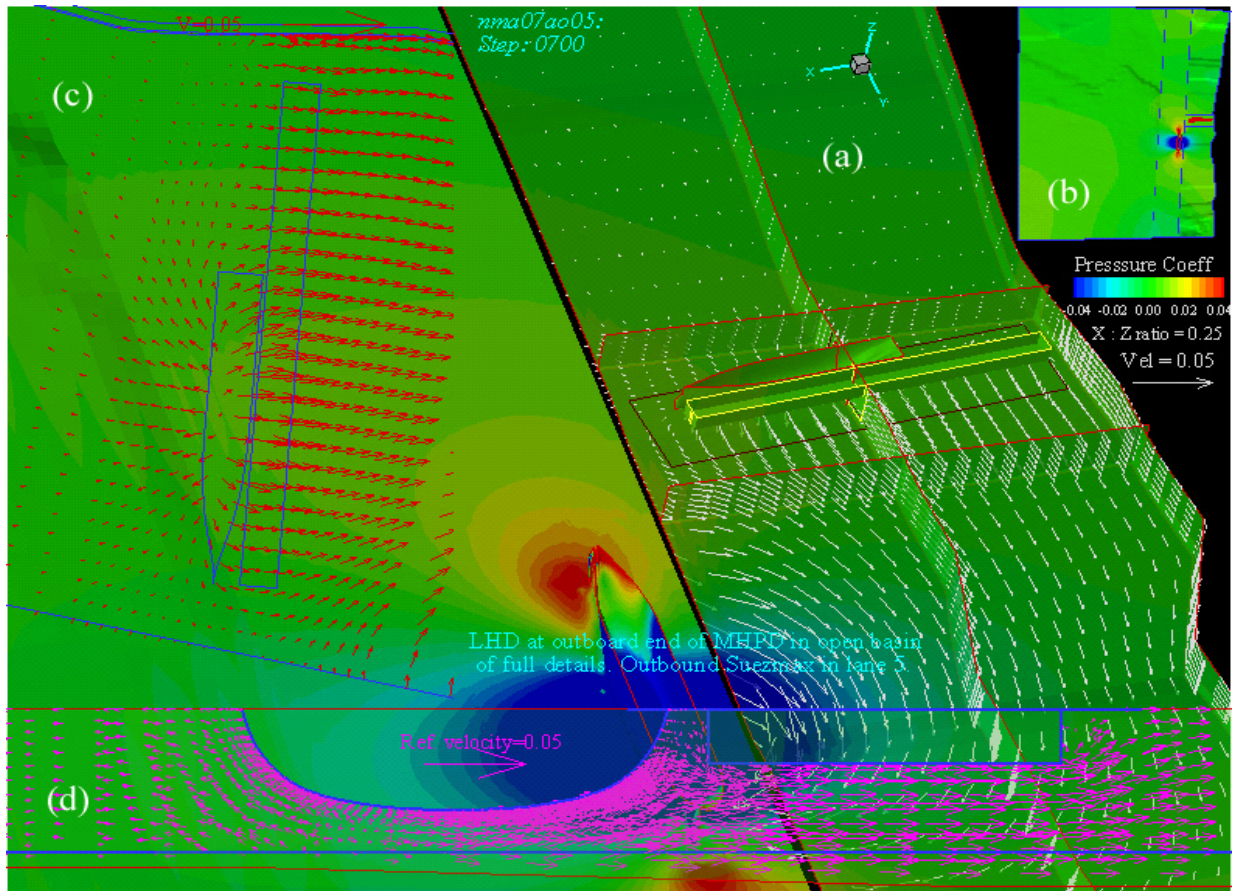
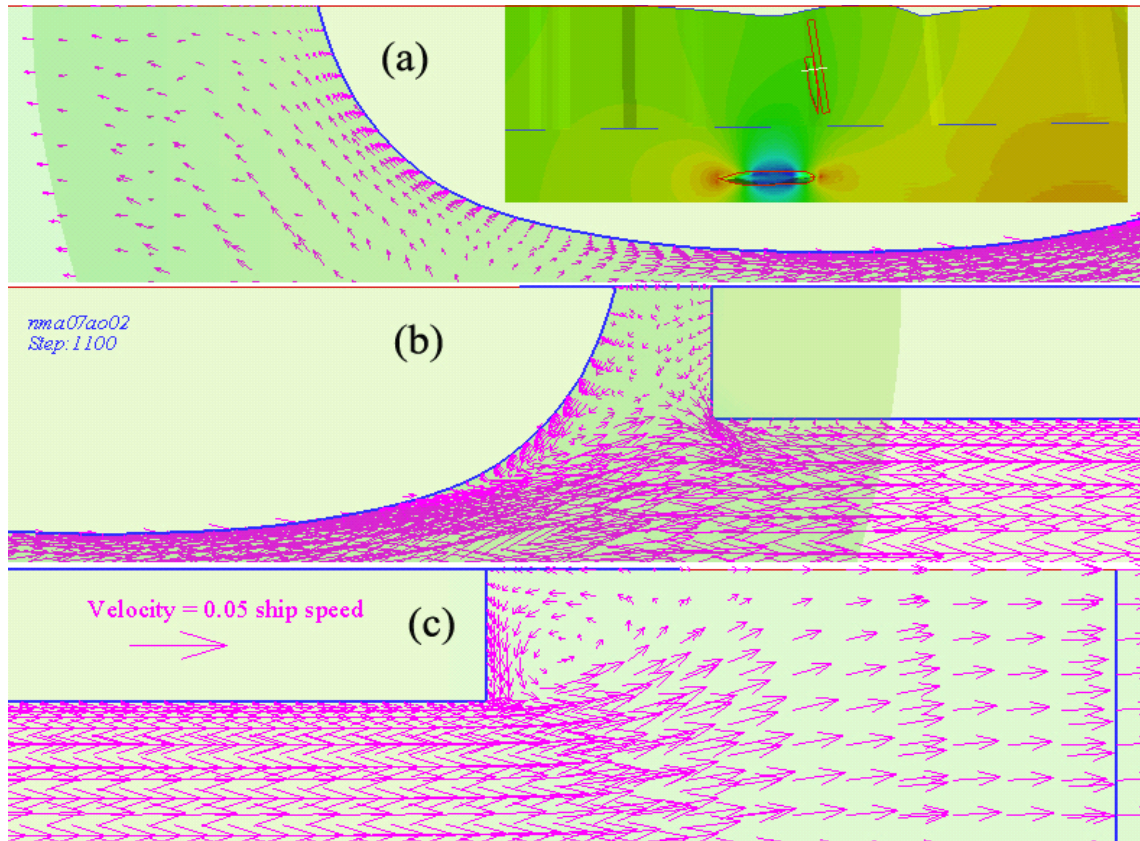


Figure 32. An example of passing ship induced flow fields.



**Figure 33. Currents under the ship hulls induced by outbound Suezmax**

**Excitation forces.** The passing ship effects were presented in terms of the excitations on the moored ship. Figure 34 is an example of the force history to show the nature of passing ship induced excitations at the NAVSTA Norfolk waterfront. Charts (a) and (b) illustrate sway forces on the LHD and the MHP induced by the outbound passing ship, with the ship in Lane 1 through Lane 5 specified in Figure 8. The locations of ship lanes measured from the bottom of the east border of the navigation channel are also provided for reference. The LHD is moored at the offshore end of the MHP as illustrated in Figure 32. In this set of simulations, both the MHP and the LHD were held fixed such that the sway forces shown represent the excitations induced by the outbound ship. No fluid reaction in response to passive motion is involved. The vertical axis indicates sway forces in Kilonewtons (KN) while the horizontal axis represents the stagger distance between the passing and moored ships as defined in Figure 9, normalized by the length of the outbound ship. A negative stagger distance indicates the approaching stage and a positive distance the departing stage. All forces refer to a coordinate system (red arrows) as shown in Figure 9. A positive sway force pushes the moored ship toward its port side.

It can be seen that the pressure pulse begins to engage the moored ship when the passing ship is at two ship lengths away. This is compliant with the pressure profiles shown in Figure 17. However, the exciting forces do not increase noticeably as the pressure profile suggests until the bow of the passing ship reaches the MHP site when the stagger distance equals zero. Before that the forces oscillate about roughly zero within a tight range. This oscillation may be attributed partially to irregular seabed geometry, particularly the reflections by quay walls and a nearby shoal just downstream of the pier (See Figure 5). Despite the oscillation, the forces remain

essentially flat before the arrival of the passing ship. This implies that the pressure pulse is not the only responsible mechanism for the passing ship induced excitations. In fact, the force history is in phase with the location of the passing ship induced circulation flow as the ship passes by. This circulating flow broadsides the moored ships and thus heavily interacts with the ships. Note that the center of the circulation is located slightly aft of midship (see the insert of Figure 34(a)). Figure 34 indicates that the sway forces on the MHP and the LHD agree with the circulation flow in both direction and intensity. The forces increase rapidly as soon as the bow of passing ship arrives at the moored ships, reach maxima when the center of circulation passes by, and taper off there after. The residual currents continue to drag the moored ship in the same direction after the stern of passing the ship clears the MHP site (stagger distance turns positive). Then the positive pressures aft stern take over and push the moored ships in the opposite direction while the circulation diminishes. The forces observed prior to the arrival of a passing ship also conform to this hypothetical model. It is very likely that the flat force history is caused by cancellation between effects due to pressure gradient effect and drag by circulation flow.

The positive sway forces decrease rapidly as the ship lane moves away from the waterfront in compliance to the theoretical anticipation. However, the negative forces present a less consistent trend instead. The limited information available at the present time suggests that this irregularity may be related to the size of under keel clearance of the moored ships. Figure 35 compares the shape of sway force on three distinct hulls of CVN, the LHD, and the MHP. Their under keel clearances normalized by their respective drafts are 0.25, 0.75, and 2.3, respectively. The force histories shown had been normalized by the maximum value of each individual case to highlight their shape. This set of data indicates that vessels of larger under keel clearances tend to experience more significant negative forces. This trend suggests a legitimate assumption that the broadside current across the ship with larger under keel clearance responds more rapidly. As such, the effect of residual current is less likely to cancel the effect of the positive pressure trailing the passing ship. The same assumption is applicable to the force history prior to the arrival of a passing ship. The CVN hull observes a significant negative force (blue line) at stagger distance near -1.3, while the MHP and the LHD observe positive forces (red and magenta). It is possible that the barrier provided by the deep hull of the CVN force the circulation to draw water from the navigation channel rather than the lee side of the ship hull through the under keel clearance. As a result, the positive pressure ahead of the passing ship is the only factor to push the CVN hull in the negative direction.

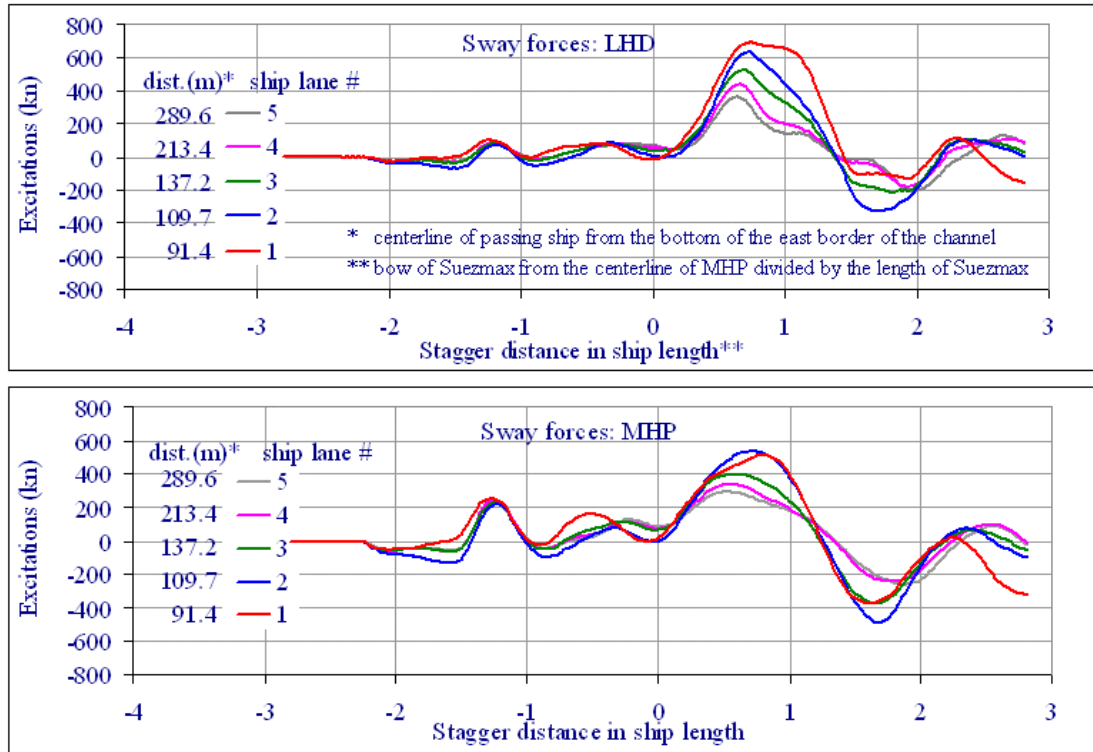


**Figure 34. Example of passing ship induced forces.**

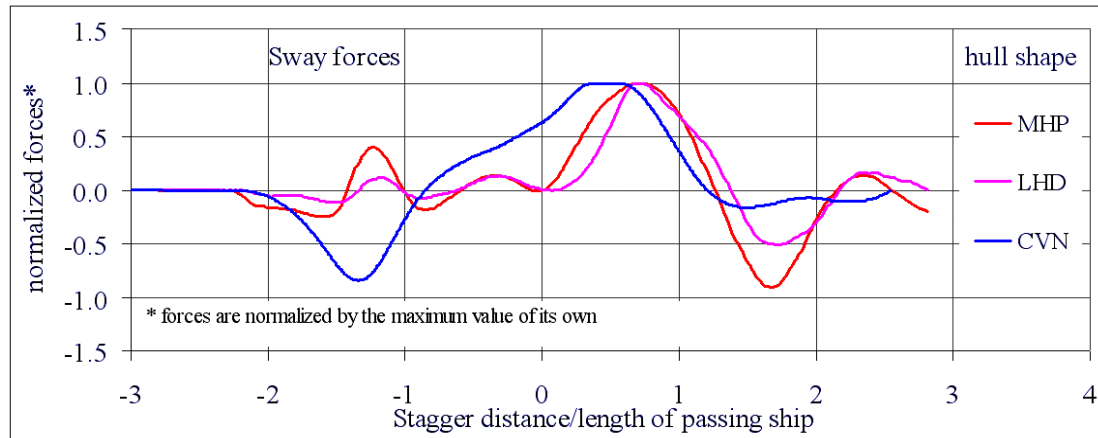


**Figure 35. Shape of force histories**

**Ship responses.** The responses of the MHP and client ships were assessed by a generalized motion tracer<sup>2</sup> at every time step throughout the entire simulation duration. Other motion kinematics may be derived from the histories of motion excursions. Figure 36 presents an example of motion responses of the MHP with a client ship, the LHD, in the scenario illustrated in Figure 19. The simulations were repeated in three different structural layouts with: (a) the LHD moored to the MHP, (b) the LHD moored to a pile supported pier, and (c) the MHP alone. In all cases, the LHD hull, if present, is located at the offshore end on the north side of the pier.

<sup>2</sup> See the section of theoretical consideration for a brief description of the motion tracer.

The setup of mooring lines and fenders remain identical for all cases. The results are summarized in the same chart for reference. The red lines and blue lines depict the responses of the LHD and the MHP, respectively. These curves refer to the vertical scales of the same color. The thin lines represent the results with the presence of one vessel alone (either the MHP or the LHD), while the thick lines represent the results with both the MHP and the LHD in the scene. The motion history basically follows the shape of excitation history. However, the LHD moves opposite directions with or without the presence of the MHP hull. Without the MHP present, the LHD was drawn southward (positive excursion) apparently by the circulation flow. With the MHP present, the LHD was pushed northward (negative excursion) most of the time except the moment the passing ship went by. It appeared like a positive pressure field was developed in the gap between their two hulls. On the other hand, the MHP moved to the same direction with or without the LHD. However, the MHP moves substantially more with the presence of the LHD, because the internal fenders have to take the hydrodynamic loads on both vessels. Figure 36 (b) and (c) are the corresponding velocity and acceleration histories. The MHP vibrates at high frequency intermittently in response to impact from the LHD.

**Reactions of coupling members.** Given the motion excursions of the vessels, the loads on coupling members can be determined according to their histories of distortion and the dynamic properties. Figure 37 summarizes the loads on internal (Trellex) fender, mooring lines, and external (foam) fenders. Again the thin lines represent the cases with one vessel alone and thick lines represent the cases with both vessels in scene. Charts (a) and (b) reflect the additional fluid forces transferred through the LHD if present. The LHD seems to contribute more than the MHP. Chart (e) reflects the fact that the LHD was moored at the piers with the bow out, subject to a higher passing ship influence and compressing the bow fender more severely.

Large ships like the LHD class are of comparable displacement to the MHP. Layouts of these client ships and coupling members heavily influence the dynamic performance of the MHP. While the ambient water drives the MHP and client ships in motion under the restraints of coupling members, the excursions of the MHP and client ships in turn influence the ambient water activities and decide the coupling forces. As such, the pier, client ships, ambient water, and coupling members are tied into an indivisible system. Their dynamic performance must be evaluated as a coupled system. Eventually, all fluid forces imposed on the MHP and client ships plus the amplification effects introduced by the elastic coupling members are to be withstood by mooring shafts. A proper assessment of the resulting forces and their allotment to the mooring shafts requires accurate knowledge of the instant phase relations among various modes of vessel excursions. There are several crucial factors which may substantially change the phase relations among the component vessels. Of the most significance to the numerical simulation is the viscous water flow associated with transverse ship motion. Uncertainties introduced by the numerical approximation of the water flow may be radically amplified by the nonlinear nature of coupling members. This process can be illustrated by Figure 38(a) for example. This figure summarizes the fluid forces experienced by a client ship under different levels of mooring constraint. The top chart compares the net fluid forces imposed on the moored ship, including exciting and radiation components. The red line illustrates the results of a tight mooring while the blue curve illustrates the results of a slack mooring. Other conditions, including the passing ship layout and seabed bathymetry, are identical for both. The white line in the same chart represents the exciting forces induced by a passing ship. It is obvious that the influence of mooring conditions is remarkable. The force on the tightly moored ship (red) essentially follows

the passing ship excitation closely. The reactive radiation forces are relatively small as the moored ship moves only slightly. The force history associated to the slack mooring (blue), on the other hand, separates from the passing ship excitations as soon as the moored ship bounces off the fender. The total fluid forces stay near zero as the moored ship drifts within the range allowed by the slack in the mooring lines. The forces, however, increase sharply when the moored ship comes to a sudden stop at the end of the initial slack and the trailing currents previously established by the drifting ship start to catch up and push against the moored ship. Mooring lines must be prepared to absorb this additional energy. The difference between the total forces on the moored ship (red and blue) and the passing ship excitation (white) represent roughly the radiation forces. The results were summarized in the bottom chart of Figure 38(b). It is seen that the reactive forces can be of the same magnitude as the driving force induced by the passing ship. More importantly, this reactive force is closely correlated to the square of the speed of the moored ship (Figure 39 (a)) and is essentially irrelevant to the acceleration of the moored ship (Figure 39 (b)). In other words, these reactive forces are dominated by form drags resulting from the flow separations (see Figure 9) around the sharp edges of the ship hulls. A proper assessment of this force component requires precise information of the flow field at the instant and fluid viscosity. A potential theory based simulation model is unlikely to capture this reactive force. Without this term, the simulation model tends to over predict the dynamic responses of a moored ship and its couplings with the pier.

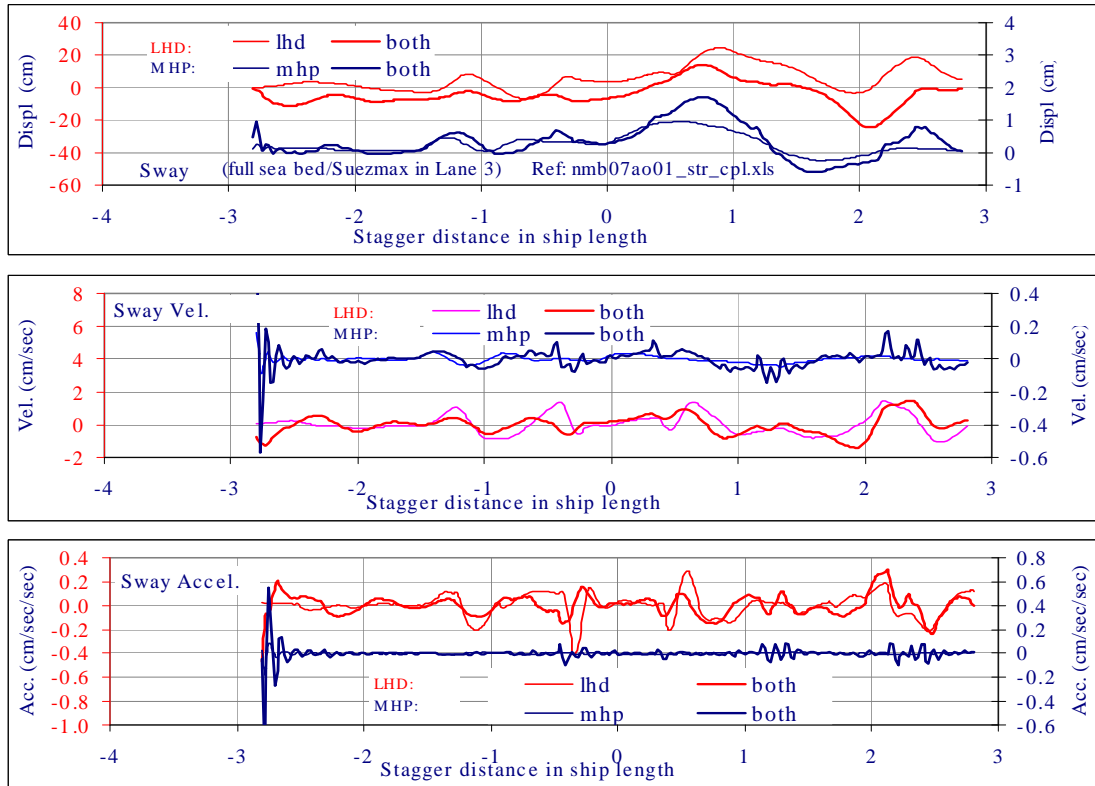


**Figure 36. Example of ship motions**

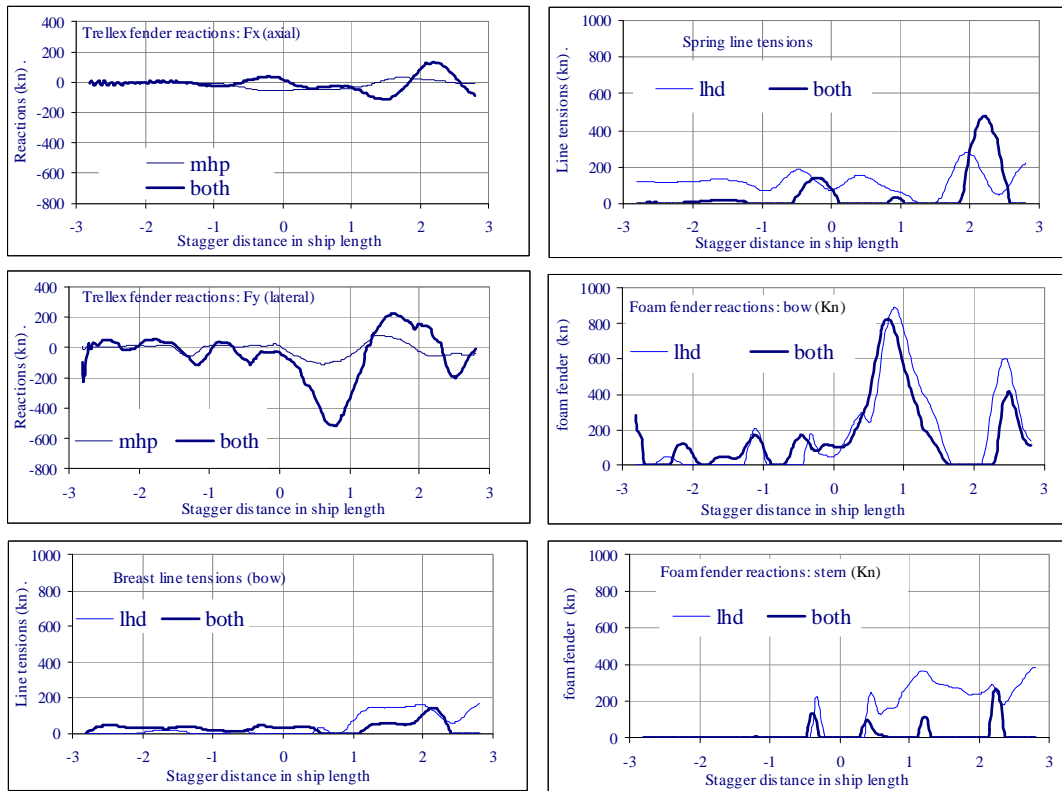


**Figure 37. Example of fender and mooring line reactions**

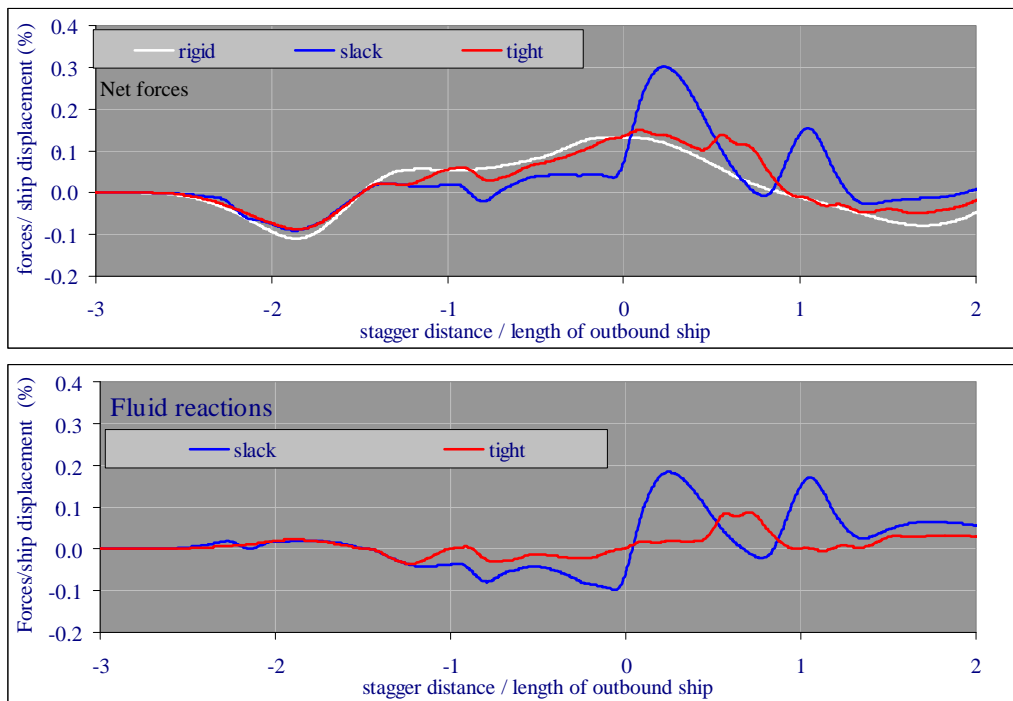


**Figure 38. Influences of mooring lines**

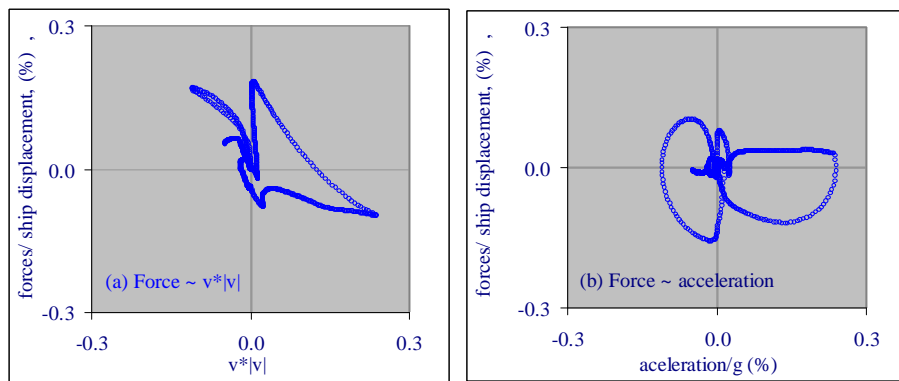


**Figure 39. Fluid reaction forces versus ship motion.**

## PASSING SHIP EFFECTS ON THE MHP SYSTEM

The MHP differs from the pile supported piers in its buoyancy hull. The Navy waterfront community expressed considerable concerns on the impact of this additional hull and its motion to the culture of pier operations. This effort conducts a series of numerical simulations to gauge the MHP intervention to: (a) the ambient water activities, (b) the hydrodynamic forces on the MHP and client ships, and (c) dynamic responses of the MHP and client ships. To provide a fair baseline, all test cases were repeated by substituting the MHP with an equivalent pile supported pier in the same site conditions and ship layouts.

### Hydrodynamic Interference Introduced by the MHP Hull

Figure 40 compares velocity profiles at the free surface of the flow fields around the MHP and an equivalent pile supported pier. Both cases assume identical ship layouts with an LHD hull moored to the offshore end of the pier (Figure 40(a)) in identical site conditions as illustrated by Figures 40(b) and 40(c). Figures 40(d) and 40(e) present a snap shot of the respective velocity profiles at the same moment, which are overlapped in Figure 40(f) for comparison. Note that the pile supported pier is not shown in Figure 40(e) because its deck is entirely above the water. The velocity profile with the presence of the MHP is shown in magenta vectors, while the profile with the equivalent pile support pier is shown in cyan vectors. Figure 41 presents the flow pattern near the sea floor in the same format.

It can be seen that the velocity profiles at the free surface are essentially identical except the space occupied by the MHP and its immediate vicinity, while the profiles near the seabed hardly show any difference. Besides, the overall flow pattern is heavily dictated by the LHD hull. The presence of the MHP hull only slightly modifies the flow pattern diffracted by the LHD alone. This trend is reasonable as the draft of the LHD is twice as deep as that of the MHP (see Table 2) and the water at the pier site is substantially deeper than both hulls. Consequently, the broadside currents induced by the passing ship tends to conform to the major barrier of the LHD hull. Most significant differences occur under the MHP hull and in the narrow gap between two hulls.

The influence of the MHP is more visible in terms of fluid forces on ship hulls. Figures 42(a) and 42(b) summarize the histories of surge and sway forces on the LHD as the passing ship cruising by the pier site. Figures 42(c) and 42(d) give the same on the MHP hull. In these figures, the blue lines indicate the cases with the LHD moored to the MHP, while red lines indicate the cases with the presence of the LHD (moored to a pile supported pier) or the MHP (with no client ship) alone. All these cases were simulated in shallow water. The case with the LHD moored to the MHP was repeated in deep water to provide a reference of the water depth effect. The results are presented in yellow lines. This set of tests confirms that the presence of the MHP hull hardly changes the fluid forces on the client ship, the LHD. The client ship, on the other hand, more noticeably influences the forces on the MHP, but the differences remain negligible. In all cases, the blue lines in essence overlap the corresponding red lines. As a matter of fact, the disturbance introduced by the MHP hull is much less than the influence of water depth as indicated by the yellow lines.

Likewise, it is anticipated that the influence of other client ships will be more pronounced than the disturbance by the MHP per se. Figure 43 compares the flow field diffracted by a pair of the LHD hulls at an open pier (purple arrows) to that by the combination of the LHD and the

MHP (blue arrows). The associated ship layouts are shown in Figure 43(a). The difference of these velocity profiles is more noticeable than that between the MHP and open pier (Figure 41). In fact, the LHD hull on the weather (south) side substantially shelters to the ship on the leeward (north) side as indicated by the force histories in Figure 44. The LHD hull on the leeward side observes only 50 percent of the fluid excitations experienced by the LHD hull on the weather side (the blue and red lines in Figure 44(b)). The green line represents the force observed by one LHD hull at the same site alone. Note that the green line is more or less in the middle of the red and blue lines. This implies a significant pressure reduction in the gap confined by the two LHD hulls as a result of hydrodynamic couplings. The pressure reduction is likely associated to energy loss due to flow separation across the keels. A viscous flow solver is required to capture this critical mechanism. A similar test at the same site with DDG hulls indicates that the significance of sheltering effect decreases with the increase of the under keel clearance relative to ship draft (Figure 44(c)).

This test was reiterated in various ship configurations and water depths to exclude site specific influence. Results are summarized in Figures 45 and 46. Figure 45(b) confirms the decreasing trend of the excitation forces with the increase of separation distance between the passing and moored ships. Figure 45(c) reinforces the previous observation that the excitation forces tend to increase as the water depth at the pier site decreases when the under keel clearances are sufficiently large. Figure 46 unanimously concludes that the MHP hardly intervene the fluid action to the client ships. The client ship actually observes almost identical excitation forces induced by passing ships.

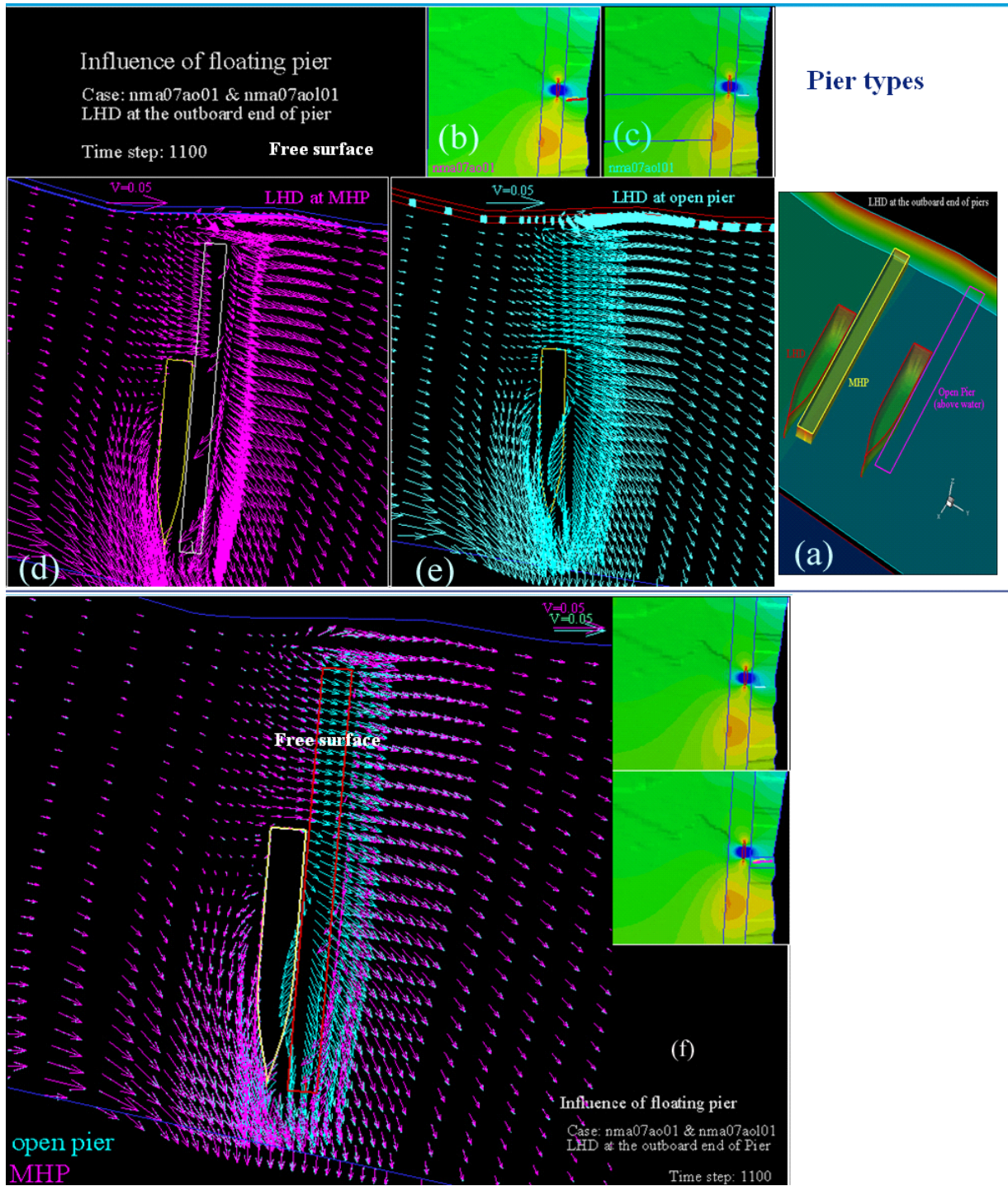


Figure 40. Comparison of flow fields at the free surface.

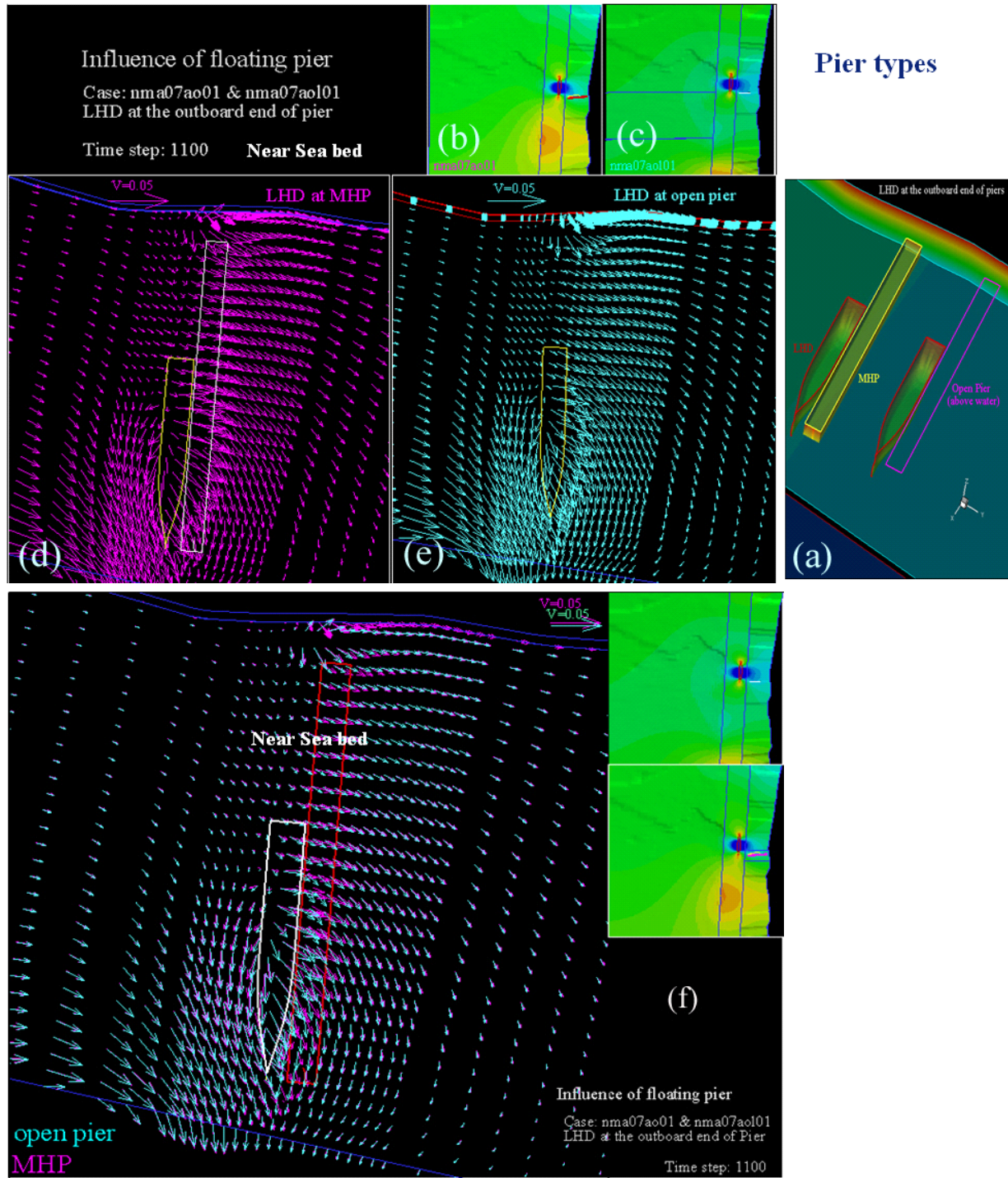
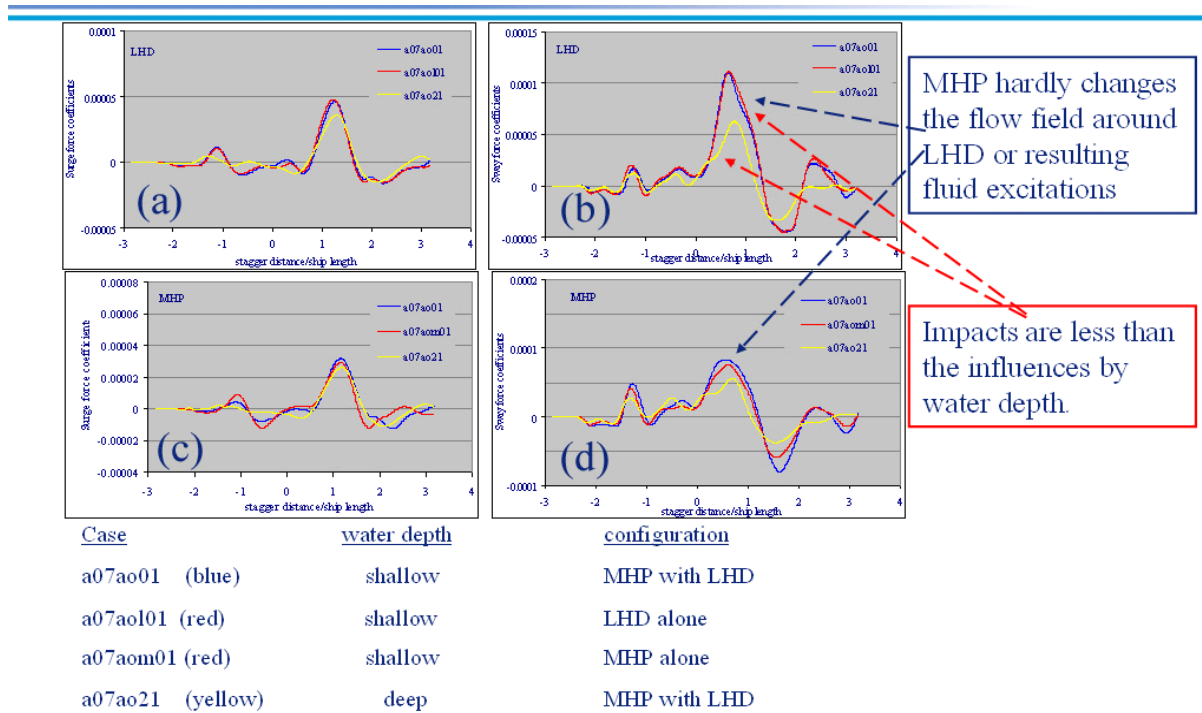
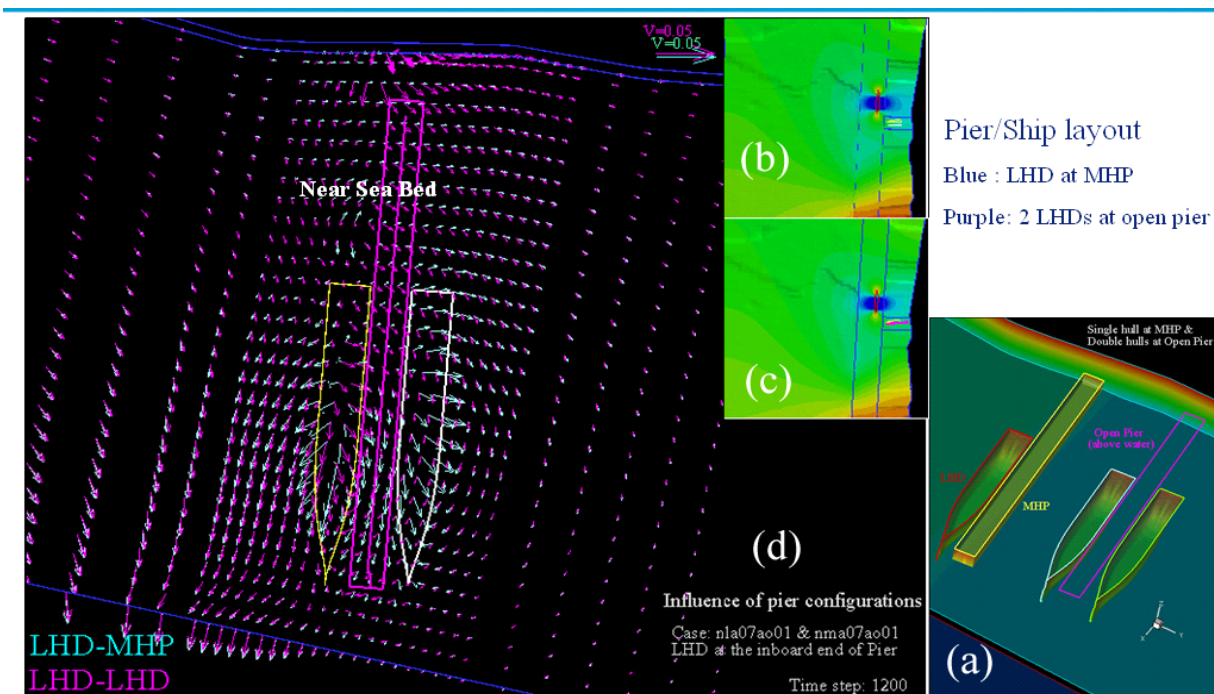


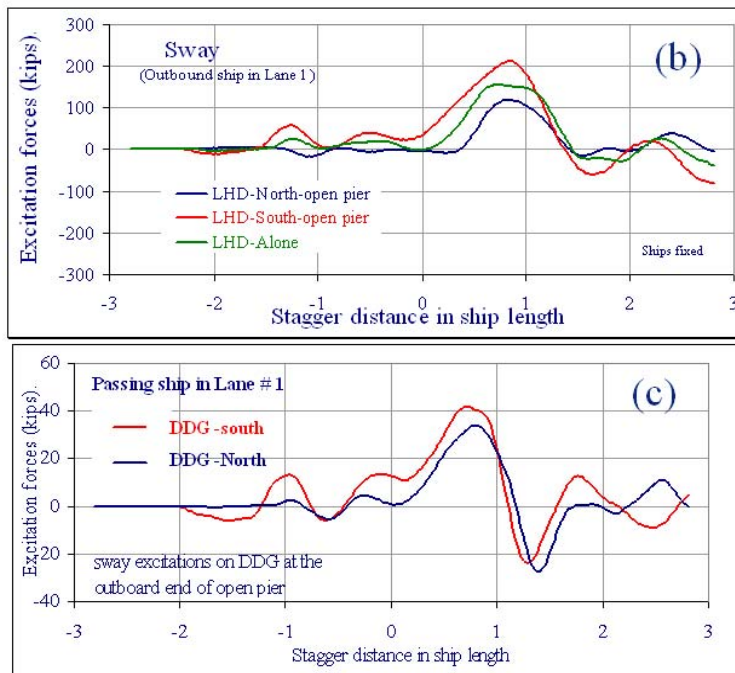
Figure 41. Comparison of flow fields near seabed.



**Figure 42. Hydrodynamic coupling between client ships and piers**



**Figure 43. Sheltering between moored ships: currents**



Other client ships provide more sheltering than does MHP

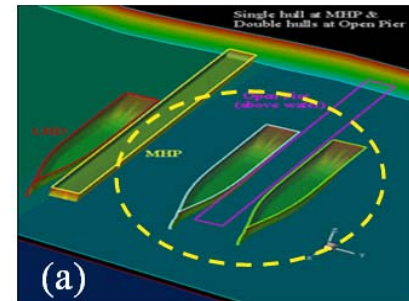


Figure 44. Sheltering between moored ships: excitation forces

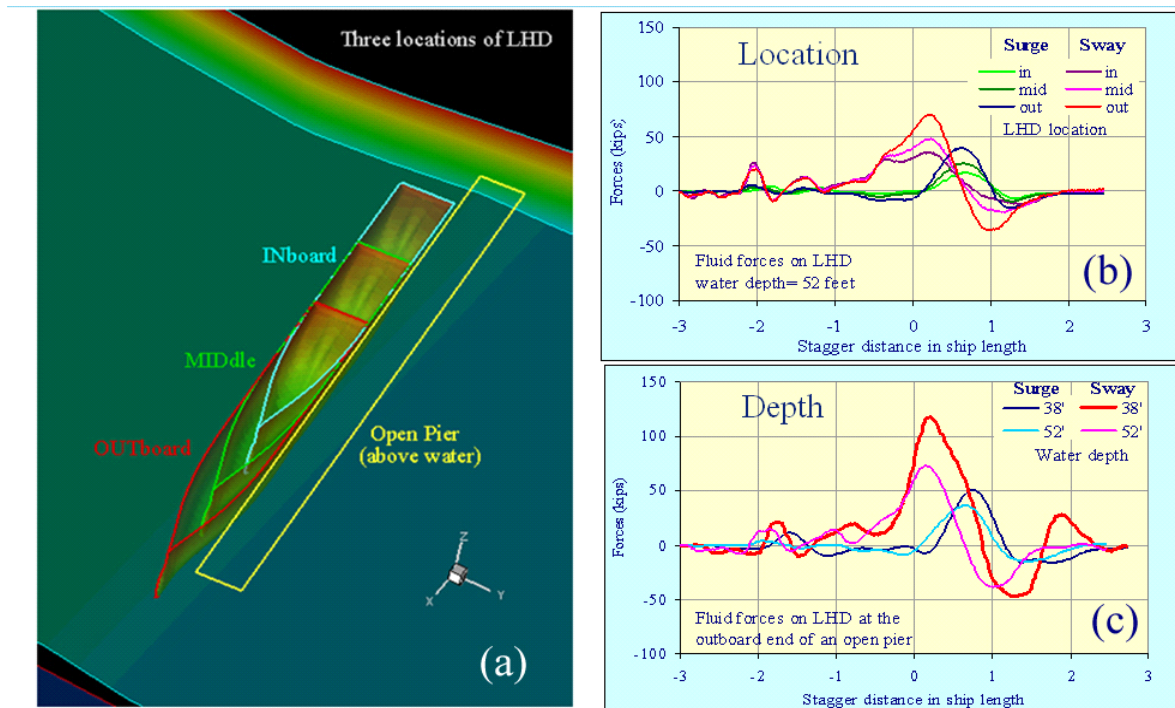
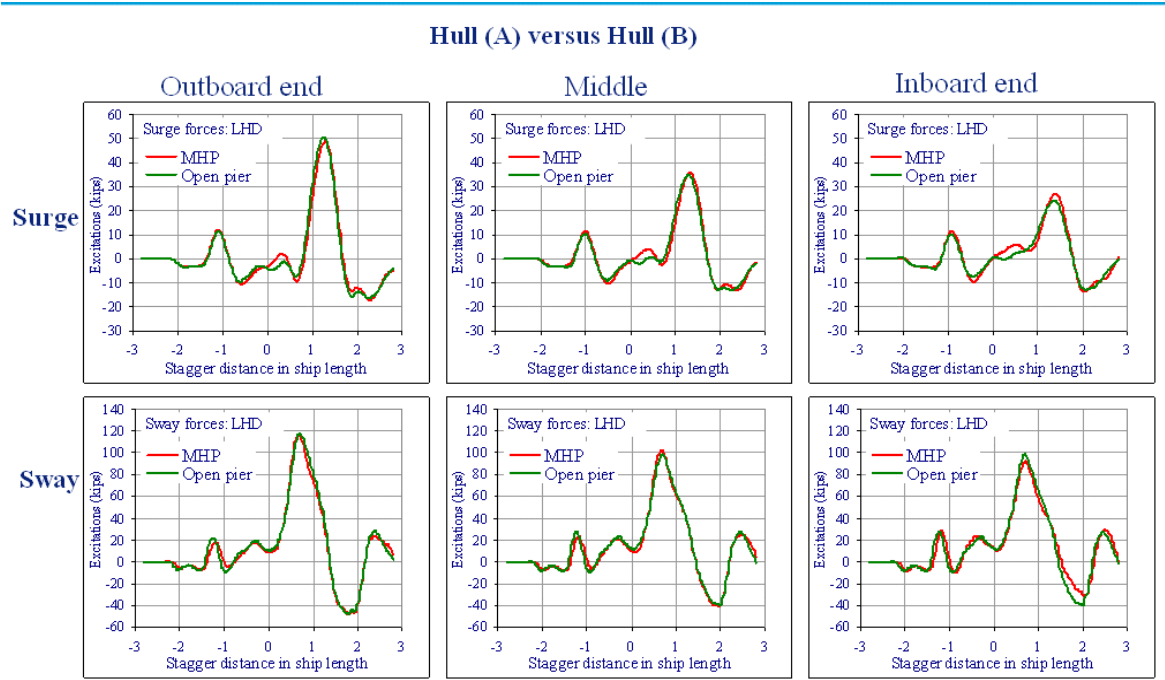


Figure 45. Influences of client ship locations and water depths.



**Figure 46. Impacts introduced by the presence of floating pier the MHP.**

## Fluid Excitations on the MHP and Client Ships

Large passing ships can generate sufficient disturbances to upset nearby piers and client ships. The consequence concerns the design and operation of a floating pier like the MHP in at least two aspects. The fluid excitations imposed on the pier and client ships are eventually withstood by the designated anchor mechanism and the resulting motion may degrade the efficiency of pier operations. A sequence of numerical simulation was exercised to check the design capacity of the mooring shafts and gauge the motion responses of the MHP and client ships in the episode of passing ship scenario. This test was conducted in a typical waterfront environment at Pier 7 of NAVSTA Norfolk with the largest cargo ship permissible to the existing navigation channel. With the close distance of this pier site to the navigation channel and high passing ship speed in consideration, the test scenario perhaps represents the worst case passing ship disturbance the MHP may face in the foreseeable future. However, this test considers only one client ship subject to the capacity limitation of the computer resources. The mooring shafts are expected to see much higher loads if multiple client ships are moored to pier simultaneously.

Figure 47 gives an overview of the passing ship induced excitations on the MHP and the LHD with the outbound Suezmax in five various ship lanes as specified in Table 3. The client ship, the LHD, is moored to the north side of the MHP at its offshore end in this case. These forces represent exclusively the fluid excitations on fixed the MHP and the LHD. Features of these force histories were discussed previously in Figure 34(a). All force components follow the general trend of decreasing with the increase of separation distance. The LHD observes substantially higher loads than the MHP even the latter is of slightly larger displacement. These forces are eventually transferred to the mooring shafts.

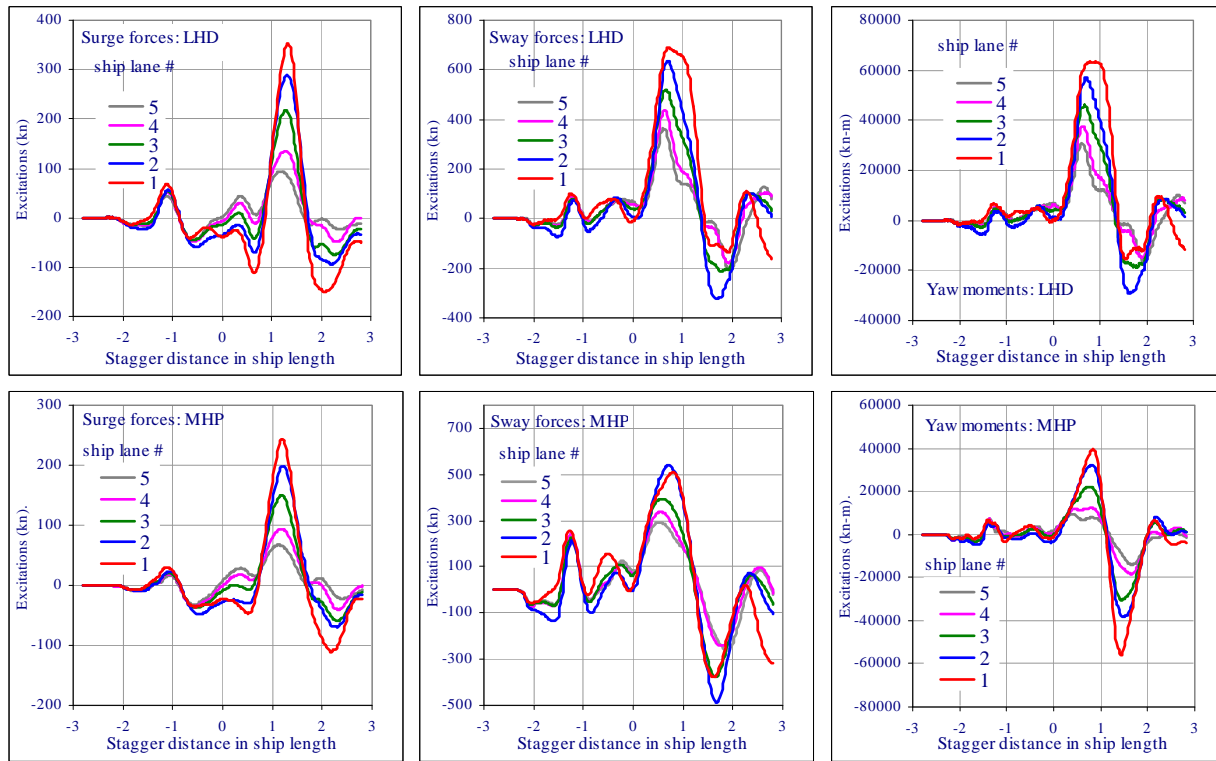


**Figure 47. Example of passing ship induced forces.**

## Dynamic Responses of the MHP and Client Ships

The motion excursions of the coupled system in response to the passing ship excitations were tracked by a versatile motion tracer at every time step throughout the simulation duration. The fluid solver automatically updates the fluid induced forces including the fluid reactions to the ship motion while the motion tracer constantly assesses the coupling loads at the instant. This seamless procedure precisely preserves the phase relationship between structural components including pier, ship, and coupling mechanisms. The results represent the true motion history rather than a statistically similar performance of the system. The difference can be devastated in a transient process. As previously mentioned, the system responses are sensitive to the layouts and dynamic nature of the coupling members. For the purpose of gauging the fender loads on the mooring shafts and motion dynamics of the MHP, the simulation model implemented the internal fenders around the mooring shafts to the design specification to date, but assumed a symbolic external coupling system composed of linear mooring lines and foam fenders. The resulting motion responses of the client ship and load distribution among mooring lines and foam fenders should be considered as nominal figures. Nevertheless, the global forces transferred from the client ship to the MHP are more stable through the averaging process unless the client ship responses diverge. This simulation assumes a stiff external coupling system to ensure smooth load transfer between pier and client ship. As such, the MHP responses and dynamic loads on the internal fenders are realistic. The results are presented in Figures 48 to 50.

Figure 48(a) illustrates the pier and ship layouts for the consideration of motion analysis. The middle system sets a baseline with one LHD moored to the offshore end of the MHP. The left system represents the same configuration at an equivalent pile support pier and the right system is a bare the MHP alone. The associated results of three systems are denoted by “both”, “lhd”, and “mhp”, respectively. The thick lines present the baseline system and the thin lines display the reduced system with the MHP or the LHD alone. The red and blue colors distinct the quantities of the LHD and the MHP, respectively. Quantities shown in Figures 47 and 48 refer to the scale of like color.

Figure 48 (b) to (d) summarizes the motion excursions in the horizontal plane. In addition to the shape and magnitudes of the motion excursions, this set of data reveals several noteworthy insights.

- (a) Coupling members significantly influence to the motion responses. Even the force excitations on the LHD are of little difference regardless of the pier type (Figure 42), the motion histories appear quite different, particularly the surge excursion of the LHD. The cause of these disparities was traced back to a small difference in the fender and mooring line setup. The external fenders and mooring lines in the baseline case were slightly preloaded to ensure a firm contact of the client ship with the MHP. Unfortunately, this initial condition was not properly enforced in the case with the LHD at a pile support pier due to a small offset in the location of the pier. This difference can be seen in the initial sway responses of the LHD at the beginning of the simulation in Figure 47(c). The LHD hull was initially pushed away from the pier in the baseline case and was pulled into the pier in the other case. The shapes of sway histories are separated by the initial offset and otherwise appear very similar. However, this offset makes some difference in the surge motion. The mooring lines are tighter in the baseline case than in case with pile supported pier and thus pull the LHD harder along the ship length to further excite the surge excursion.
- (b) The LHD moves 100 times more than the MHP, because the internal fenders are about 100 times stiffer than the external coupling system.
- (c) The MHP with the LHD sways twice as much as does the pier in the same condition alone (see blue lines in Figure 48(c)). This is in line with the fact that the LHD bears the same magnitude of fluid excitations as the MHP hull.
- (d) MHP responses are sensitive to the client ship layout along the pier. The difference in the yaw excursions of the MHP with and without the LHD is drastically more pronounced than the difference in the sway excursions, obviously due to the eccentric location of the LHD off the midship of the MHP.

Figures 49(a) and 49(b) summarize the time histories of the velocities and accelerations. The quantities of the MHP present the high frequency component associated to the internal fender and low frequency component associated to the external coupling system. The acceleration history of the MHP further marks the signature when the LHD hull hits hard on the external fenders.

Figures 49 (c) and 49(d) on the other hand present the total (net) fluid forces on the ships, including the passing ship induced excitations and fluid reactions to the ship motion. The differences between the baseline case and cases with the LHD or the MHP alone are minor, except the obvious phase shift in the surge forces on the MHP.

Recall that fender reactions and mooring loads are sensitive to the layouts of coupling members and client ships. Figure 50 provides an overview of the forces on selected fenders and mooring lines to illustrate their nominal magnitudes and nature of great variability. In general, the client ship adds substantial loads on the internal Trellex fenders as anticipated (Figure 50 (a) and (b)). The influence of pier types between floating and pile supported is less visible (Figure 50 (c) to (f)). It is clear that ship excursion dictates the coupling forces and the coupling forces also affect the ship excursion to a great extent. The spring lines, particularly, are nearly parallel to the client ships and thus induce substantial cross coupling effects to complicate the ship excursion. A transverse ship excursion may result in large mooring loads along the ship length and vice versa. The influences are then passed onto the ambient water activities through ship excursions. As a result, the MHP, client ships, coupling members, and ambient water form an inseparable system. The mechanism of fluid-structure coupling is the most sophisticated link of the entire system. Both the fluid force history and phase relations between various fluid force components are crucial to the system performance. Numerical errors in fluid force assessment tend to grow through the amplification effects by the coupling members over time.

Figures 51 and 52 recapitulate the passing ship effects on the MHP and concerning anchor system design for the pier. These results were extracted from a numerical exercise at a real waterfront fully exposed to a major navigation channel of heavy ship traffic as illustrated in Figure 51(a). Details of the water domain, seabed bathymetry, and channel configurations were illustrated in Figure 5 and discussed in the section of site descriptions. The numerical exercise considered an adverse passing ship scenario in the typical naval waterfront environment close to the worst case event that a future the MHP may face in reality. The scenario features a large cargo ship of Suezmax class cruising by the model pier site at 14 knots at various distances from 150 to 200 meters from the offshore end of the pier. This range encloses the passing ship Lanes 1, 2, and 3 as shown in Figure 51(b). Actually, Lanes 2 and 3 specify roughly the existing outbound lane at the NAVSTA Norfolk while Lane 1 is near the border of the navigation channel of Norfolk Harbor Reach. Large passing ships are unlikely to approach any closer in reality. Figures 51 (c) and (d) illustrate the fluid excitations observed by the MHP and client ships for the model passing ship in Lane 1 and Lane 3, respectively. A prescribed passing ship in Lane 3 will impose a sway force of 400 Kilonewtons (KN) and a surge force of 150 KN on the MHP and a sway force of 520 KN and a surge force of 220 KN on the LHD hull moored to the leeside of the pier, respectively. Figure 52 indicates the maximum load on a mooring shaft is 520 KN, which is about 8 percent of the design buckling load of these fenders. Under this condition, the MHP surges 1 centimeter (cm), sways 2 cm, and yaws 0.005 degrees at the maxima. Note that the fluid excitations increase by roughly 50 percent if the passing ship moves to Lane 1, which is 50 meters toward the MHP and that the LHD hull bears the same amount of excitations as the MHP. Considering the worst case conditions with the passing ship in Lane 1 compound with four of the LHD hulls at the offshore end of the MHP in double mooring, the maximum load on the internal fenders could reach 40 percent of their design buckling load by linear extrapolation.

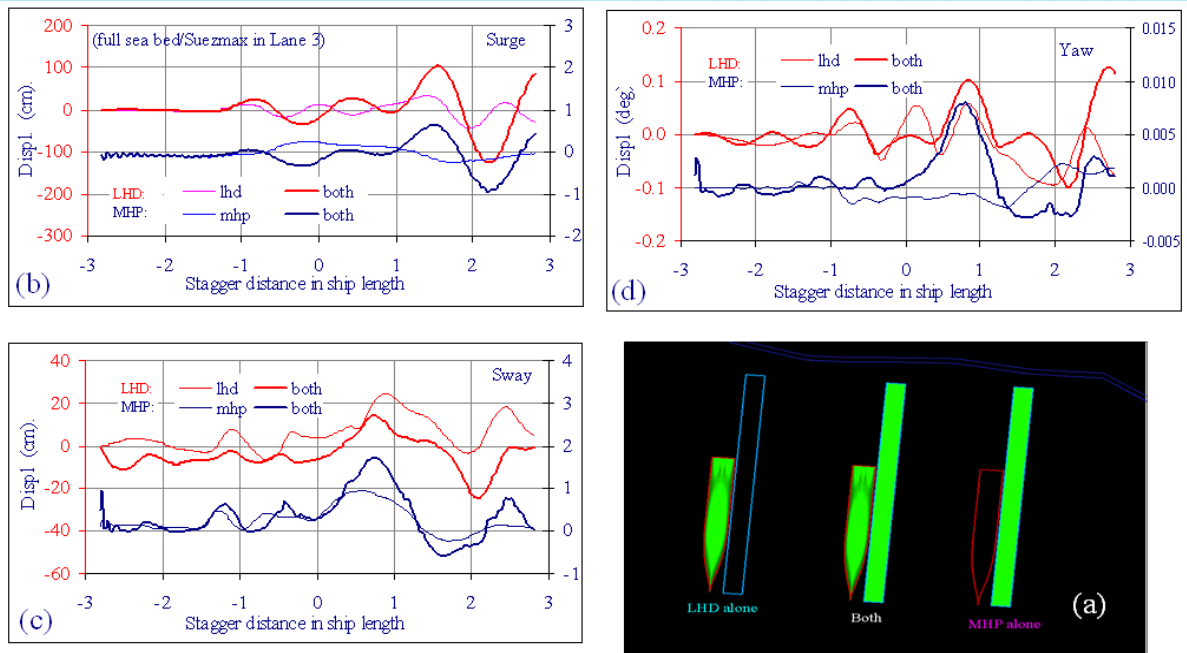


**Figure 48. Impacts introduced by the MHP hull: motion excursions.**

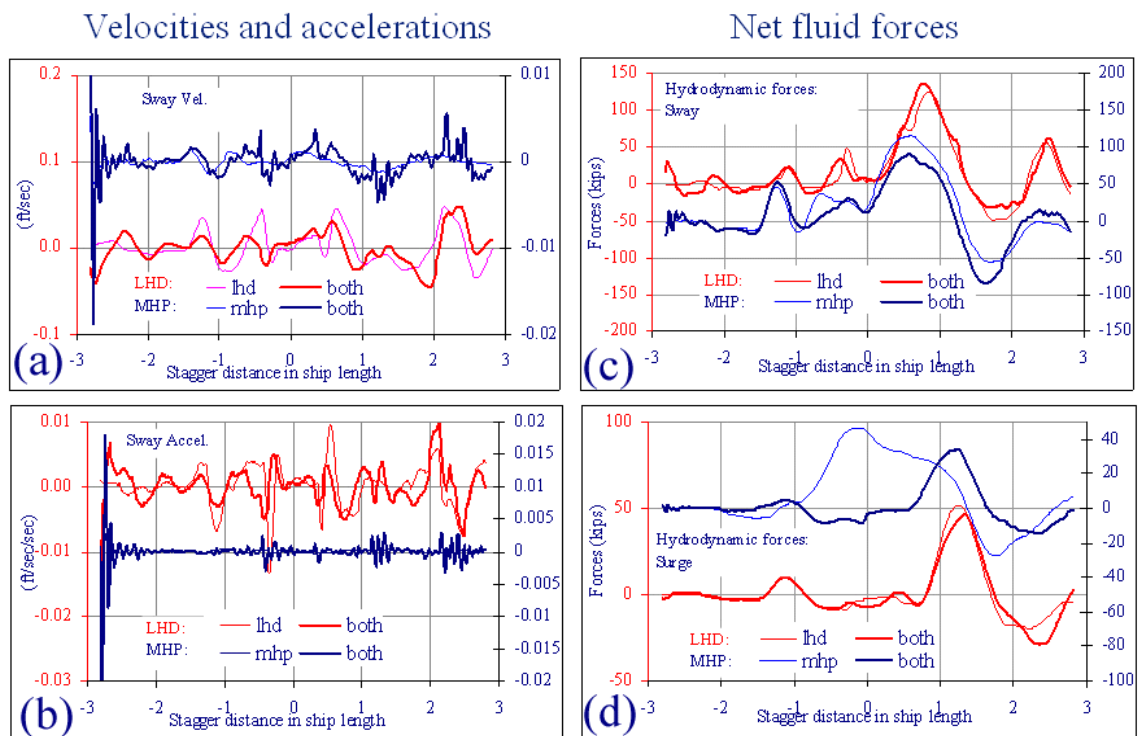


**Figure 49. Impacts introduced by the MHP hull: kinematics and excitations.**

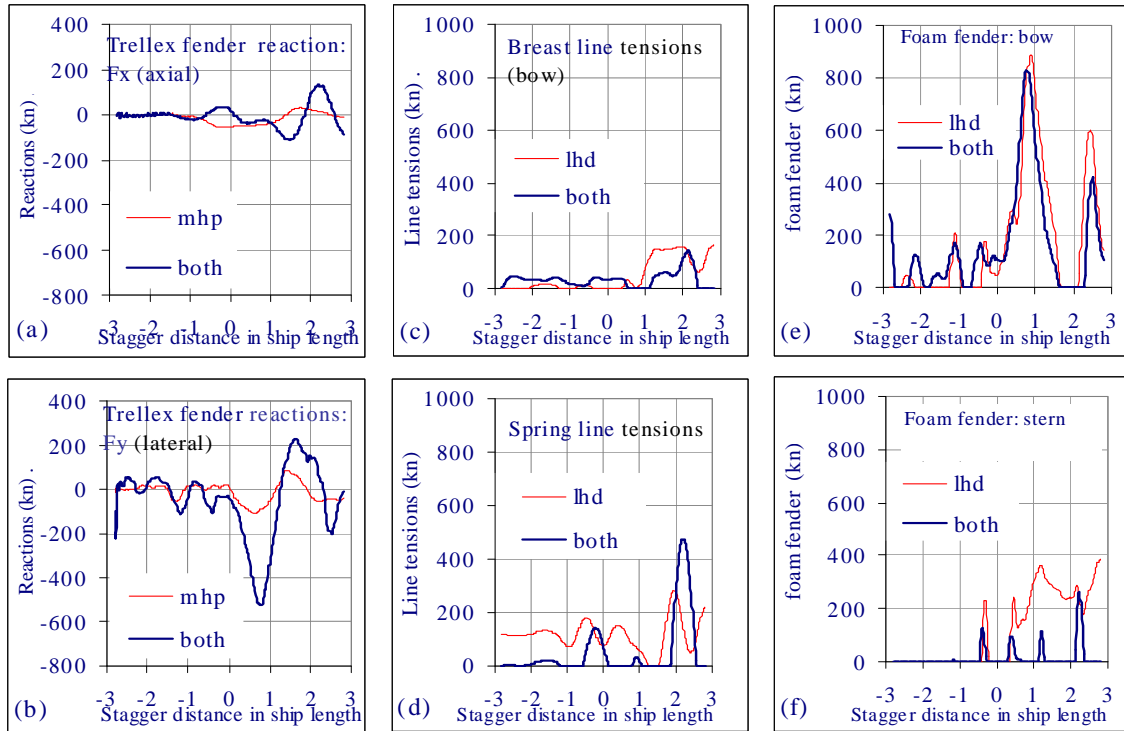


**Figure 50. Impacts introduced by the MHP hull: coupling member reactions.**

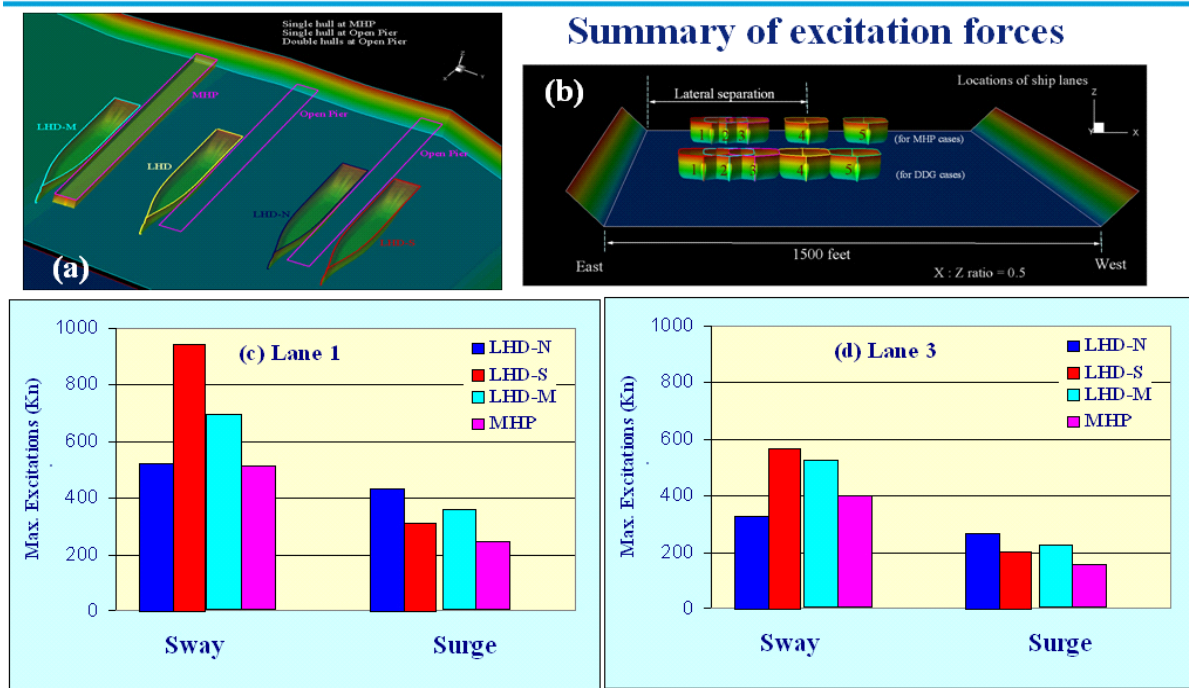


**Figure 51. Summary of passing ship induced excitations on the MHP and client ship.**

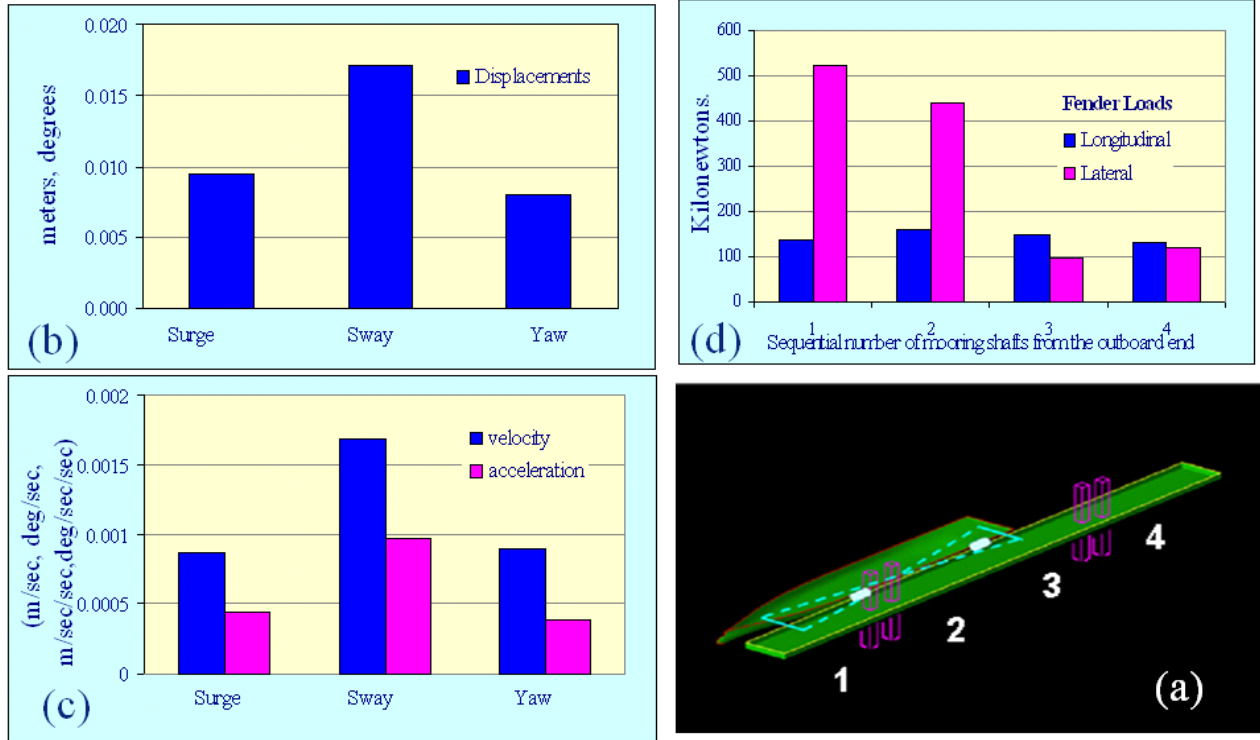


**Figure 52. The MHP responses and fender reactions.**

## CONCLUSIONS

Passing ships engage the MHP and its client ships through pressure pulses in inland water. Their effects are dictated by the speed of the passing ship, its separation distance from the pier, and the water depth at the pier site relative to the drafts of client ships. Typical MHP sites are relatively deep for their design client ships. Under this circumstance, the flow patterns around a pier of a specific ship layout are similar. This nature allows the passing ship induced excitations be assessed with parametric models. However, these models are site, hull shape, and ship layout dependent and hence require extensive calibrations by empirical data. Besides, a full account of passing ship effects shall address the dynamics of pier, client ships, fenders, mooring lines, and ambient fluid. These induced entities are highly transient and fully coupled. A seamless, self-sustain model capable of assessing the instant structure and fluid activities concurrently is required to preserve the phase relations among the component entities for a faithful description of the pier and client ship performances. Otherwise, numerical uncertainties in one entity are likely to propagate to the others and accumulate in time.

This study indicates that the MHP hull does not substantially disturb the ambient flow and client ship performance. The disturbance introduced by the presence of the MHP hull is much less significant than the influence due to water depth variations at the pier site. In fact, a client ship on the weather side provides far more sheltering than does the MHP hull. This

observation is substantiated by evidences extracted from flow patterns around the pier site and fluid excitations on the MHP and client ships.

Passing ship induced fluid excitations are roughly proportional to the displacement of the MHP and client ships. Large client ships of the LHD class draw comparable fluid forces as does the MHP. A smaller hull of DDG class bears about 20 percent of the forces on the MHP. These forces are eventually transferred to the anchor system of the pier. For instance, the mooring shafts of the MHP may endure three to five times the fluid forces on the pier alone in a scenario with four of the LHD hulls in double mooring. Nevertheless, an equivalent pile supported pier with the same client ships would experience similar fluid excitations. The MHP differs from the pile supported berthing pier in the load transfer path to the anchor system. The MHP is apparently more sensitive to the layout of client ships.

The present simulation addresses an adverse passing ship scenario in the typical naval waterfront environment close to the worst case event that a future MHP may face in reality. Lessons learned from this effort provide a tangible scale to gauge the design load for the anchor system. The scenario features a large cargo ship of Suezmax class cruising by the model pier site at 14 knots in a ship lane at 190 meters from the offshore end of the pier. The MHP is secured to the seabed with four mooring shafts and stands nearly perpendicular to the navigation channel. Each mooring shaft interfaces the MHP hull through a set of internal fenders around the shaft. One of the LHD hull is moored to the offshore end of the pier on its downstream side. Figures 51 and 52 summarize the passing ship effects in terms of fluid excitations and system responses, respectively. Under the prescribed conditions, the passing ship imposes a sway force of 520 KN and a surge force of 220 KN on the LHD hull and 400 KN and a surge force of 150 KN on the MHP, respectively. These forces hardly move the MHP. The MHP surges 1 centimeter (cm), sways 2 cm, and yaws 0.005 degrees at the maximum. The maximum load on a mooring shaft is 520 KN, which is about 8 percent of the design buckling load of these fenders. Taking the passing ship scenario and client ship layout to the worst conditions possible for a 396-meter the MHP at the waterfront under consideration, the maximum load on the internal fenders could reach 40 percent of their design buckling load by linear extrapolation.

## REFERENCES

- Berger/Abam Engineers Inc. (2001), "Modular Hybrid Pier - Phase 2 Report," December
- Chen, Hamn-Ching, and Huang, Erick T. (2003), "Time-Domain Simulation of Floating Pier and Multiple-Vessel Interactions by a Chimera RANS Method," presented to 7<sup>th</sup> International Symposium on Fluid Control, Measurement and Visualization, Sorrento, Italy, August
- Chen, H.C., Liu, T., Huang, E.T. and Davis, D.A. (2000), "Chimera RANS Simulation of Ship and Fender Coupling for Berthing Operations," International Journal of Offshore and Polar Engineering, Vol. 10, No. 2, pp. 112-122.
- Chen, H.C., Liu, T., Chang, K.A., and Huang, E.T. (2002c), "Time-Domain Simulation of Barge Capsizing by a Chimera Domain Decomposition Approach," Proceedings of the 12<sup>th</sup> ISOPE Conference, Vol. III, pp. 314-320, Kitakyushu, Japan, May 26-31.
- Chen, H.C., Lin, W.M., Liut, D. A. and Hwang, W.Y. (2003), "An Advanced Viscous Flow Computational Method for Ship-Ship Interactions in Shallow and Restricted Waterway," MARSIM'03, Japan.
- Chen, H.C., Lin, W.M. and Hwang, Y.W., (2002a) "Application of Chimera RANS Method for Multiple-Ship Interactions in a Navigation Channel," Proceedings of the 12th ISOPE Conference, Vol. III, pp.330-337, Kitakyushu, Japan, May 26-31.
- Chen, H.C., Lin, W.M. and Hwang, Y.W., (2002b) "Validation and Application of Chimera RANS Method for Multiple-Ship Interactions in Shallow Water and Restricted Waterway," 24<sup>th</sup> Symposium of Naval Hydrodynamics, Fukuoka, Japan, July 8-13
- Dand, I.W., (1981) "Some Measurements of Interaction between Ship Models Passing on Parallel Courses," Report R 108, 1981, National Maritime Institute, Feltham, Middlesex, United Kingdom.
- Hammell, T. J., Hwang, W. Y., Puglisi, J. J., and Liotta, J. W. (2002), "Norfolk Harbor Reach Simulator Study Final Report," CAORF 20-0005-01, Computer Aided Operations Research Facility, United States Merchant Marine Academy, Kings Point, NY 11024
- Huang, E. T. and Chen, H. C., (2008) "Passing Ship Effects on Moored Ships at Naval Station Norfolk," Special Site Report SSR-3284-AMP, NAVFAC ESC, 1100 23rd Ave, Port Hueneme CA 93043-4370
- Kriebel, D. (2007), "Mooring Loads due to Perpendicular Passing Ships," Technical Report TR-6069-OCN, NAVFAC ESC, 720 Kennon Street SE, Bldg. 36, Suite 333, Washington Navy Yard, DC 20374

- Muga, B. J. and Fang, S. (1975) "Passing Ship Effects – From Theory and Experiment," Proceedings of 7th Offshore Technology Conference, Houston, Texas, May 5-8,
- Remery, G.F.M. (1974), "Analysis of Model Tests of Passing Ship Effects," Proceedings of Sixth Offshore Technology Conference, Houston, Texas, May 6-8.
- Suhs, N.E. and Tramel R.W., "PEGSUS 4.0 Users Manual," Report AEDC-TR-91-8, 1991, Arnold Engineering Development Center, Arnold Air Force Station, TN.
- Tuck, E. O. and Newman, J. N. (1974) , "Hydrodynamic Interactions between Ships," Proceedings of Tenth Naval Hydrodynamics Symposium.
- Varyani, K. S., and M. Vantorre (2006), "New Generic equation for Interaction Effects on a Moored Containership Due to a Passing Tanker," Journal of Ship Research, Vol. 50, No. 3, September 2006, pp. 278-287
- Wang S., (1975), "Dynamic Effects of Ship Passage on Moored Vessels," Journal of ASCE, the Waterways, Harbors and Coastal Engineering Division, Page 247 – 258, WW3, August.
- Chen, H.C. and Patel, V.C. (1988), "Near-Wall Turbulence Models for Complex Flows Including Separation," AIAA Journal, Vol. 26, No. 6, pp. 641-648.
- Chen, H.C., Patel, V.C. and Ju, S. (1990), "Solutions of Reynolds-Averaged Navier-Stokes Equations for Three-Dimensional Incompressible Flows," Journal of Computational Physics, Vol. 88, No. 2, pp. 305-336.
- Suhs, N.E. and Tramel R.W., "PEGSUS 4.0 Users Manual," Report AEDC-TR-91-8, 1991, Arnold Engineering Development Center, Arnold Air Force Station, TN.
- Chen H. C. and Korpus, R., "A Multi-block Finite-Analytic Reynolds-Averaged Navier-Stokes Method for 3D Incompressible Flow," ASME FED-Vol. 150 pp. 113-121, ASME Fluid Engineering Conference, Washington, DC, June 20-24 1993
- Chen, H.C. and Chen, M. (1998), "Chimera RANS Simulation of a Berthing DDG-51 Ship in Translational and Rotational Motions," International Journal of Offshore and Polar Engineering, Vol. 8, No. 3, pp. 182-191.
- Huang, E.T. and Chen, H.C., (2003) "Ship Berthing at a Floating Pier," Proceedings of the 13<sup>th</sup> ISOPE Conference, Vol. III, pp. 683-690, Honolulu, Hawaii, May 25-30.
- Huang, T.S. (1990), "Interaction of Ships with Berth at Floating Terminals," TM-65-90-03, Naval Civil Engineering Laboratory, Port Hueneme, California.
- Chen, H.C., Liu, T. and Huang, E.T., "Calculations of Nonlinear Free Surface Flows Around Submerged and Floating Sea Caches," Proceedings, 10th International Offshore and Polar Engineering Conference, Vol. III, pp. 193-200, Seattle, Washington, May 28-June 4, 2000.

Chen, H.C., Liu, T., and Huang, E.T., “Time-Domain Simulation of Large Amplitude Ship Roll Motions by a Chimera RANS Method,” 11th International Offshore and Polar Engineering Conference, Vol. III, pp. 299-306, June 17-22, Stavanger, Norway, 2001.

Chen, H.C., Chang, K.A, Liu, T., and Jung, K.H., “Stability of Small Pontoon-Based Platforms at High Sea States,” COE Report No. 379, 126 pages, Texas Engineering Experiment Station, Texas A&M University, College Station, TX, September 2003.

Chen, H.C., Liu, T., Huang, E.T. and Davis, D.A. (2000), “Chimera RANS Simulation of Ship and Fender Coupling for Berthing Operations,” International Journal of Offshore and Polar Engineering, Vol. 10, No. 2, pp. 112-122.

Chen, H.C., Liu, T., and Huang, E.T. (2001) “Time-Domain Simulation of Large Amplitude Ship Roll Motions by a Chimera RANS Method,” Proceedings of the 11th ISOPE Conference, Vol. III, pp. 299-306, Stavanger, Norway.

Chen, H.C., Liu, T., Chang, K.A., and Huang, E.T. (2002c), “Time-Domain Simulation of Barge Capsizing by a Chimera Domain Decomposition Approach,” Proceedings of the 12<sup>th</sup> ISOPE Conference, Vol. III, pp. 314-320, KitaKyushu, Japan, May 26-31.